Vol. 59 • No. 1

Microwave® Journal

.com

FIGHTING FOR IFF

horizon house®

Founded in 1958

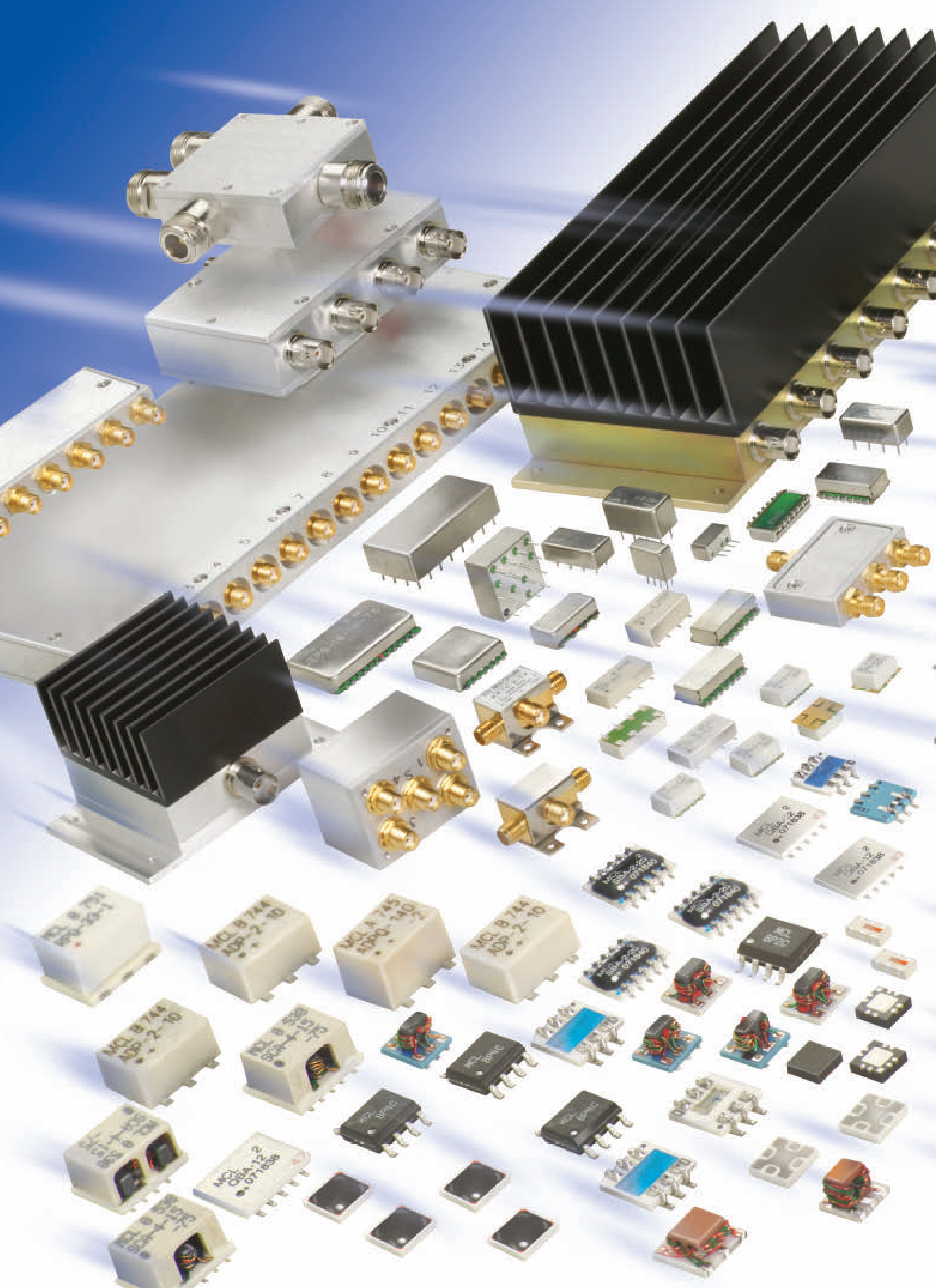
MCL B 744
ADP-2-10
MCL
QBA-12

Microwave Journal

CONTENTS

January 2016
Vol. 59 • No. 1
Radar and Antennas
mwjournal.com

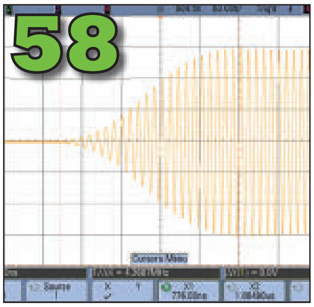

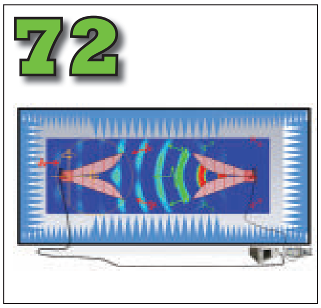

AUGMENTED REALITY: HOW IT WORKS

STEP 1	STEP 2	STEP 3
Download the free Layar app from the iTunes (iOS) or Google Play (Android) store.	Launch the app to view enhanced content on any page with the layar logo.	Frame the entire page in the screen and tap to experience enhancements (tap screen again for full screen view).

Look for the Layar logo on participating pages.

AR pages may expire after 30 days.

59 YEARS OF PUBLISHING EXCELLENCE

Microwave Journal

CONTENTS

mwjournal.com

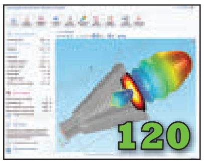

Product Features

Tech Briefs

Departments

Microwave Journal (USPS 396-250) (ISSN 0192-6225) is published monthly by Horizon House Publications Inc., 685 Canton St., Norwood, MA 02062. Periodicals postage paid at Norwood, MA 02062 and additional mailing offices.

POSTMASTER: Send address corrections to *Microwave Journal*, PO Box 1143, Skokie, IL 60076 or e-mail mwj@halldata.com. Subscription information: (847) 763-4943. This journal is issued without charge upon written request to qualified persons working in the RF & microwave industry. Other subscriptions are: domestic, $120.00 per year, two-year subscriptions, $185.00; foreign, $200.00 per year, two-year subscriptions, $370.00; back issues (if available) and single copies, $10.00 domestic and $20.00 foreign. Claims for missing issues must be filed within 90 days of date of issue for complimentary replacement.

STAFF

Publisher: Carl Sheffres
Editor: Patrick Hindle
Technical Editor: Gary Lerude
Managing Editor: Jennifer DiMarco
Associate Technical Editor: Cliff Drubin
Multimedia Staff Editor: Leslie Nikou
Multimedia Staff Editor: Barbara Walsh
Consulting Editor: Harlan Howe, Jr.
Consulting Editor: Frank Bashore
Consulting Editor: David Vye
Consulting Editor: Raymond Pengelly
Electronic Marketing Manager: Chris Stanfa
Client Services Manager: Kristen Anderson
Event Coordinator: Jacqueline Williams
Audience Development Manager: Carol Spach
Traffic Manager: Edward Kiessling
Director of Production & Distribution: Robert Bass
Art Director: Janice Levenson
Graphic Designer: Sachiko Stiglitz

EUROPE

International Editor: Richard Mumford
Office Manager: Nina Plesu

CORPORATE STAFF

CEO: William M. Bazzy
President: Ivar Bazzy
Vice President: Jared Bazzy

EXECUTIVE EDITORIAL OFFICE
685 Canton Street, Norwood, MA 02062
Tel: (781) 769-9750
FAX: (781) 769-5037
e-mail: mwj@mwjournal.com

EUROPEAN EDITORIAL OFFICE
16 Sussex Street, London SW1V 4RW, England
Tel: Editorial: +44 207 596 8730 Sales: +44 207 596 8740
FAX: +44 207 596 8749

SUBSCRIPTION SERVICES
Send subscription inquiries and address changes to:
Tel: (847) 763-4943
e-mail: mwj@halldata.com

BPA WORLDWIDE

www.mwjournal.com

Printed in the USA

Microwave Journal Online

Scan page using layar app

Visit us @ mwjournal.com

eLEARNING free webinars

Access webinars on-demand at www.mwjournal.com/webinars.

Web Survey

What is the biggest innovation in antenna technology?

Look for our multiple choice survey online at mwjournal.com

November Survey

What was the most significant development in radar technology during the past decade?

- AESAs (18%)
- GaAs MMICs (13%)
- Digital IC processing (10%)
- GaN PAs and MMICs (41%)
- Single-chip T/R or AESA (18%)

Executive Interviews

Paul Hart, NXP SVP and GM of RF Power, outlines the market and technology direction of the business following NXP's acquisition of Freescale and the sale of their own RF power unit.

Reinier Beltman, CEO of **Ampleon** offers background to the company's formation and commits to continued development of mobile broadband initiatives, advancement of its RF energy activity and increased investment in R&D.

FOLLOW US ON TWITTER

Pat Hindle @pathindle	Gary Lerude @MWJGary	Leslie Nikou @MWJeditor
Jacqui Williams @MWJevents	Jenn DiMarco @jndimarco	Mike Hallman @mphallman

Catch *Frequency Matters*, the industry update from *Microwave Journal*, www.microwavejournal.com/FrequencyMatters

COM

TIP 1 For an inductor with the absolute maximum Q, pick one of these air core "Springs". They have flat tops for easy mounting and exceptional current ratings.

TIP 2 If you prefer conventional chip inductors, you'll get the highest Q with our new ceramic body 0402HP and 0603HP families. These tiny wirewound coils handle up to 2 times more current than the nearest competitor.

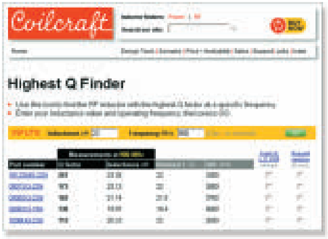

This new web tool finds inductors with the highest Q at your operating frequency

TIP 3 Need to find coils with the best Q at your L and frequency? Our **Highest Q Finder** web tool tells you in just seconds. Click again to plot the L, Q, Z and ESR of up to 4 parts simultaneously.

TIP 4 When it's time to build your prototypes, be sure to ask us for evaluation samples. They're always free and we can get them to you overnight.
To get started, visit **www.coilcraft.com/Q**

Here are some high Q tips

photo courtesy of the
U.S. Military & NASA

ULTRA-REL® *10 MHz to 7GHz*

CERAMIC MMIC AMPLIFIERS

Low NF from 0.5 dB *High IP3 up to +42 dBm* *Low DC current 65 mA* from $4.95 ea. (qty 20)

When failure is not an option. Our CMA family of ceramic MMIC amplifiers is expanding to meet your needs for more critical applications. Designed into a nitrogen-filled, hermetic LTCC package just 0.045" high, these rugged models have been qualified to meet MIL standards for a whole battery of harsh environmental conditions:

Qualified for: *(see website for complete list and details)*

- *Gross and Fine Leak*
- *Mechanical Shock*
- *Vibration*
- *Acceleration*
- *PIND*
- *HTOL (1700 hours @ +105°C)*
- *Steam Aging*
- *Solder Heat Resistance*
- *Autoclave*
- *And More!*

Robust performance across wide bandwidths makes them ideal for instrumentation, or anywhere long-term reliability adds bottom-line value. Go to minicircuits.com for all the details today, and have them in your hands as soon as tomorrow!

Electrical Specifications *(-55 to +105°C)*

3 x 3 x 1.14 mm

	Model	Freq. (GHz)	Gain (dB)	P_{OUT} (dBm)	IP3 (dBm)	NF (dB)	DC (V)	Price $ ea. (qty 20)
New	CMA-81+	DC-6	10	19.5	38	7.5	5	6.45
New	CMA-82+	DC-7	15	20	42	6.8	5	6.45
New	CMA-84+	DC-7	24	21	38	5.5	5	6.45
	CMA-62+	0.01-6	15	19	33	5	5	4.95
	CMA-63+	0.01-6	20	18	32	4	5	4.95
	CMA-545+	0.05-6	15	20	37	1	3	4.95
	CMA-5043+	0.05-4	18	20	33	0.8	5	4.95
	CMA-545G1+	0.4-2.2	32	23	36	0.9	5	5.45
	CMA-162LN+	0.7-1.6	23	19	30	0.5	4	4.95
	CMA-252LN+	1.5-2.5	17	18	30	1	4	4.95

RoHS compliant

Mini-Circuits®

www.minicircuits.com P.O. Box 350166, Brooklyn, NY 11235-0003 (718) 934-4500 sales@minicircuits.com

FEBRUARY

MARK YOUR CALENDAR

4

WEBINAR **5G Physical Layer Modeling: A Communication System Architect's Guide**

Sponsored by: KEYSIGHT TECHNOLOGIES

5

Call for Papers Deadline

EUROPEAN MICROWAVE WEEK, LONDON, UK, 3-7 OCTOBER 2016, www.eumweek.com, EuMW 2016

www.eumweek.com/conferences/callforpapers.html

18

WEBINAR **RF and Microwave Heating Simulation Apps**

Sponsored by: COMSOL

22-25

Mobile World Congress
Barcelona, Spain

MOBILE WORLD CONGRESS

The GSMA Mobile World Congress is where senior mobile leaders and visionaries network, collaborate and celebrate how mobile technology is at the forefront of discovery and innovation. The event provides the planet's best venue for mobile industry business opportunities and deal-making. MWC includes a product and technology exhibition showcasing 2,000+ companies; a world-class conference featuring visionary keynotes and discussions; the industry's best networking; and the annual Global Mobile Awards ceremony celebrating mobile solutions and initiatives.

www.mobileworldcongress.com

23

WEBINAR **Large Signal Device Characterization for RF Power Amplifier Design**

Sponsored by: NATIONAL INSTRUMENTS

24

WEBINAR **Millimeter Wave and E-Band Vector Network Analyzer Solutions**

Sponsored by: Anritsu envision : ensure

23-25

International Exhibition and Conference on Electromagnetic Compatibility (EMC)
Düsseldorf, Germany

emv

Europe's leading application-oriented conference on electromagnetic compatibility is held parallel to the EMV exhibition. EMC has become an important factor for innovation and social acceptance of new technology. Safety engineering in vehicles, automation technology in industrial environments, information supply — nothing works without electrical signals, electrical currents and electrical voltage. And everything has to operate without influencing each other. The bi-annual EMV conference provides a comprehensive program. Specialists from all over the world report on the latest products and developments and are available for technical discussions. This is the ideal platform for the dialogue between research, product development and application.

www.mesago.de/en/EMV/home.htm

2/29-3/2

IDGA 9th Annual Military Radar Summit
Washington, DC

9th Annual Military Radar Summit

As the only event in the United States that focuses exclusively on Military Radar, the summit again will bring together experts and thought leaders responsible for advancing critical discussion on this narrow and deep subject. Whether by land, sea, or air, military radar is used everywhere and requires consistent reexamination to achieve maximum performance. Come ready to learn and engage as this community works towards developing the next generation of capabilities for this essential technology.

www.militaryradarsummit.com

FOR DETAILS, VISIT MWJOURNAL.COM/EVENTS

Coming**Events**

CALL FOR PAPERS

EDI CON USA
February 1, 2016

EuMW 2016
February 5, 2016

ARMMS RF & Microwave Society Conference
February 19, 2016

mwjournal.com

FEBRUARY

Mobile World Congress
February 22–25, 2016 • Barcelona, Spain
www.mobileworldcongress.com

EMV 2016
February 23–25, 2016 • Düsseldorf, Germany
www.mesago.de/en/EMV/home.htm

IDGA Military Radar Summit
February 29–March 2, 2016 • Washington, DC
www.militaryradarsummit.com

MARCH

Satellite 2016
March 7–10, 2016 • National Harbor, Md.
www.satshow.com

GOMACTech
March 14–17, 2016 • Orlando, Fla.
www.gomactech.net

IWCE
March 21–25, 2016 • Las Vegas, Nev.
www.iwceexpo.com

Microwave & RF
March 23–24, 2016 • Paris, France
www.microwave-rf.com

APRIL

WAMICON 2016
April 11–13, 2016 • Clearwater Beach, Fla.
www.wamicon.org

ARMMS RF & Microwave Society Conference
April 18–19, 2016 • Oxfordshire, UK
www.armms.org

EDI CON China 2016
April 19–21, 2016 • Beijing, China
www.ediconchina.com

MAY

AUVSI Xponential 2016
May 2–5, 2016 • New Orleans, La.
www.xponential.org

EW Europe
May 10–12, 2016 • Rotterdam, Netherlands
www.eweurope.com

DAS & Small Cells Congress
May 16–18, 2016 • Las Vegas, Nev.
www.dascongress.com

CS Mantech 2016
May 16–19, 2016 • Miami, Fla.
www.csmantech.org

RFIC 2016
May 22–24, 2016 • San Francisco, Calif.
www.rfic-ieee.org

IMS 2016
May 22–27, 2016 • San Francisco, Calif.
http://ims2016.mtt.org

Space Tech Expo
May 24–26, 2016 • Pasadena, Calif.
www.spacetechexpo.com

87th ARFTG Microwave Measurement Symposium
May 27, 2016 • San Francisco, Calif.
www.arftg.org

JUNE

Sensors Expo & Conference
June 21–23, 2016 • San Jose, Calif.
www.sensorsexpo.com

JULY

IEEE EMC International Symposium on Electromagnetic Compatibility
July 25–29, 2016 • Ottawa, Ontario
www.emc2016.emcss.org

AUGUST

RFIT 2016 IEEE International Symposium on Radio-Frequency Integration Technology
August 24–26, 2016 • Taipei, Taiwan
www.rfit2016.org

SEPTEMBER

CTIA Super Mobility
September 7–9, 2016 • Las Vegas, Nev.
www.ctiasupermobility2016.com

EDI CON USA
September 20–22, 2016 • Boston, Mass.
www.ediconusa.com

Staying Engaged

Carl Sheffres
Microwave Journal *Publisher*

This holiday season, I found myself reflecting on my good fortune; of good friends, family and health. I also recognized, and certainly not for the first time, how much I enjoy this industry. I love that the technology is transformative. I love that we're such a close-knit community and I love the people in it. My favorite part of this job is when I'm able to interact with the knowledgeable, interesting and friendly people that comprise our community and these days, there are more opportunities to engage than ever before.

We shot the 50th edition of "Frequency Matters" last month, the bi-weekly video series in which MWJ editors discuss the latest industry news and highlight the features of the current issue of the magazine. The editors allowed me a brief cameo in this special edition, and in it, I mentioned how the series provides us with yet another way to interact and engage with the industry. I've found it to be informative and entertaining, and I'm glad to see that a growing number of our readers are tuning in to this program and to our new video channel. We launched the "Microwave Media" video platform last year and it now hosts hundreds of educational videos, product demos and webinars, along with the archive of 50-plus episodes of "Frequency Matters." I encourage you to check it out on our website at mwjournal.com.

Our webinar program continues to grow every year, with more than 75 events produced and delivered in 2015. Some of these webinars are presented by companies who are looking to share their latest design and manufacturing solutions. Others are presented by experts from Besser Associates, as well as industry experts Liam Devlin, John McNeil and Henry Lau, to name a few. This year, we're teaming with the RF Energy Alliance on a series of webinars addressing applications in solid-state RF power for consumer and industrial products. You'll also see a series on GaN applications moderated by Ray Pengelly, radar applications presented by Dr. Eli Brookner as well as 5G and IoT related events. These webinars are reasonably short and informative and provide the opportunity to interact with presenters during the Q&A portion. You can find hundreds of archived webinars on our site available for on-demand viewing.

The "RF and Microwave Community" on LinkedIn continues to grow, with nearly 30,000 members. This resource provides an excellent platform for dialogue and interchange. It's an active forum that allows members to share content and network with other industry professionals. If you haven't yet joined, I highly recommend it.

While the Internet has provided us with many new ways to connect, live events remain perhaps the most effective way to learn about new developments and to network with our peers. I attend numerous events each year and come away from each one with new ideas, new contacts and renewed friendships.

2016 will be a banner year for events. There are excellent conferences that address nearly every technical aspect of our industry and exhibitions that allow us to preview the latest solutions from a wide range of providers. *Microwave Journal* supports many industry events and, as you may know, we organize some of the world's leading RF and microwave events.

We launched the Electronic Design Innovation Conference (EDI CON) in China in 2013 and are preparing now for the fourth annual event in Beijing on April 19-21. This year's event has expanded to include the China Electrotechnical Society's EMC conference and the China Radar Industry Association (CRIA) Conference. Dr. Wai Chen, chief scientist and general manager of IoT for China Mobile will be the chairman for 2016, so delegates will find increased content in this important and growing arena. I have truly enjoyed the opportunity that this show has provided me to learn more about the growing technology base in China, to become more familiar with the culture and to meet many new colleagues.

We organize European Microwave Week for the European Microwave Association (EuMA) every fall, and this year, the event takes place in London on October 3-7 at the ExCel Center. London hasn't hosted EuMW in 15 years, so this one's particularly noteworthy. The call for papers is happening now, for those interested in participating.

The big news, and hopefully you've seen our promotions already, is the debut of EDI CON USA, which will take place on September 20-22 in Boston, at the Hynes Convention Center. Our goal is to bring the successful model we deployed in China to North America. That model aims to deliver practical, hands-on training and the opportunity to engage and network with your peers. Many leading companies are participating, along with some of the industry's most recognized experts. I hope to see you there.

Last, but hardly least, we're proud to bring you this publication, now in its 59th year. Whether you're reading it in print, digital, online or on our mobile app, I hope that you find its content beneficial to your work. Our advertisers make it possible to deliver your monthly edition at no cost to you. All we ask is that you renew yearly, so please do so at mwjournal.com/subscribe.

I look forward to another year of engagement, whether it's virtual or in-person. On behalf of the entire MWJ team, we wish all of our readers a prosperous and healthy New Year. ■

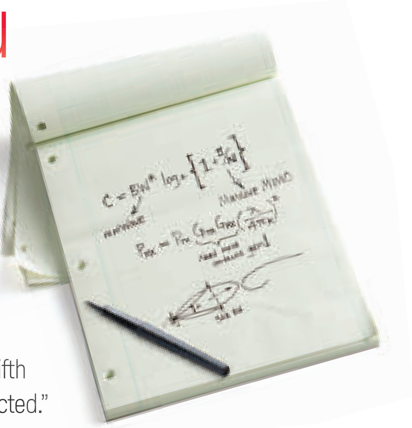

COVER FEATURE
INVITED PAPER

Solid-State Transmitters for IFF and SSR Systems

John Walker and James Custer
Integra Technologies Inc.

Identify Friend or Foe (IFF) and Secondary Surveillance Radar (SSR) systems are, from a hardware point of view, essentially the same system although the application is different. The radar systems developed in World War II could determine the range and bearing of aircraft but could not distinguish between friendly and hostile planes. IFF systems were developed at the same time to solve that deficiency.

The basic concept is illustrated in ***Figure 1***. Although today's systems are digital rather than analog and the frequencies used are different, the basic concept shown in Figure 1 has not changed. A ground-based transmitter sends out an interrogating pulse, which today is at 1030 MHz, to the aircraft. On receipt of this pulse the aircraft on-board transponder sends back a reply at a different frequency of 1090 MHz which, if it is a friendly aircraft, will contain a coded message that identifies it as a friendly aircraft. Thus IFF systems are basically military in nature. Further details about IFF and SSR systems can be found in[1-3].

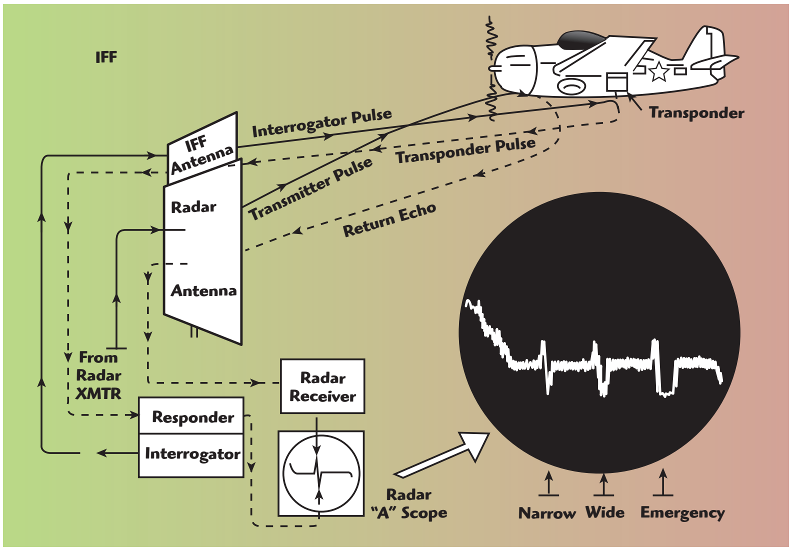

Fig. 1 Principle of an IFF system. Source: Radar Bulletin 8A, U.S. Navy, 1950.

Civil aviation has a different need to the military, requiring information such as the aircraft's flight number, its altitude etc. The basic difference between the military and civil uses of the IFF system is the information that is sent back to the ground station in the return pulse at 1090 MHz. Civil aviation labels this system a Secondary Surveillance Radar, but this is a misnomer since the returned pulse contains a data stream containing information about the flight, so in reality it is a communication system rather than a radar system. Nevertheless, it is universally termed an SSR and so this nomenclature will be used in this article. ***Figure 2*** shows a typical SSR system co-located with the S-Band primary radar system which is used to detect any object in the path of the radar beam.

SSR message formats have evolved over the years and the system that is in the most widespread use today is the Mode S version which transmits a train of 128 pulses of 0.5 µs on, 0.5 µs off with a long term duty cycle of 1 percent. As far as transistors are concerned, this is a very benign pulse train from a thermal point of view and any transistor technology can easily withstand this. However, a newer version of Mode S is being implemented called Extended Length Message (ELM) which uses a

RF & MICROWAVE FILTERS

RLC has the customized filter solutions you need.

RLC manufactures a complete line of RF and Microwave filters covering nearly every application in the DC to 50 GHz frequency range. We offer different filter types, each covering a specific engineering need.

In addition, our large engineering staff and high volume production facility give RLC the ability to develop and deliver both standard and custom designed filters at competitive costs, within days or a few weeks of order placement.

- Band Pass, Low Pass, High Pass & Band Reject
- Connectorized, Surface Mount, PCB Mount or Cable Filters
- Wave Guide Bandpass and Band Reject
- 4th Order Bessel Filters
- Spurious Free, DC to 50 GHz, Low Loss, High Rejection
- Custom Designs

For more detailed information, or to access ***RLC's exclusive Filter Selection Software****, visit our web site.*

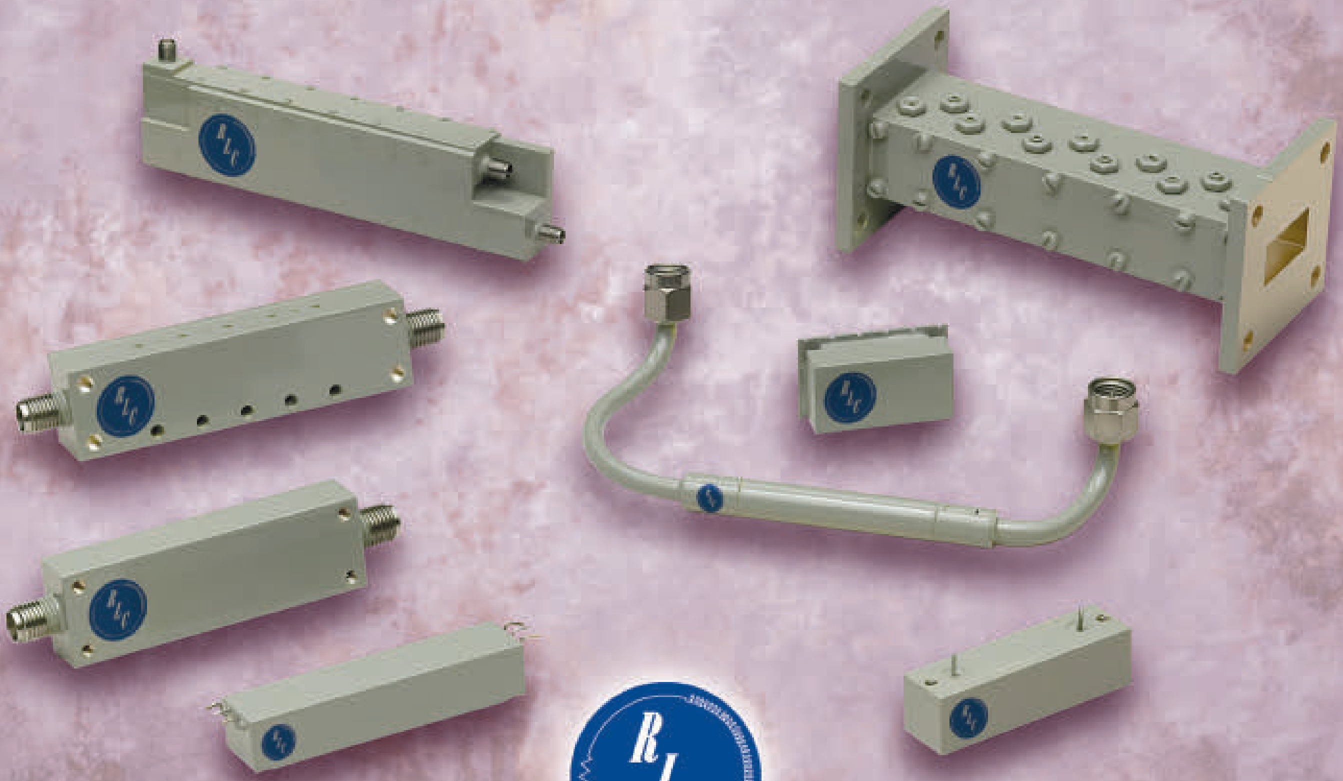

RLC ELECTRONICS, INC.

83 Radio Circle, Mount Kisco, New York 10549 • Tel: 914.241.1334 • Fax: 914.241.1753
E-mail: sales@rlcelectronics.com • www.rlcelectronics.com

ISO 9001:2000 CERTIFIED

RLC is your complete microwave component source...
Switches, Filters, Power Dividers, Terminations, Attenuators, DC Blocks, Bias Tees & Detectors.

48 pulse burst of 32 μs on, 18 μs off (i.e., 67 percent duty cycle within the pulse) with a long-term duty cycle of 6.4 percent.

As far as the transistor is concerned the off period during the pulse burst is not long enough for the transistor to fully cool down so from a thermal perspective the ELM Mode S pulse train looks like a 2.4 ms pulse with an overall duty cycle of 6.4 percent. This very long effective pulse means that the transistor is running close to CW conditions and many of the early generations of high-power pulsed RF transistors cannot be run CW without substantial de-rating.

This has necessitated the redesign of many SSR systems. The typical output power of a SSR transmitter is around 4 kW for the ground station while the airborne transponder is lower power at 1 to 2 kW. There is no requirement for linearity and so the transistors are often operated at about 2 dB into compression which helps achieve high efficiency.

The following is an assessment of the merits and disadvantages of silicon bipolar, silicon LDMOS and gallium nitride HEMT technologies for this application.

SILICON BIPOLAR TRANSISTORS

Early solid-state SSR systems used Si bipolar junction transistors (BJT) as this was the only transistor technology available and BJT-based SSRs are still being manufactured today. In fact, the standard mode S waveform[3] suits the characteristics of BJTs very well because the thermally benign waveform enables full advantage to be taken of the high power density capability of a BJT. With a requirement for around 4 kW of output power, the ‘holy grail’ for an SSR manufacturer has been a transistor with an output power of at least 1 kW since then it is easy to combine four of these devices to achieve 4 kW.

▲ *Fig. 2 Airport co-located primary and secondary radar system. The SSR radar antenna is at the top with the S-Band antenna immediately beneath it. (Photo courtesy of Shutterstock.com).*

In fact, a little more than 1 kW is needed to allow for losses in the combiner and the insertion loss of the isolator used at the output to protect the transistor from a high VSWR mismatch. BJTs fulfill this requirement nicely with devices up to 1.5 kW[4]. BJTs for this application are always operated in Class C mode with no applied DC voltage to the base-emitter junction and the typical efficiency is about 60 to 65 percent for a 1 kW device.

BJTs have the simplest RF circuitry of any technology. ***Figure 3*** shows the circuit for the 1.5 kW 1030 MHz BJT, just two capacitors are used on the PCB plus a large external reservoir capacitor that is common to all types of transistors. It also only requires a single positive supply voltage.

BJTs also have one other extremely important attribute that is not enjoyed by either GaN HEMTs or LDMOS transistors. BJTs are operated in Class C so that when there is no applied RF pulse the transistor does not pass any DC current. Consequently, BJT-based SSRs inherently emit almost zero shot noise in the off period. LDMOS and GaN HEMTs, on the other hand, are always biased Class A/B and so emit shot noise in the off-period which is injected into the receiver along with the returned signal from the aircraft transponder causing receiver de-sensitization.

The required quiescent current for LDMOS and GaN is roughly proportional to the output power of the transistor so it is more of an issue for the kW-level transistors used in SSR systems than in low power systems. The solution to this problem is to use

more complex DC circuitry which shuts down the transistor completely in the off-period but which turns the gate bias on ahead of the RF pulse[5].

BJTs can also be designed for the ELM version of mode S, but the maximum output power drops to about 500 W due to thermal limitations. This means that a minimum of 8 BJTs are needed for a complete SSR. This has serious size and cost implications for the system. Thus, although BJT technology is well-proven and extremely reliable it is unlikely that any new systems will be designed using BJTs.

BJTs also have three other disadvantages, namely they use environmentally unfriendly BeO packages which are also expensive, and they have much lower gain than either LDMOS or GaN HEMTs which means that more gain stages are needed in the amplifier which, of course, adds to size and cost. Finally, the VSWR withstand capability for a 1 kW device is normally specified at 3:1 which means that the device needs to be protected by a high power isolator which also adds to the overall cost.

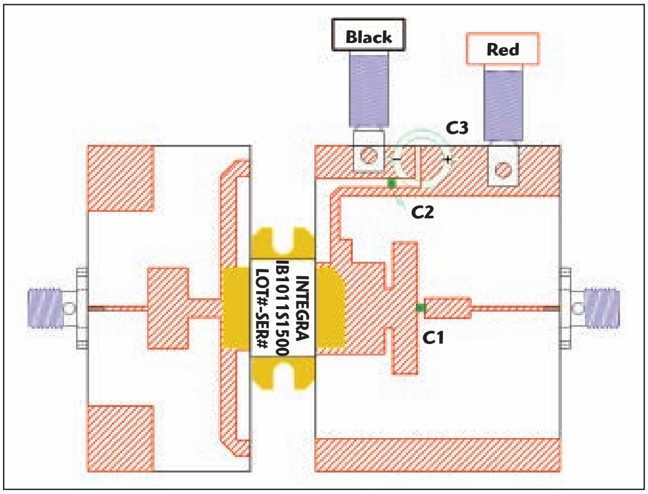

Fig. 3 Circuit for IB1011S1500 1.5 kW Si bipolar junction transistor for SSR applications.

SILICON LDMOS

Silicon LDMOS became the main technology for communications and basestations in the mid 1990s, and it has since become widely accepted for L-Band avionics and radar applications, not least because it can be manufactured in a standard 8" CMOS wafer fabrication facility resulting in lower cost than bipolar RF power transistors. Also, kW-level LDMOS transistors are readily available that can withstand a 20:1 VSWR mismatch and this leads to a further system-level cost reduction since the expensive isolator that needs to be added at the output of a bipolar transistor amplifier can be eliminated.

A 1 kW LDMOS transistor typically has about 10 dB more gain than the corresponding BJT device so fewer driver stages are needed leading to further cost and size reduction. 1 kW LDMOS transistors are available in both single-ended and push-pull formats. Single-ended versions have simpler, smaller and cheaper circuits than push-pull versions since no balun is needed.

While the above highlights the plus points of LDMOS, there are also a couple of negative features. Firstly, since LDMOS is always operated in Class A/B rather than the Class C used by BJTs, the efficiency of an LDMOS amplifier is typically 5 to 10 percent lower than is achieved with a bipolar-based transmitter, usually in the mid 50 percent range. It is worth examining why the efficiency is much lower than the theoretical 78.5 percent that an ideal Class B amplifier would have. Class A/B bias is used as a compromise between the best gain which occurs in Class A but which has the worst efficiency, and Class B which has the best efficiency but the lowest gain. This fact alone accounts for a few percentage points reduction in the maximum efficiency from 78.5 percent which would occur in an ideal class B amplifier without any waveform clipping.

However, it was mentioned earlier that the transistors in an SSR are typically operated about 2 dB into compression. This is very beneficial in terms of increasing the power output, if this didn't happen then to get 1 kW would require an even larger and more expensive transistor but,

as Cripps[6] has shown, this also gives rise to another small reduction in efficiency.

A 1 kW transistor operated from a 50 V supply requires that the current generator in the transistor sees a load resistance of $50^2/2*1000\ \Omega$ ($V^2_{rf}/2P_{out}\Omega$) if full voltage modulation occurs, i.e., the transistor has zero on-resistance or knee voltage. Thus the transistor needs to see a load of 1.25 Ω but the RF path from the plane of the current generator to the external 50 Ω load is bound to have some series resistance, even 0.1 Ω would cause the efficiency to be reduced to 90 percent of its theoretical maximum value, for example, the ideal Class B efficiency would fall to 70 percent maximum.

All of the above efficiency-reduction mechanisms apply equally well to both GaN and LDMOS, but the next issue is more of a problem for LDMOS than GaN. Real transistors always have a finite on-resistance or, equivalently, knee voltage. This prevents full voltage modulation from occurring and leads to a further efficiency reduction[7]. GaN HEMT devices have a lower on-resistance for the same output power than LDMOS, and so do not suffer from this efficiency reduction mechanism to the same extent. Taken together, it is easy to see why all these efficiency degradation mechanisms result in LDMOS 1 kW transistors operated in Class A/B have typical efficiencies in the low to mid 50 percent range regardless of whether they are push-pull or single-ended.

The obvious solution to achieve better efficiency is to use one of the very high efficiency modes such as Class E or F, but this is where LDMOS is at a distinct disadvantage compared with GaN. These high efficiency modes all involve non-sinusoidal waveforms which mean that the output matching circuit must present a specific impedance to the transistor not just at the fundamental frequency but at the harmonics as well. In the case of Class F it is required that the circuit presents a very high impedance to the transistor's internal current generator at odd-order harmonics and a short-circuit to even-order harmonics. Conversely, for Inverse Class F, a short-circuit to odd-order harmonics and an open-circuit to even-order harmonics is needed. However, the output capacitance of a 1 kW LDMOS transistor is so high that the harmonics are shorted to ground by the transistor's own internal capacitance so that it isn't possible to present the required high impedance needed for either Class F or Inverse Class F operation.

The second issue with LDMOS is that it has an inherent and unfortunate attribute, namely there is an unwanted parasitic bipolar transistor inside every LDMOS device. ***Figure 4*** shows where this is formed in an LDMOS device. Early LDMOS devices had a checkered start when first tested for high-power pulsed applications with devices failing. The problem was soon diagnosed[8] as being caused by latch-up of the parasitic bipolar transistor under fast rise and fall times associated with pulsed operation. Invariably, the drain bias to the transistor is applied via an inductor as shown in ***Figure 5***, but under fast rise and fall times a large enough voltage spike can be generated via L di/dt action to turn-on the parasitic bipolar transistor and cause device failure.

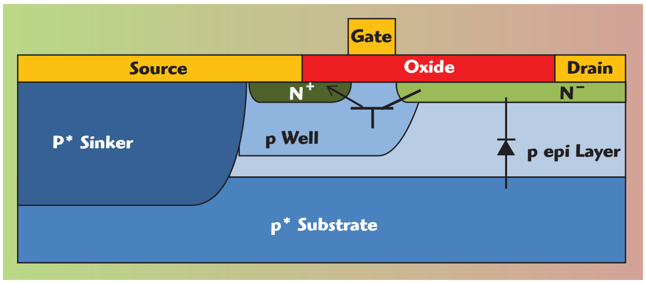

Fig. 4 Parasitic bipolar transistor inside every LDMOS device.

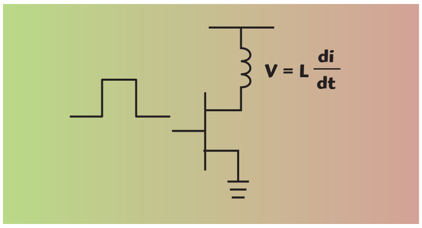

Fig. 5 The drain bias inductor creates a voltage spike under pulsed operation.

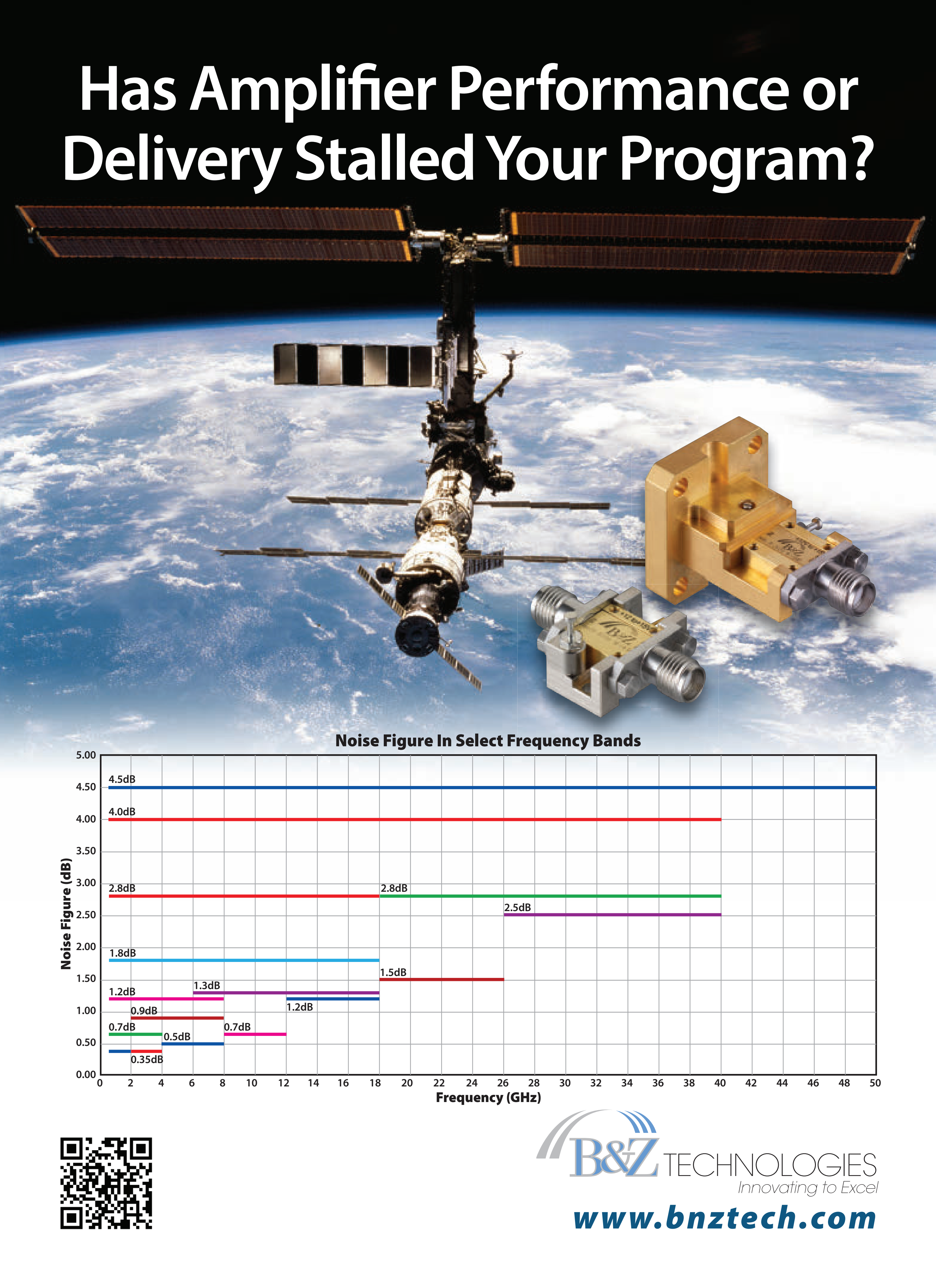
Has Amplifier Performance or
Delivery Stalled Your Program?
Noise Figure In Select Frequency Bands
Noise Figure (dB)
5.00
4.50
4.00
3.50
3.00
2.50
2.00
1.50
1.00
0.50
0.00
4.5dB
4.0dB
2.8dB
2.8dB
2.5dB
1.8dB
1.5dB
1.3dB
1.2dB
1.2dB
0.9dB
0.7dB
0.7dB
0.5dB
0.35dB
0 2 4 6 8 10 12 14 16 18 20 22 24 26 28 30 32 34 36 38 40 42 44 46 48 50
Frequency (GHz)
B&Z TECHNOLOGIES
Innovating to Excel
www.bnztech.com

The higher the power of the transistor, the higher is the value of the di/dt term and so high power transistors are more prone to this problem than low power devices. Manufacturers have devised proprietary methods of reducing this effect, but in truth these techniques merely suppress the problem rather than eliminate it. Device failures can still occur if the rise/fall time is fast enough.

GaN HEMT TRANSISTORS

GaN HEMT devices use SiC substrates rather than Si substrates which greatly add to their cost, and the much smaller wafer size (4" versus 8") exacerbates the cost issue still further. Although GaN devices are moving to 6" SiC substrates, there will still be a cost penalty for using GaN. However, there is a mitigating factor; GaN HEMT devices have a much higher power density than LDMOS and so the die size is a little smaller for a given output power — but nowhere near enough to fully compensate the smaller size and higher cost of the substrate. Consequently, GaN must offer substantial performance advantages compared with LDMOS to justify its use in this application, so what are these advantages?

Probably the single most significant advantage is the much lower capacitance per watt that GaN HEMTs offer compared with LDMOS. This much lower capacitance is a consequence of the much greater power density (capacitance is proportional to gate periphery so if the same power is achieved from a smaller periphery then you get lower capacitance). The greater power density of GaN is often cited as its greatest advantage, but this is a very debatable attribute. The high power density creates thermal problems, especially in CW applications, which is why the GaN epitaxial layer has to be grown on SiC substrates rather than Si for high power transistors since SiC has a four-fold higher thermal conductivity than Si.

Consequently, the higher power density attribute is actually a cost driver. However, the low capacitance per watt has several very desirable consequences. Firstly, it enables higher power transistors to be produced. In pulsed applications, the fundamental limit on how much power a transistor can deliver is not set by thermal limitations but on the ability of the output matching network to transform an ever-lower output impedance to 50 Ω. At first sight it might be thought that GaN HEMTs have no advantage over LDMOS in this regard since $R_L=V_{rf}^2/2P_{out}\Omega$ is identical for both types of transistor if operated from the same supply voltage — ignoring any difference in the maximum voltage modulation that each transistor can accommodate. However, all transistors have a finite output capacitance and this forms the first element in the output matching network. Hence the matching network external to the transistor has to transform not R_L to 50 Ω, but R_L in parallel with C_{ds} to 50 Ω. The bandwidth over which it is possible to match R_L in parallel with C_{ds} is limited by Fano's law[9], R_L becomes lower and C_{ds} becomes higher as the power output increases and so the usable

bandwidth of the transistor becomes smaller as the power increases.

The lower capacitance of GaN enables much higher power transistors to be produced than is possible with LDMOS, 1 kW devices[10] are already commercially available and 1.5 to 2 kW devices will shortly be released. In fact, the limit on the power output from GaN under pulsed conditions is set not by the impedance but on the availability of a suitable package to fit all the GaN die inside.

The low capacitance per watt also results in higher efficiency. It was mentioned in the LDMOS section that the high output capacitance of the device results in all harmonics being terminated in a short-circuit within the transistor die itself. This is just what one wants for Class B operation but not what is needed if you want to use one of the higher efficiency modes such as Class F. The recommended circuit for the device shown in ***Figure 6***, for example, presents a specific impedance to the transistor at the second harmonic to increase the efficiency.

The fact that the efficiency can be increased by altering the value of impedance at the second harmonic implies that the capacitance within the GaN chip is sufficiently low that the second harmonic is not being completely shorted within the die itself. Figure 6 shows a graph of gain and efficiency versus output power from which it can be seen that the typical efficiency during the pulse under Mode S ELM operation at 1 kW is 80 percent, about 25 percent higher than is achieved using LDMOS, and better even than is achieved with a Class C BJT. The 1 kW output power is achieved at 1 dB gain compression. A further advantage of GaN HEMTs over LDMOS is the lower on-resistance, or knee voltage if you prefer that terminology, which means that a larger voltage modulation can be obtained which directly aids the achievement of higher efficiency[7].

Finally, another aspect where GaN significantly differs from LDMOS is the ability to operate at voltages well in excess of 50 V where state-of-the-art avionics LDMOS technology operates. For instance, UHF GaN radar transistors have recently been reported[11] successfully operating at 125 V drain bias, and there is no particular reason why such capabilities could not be extended to IFF and SSR applications in L-Band. From the same equation it emerges that for the same load impedance R_L, increasing the supply voltage to 100 V would allow a four-fold power output increase under pulsed conditions or, alternatively, keeping the same output power would result in a four-fold reduction in the transistor gate periphery leading to smaller die that would fit in a smaller package; this translates to lower weight for airborne

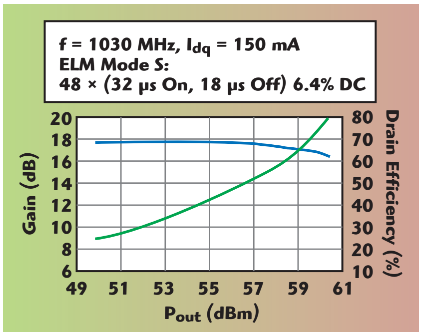

▲ *Fig. 6 Gain and efficiency with harmonic tuning for IGN1030L1000.*

systems. The higher impedance also facilitates harmonic tuning to boost efficiency even further.

The reason why GaN is better suited than LDMOS for operation in the 100 V range is that GaN fundamental physics material properties allow higher breakdown voltage without a significant increase of the on-resistance of the device, which is mostly controlled by the gate-drain spacing or drift region of the transistor.

CONCLUSION

The upgrade of ATC systems to be capable of operating under ELM mode has created the need for RF power transistors that can deliver >1 kW under almost CW conditions. BJT devices have been the dominant transistor technology for previous generations of ATC equipment but they are not the best technology for new equipment. LDMOS is the clear winner when it comes to cost, not just because they are the cheapest but also because the very high VSWR ruggedness that they offer enables the expensive protection isolator to be eliminated. However, they have the lowest efficiency of any of the three transistor technologies, and care needs to be taken to control the pulse rise/fall times to prevent transistor failure due to latch-up of their inherent parasitic BJT.

GaN HEMT devices have by far the highest efficiency but are more expensive than LDMOS, and current generations of 1 kW GaN do not have the same VSWR ruggedness as LDMOS, which means that the protection isolator cannot be eliminated. However, the VSWR issue can be fixed by improving the thermal design of the transistor. Finally, GaN offers the potential for offering much higher power than is possible with LDMOS by using higher supply voltages, and this will help overcome the cost disadvantage.

ACKNOWLEDGMENTS

The authors would like to acknowledge the contribution made by many other engineers at Integra without whom this article would not have been possible, in particular Gabriele Formicone and Jeff Burger. ■

References

1. https://en.wikipedia.org/wiki/Identification_friend_or_foe.
2. https://en.wikipedia.org/wiki/Secondary_surveillance_radar.
3. V.A. Orlando, "The Mode S Beacon Radar System," *The Lincoln laboratory Journal*, pp. 345–362, Vol. 2, No. 3, 1989.
4. http://www.integratech.com/ProductDoc.ashx?Id=135.
5. Daniel Koyama, Apet Barsegyan and John Walker, "Implications of Using kW-level GaN Transistors in Radar Systems," *IEEE COMCAS Conference*, Tel Aviv, Nov. 2–4, 2015.
6. S.C. Cripps, "RF Power Amplifiers for Wireless Communications," p. 142, *Artech House*.
7. S.C. Cripps, "RF Power Amplifiers for Wireless Communications," pp. 59–61, *Artech House*.
8. S.J.C.H. Theeuwen, J.A.M. de Boet, V.J. Bloem and W.J.A.M Sneijers, "LDMOS Ruggedness Reliability," *Microwave Journal*, April 2009.
9. H.W. Bode, "Network Analysis and Feedback Amplifier Design," Van Nostrand Reinhold.
10. http://www.integratech.com/ProductDoc.ashx?Id=1235.
11. G. F. Formicone and J. Custer, "Analysis of a GaN/SiC UHF Radar Amplifier for Operation at 125V Bias," *Proceedings of European Microwave Conference*, 6-11 September 2015, Paris, France.

Scan page using layar app

DefenseNews
Cliff Drubin, Associate Technical Editor

Global Electronic Attack (EA) Market Growing to $8.5B

RF-based Electronic Attack (EA) systems such as radar, communications and RCIED (radio controlled improvised explosive device) jammers will dominate the market for EA system spending, increasing to 70 percent of the total market in 2024. The North American region, and specifically the U.S., will drive spending on EA systems especially for airborne and shipborne EA systems and account for the largest end market over the entire forecast period. Land-based EA systems will represent the second largest market in dollar terms and dominate total shipments. The total number of EA system shipments is forecast to grow at a CAGR of 3.9 percent through 2024 to reach 10,844 units.

> The EA Market is forecast to grow at a CAGR of 3.9 percent through 2024.

"There will be an increasing emphasis towards systems that can support multi-band and/or wideband operation to combat the increasingly complex spectrum environment. Key drivers for growth will include the upgrading of capabilities by leveraging the advantages of wideband materials such as gallium nitride (GaN) and digital RF memory (DRFM) capabilities," notes Asif Anwar, director at Strategy Analytics. "The associated market for component technologies will grow from $457 million to almost $1.2 billion in 2024. While vacuum tube-based solutions will continue to dominate, programs such as the U.S.-based Next Generation Jammer (NGJ) and Surface Electronic Warfare Improvement Program (SEWIP) programs will contribute to the market for GaN becoming a staple ingredient in the makeup of future EA systems."

Capabilities Boeing, US Navy Enhance EA-18 Targeting, Situational Awareness

The U.S. Navy and Boeing recently demonstrated new targeting technologies that greatly enhance aircrew safety and effectiveness through the rapid integration and distribution of target information across multiple aircraft.

Utilizing an advanced targeting processor, an open architecture, high-bandwidth data link, and a Windows-based tablet integrated with the mission system, the demonstration proved that Boeing EA-18G Growler electronic attack aircraft can detect targets over longer distances and share information more rapidly than ever before.

"This enhanced targeting capability provides our aircrews with a significant advantage, especially in an increasingly dense threat environment where longer-range targeting is critical to the fight," said Capt. David Kindley, U.S. Navy F/A-18 and EA-18G program manager.

Naval aviation history was made during the Navy fleet experimentation campaign when data was integrated from multiple Growlers operating with an E-2 Hawkeye aircraft, utilizing the new high-bandwidth data link and increasing the speed and accuracy of target locating.

Use of the tablet device integrated with the aircraft mission system was another first for a Navy platform. That technology allowed aircrews to more easily access data and communicate with crews in other aircraft.

Existing Growlers will be retrofitted with the upgrades while the technology will be included as a standard offering on all new aircraft currently in production.

"The complexity of global threat environments continues to evolve," said Dan Gillian, Boeing F/A-18 and EA-18G programs vice president. "This long-range targeting technology is essential as we advance electronic attack capabilities for the conflicts of today and tomorrow."

The EA-18G Growler is derived from the combat-proven F/A-18F Super Hornet and is the United States' newest and most advanced airborne electronic attack platform, providing electronic intelligence, surveillance and reconnaissance data to other aircraft. The Growler has been deployed since 2010 supporting U.S. and allied forces.

EA-18 Growler (U.S. Navy Photo)

US Navy Accepts 4th MUOS Satellite for Secure Communications Network

VIEW VIDEO

Following the completion of successful on-orbit testing, on Nov. 30, the U.S. Navy accepted the fourth Lockheed Martin-built Mobile User Objective System (MUOS) satellite.

Launched Sept. 2, MUOS-4 is the latest addition to a network of orbiting satellites and relay ground stations that is revolutionizing secure communications for mobile military forces. Users with operational MUOS terminals can seamlessly connect beyond line-of-sight around the world and into the Global Information Grid. MUOS' new commercial, cellular-based capabilities include simultaneous, crystal-clear voice, video and mission data, over a secure high-speed Internet Protocol-based system.

"MUOS-4 completes the initial constellation, providing the MUOS network with nearly global coverage. Mo-

For More Information Visit mwjournal.com for more defense news

> "MUOS-4 completes the initial constellation, providing the MUOS network with nearly global coverage..."

bile forces, equipped with MUOS terminals, will soon be able to communicate with each other – including voice, data and exchanging imagery – real-time, virtually anywhere on the Earth," said Iris Bombelyn, Lockheed Martin's vice president for Narrowband Communications. "This is a tremendous upgrade in communications capabilities over what currently exists for our nation and our allies."

MUOS-4 will be relocated in Spring 2016 to its on-orbit operational slot in preparation for operational acceptance. The satellite joins MUOS-1, MUOS-2 and MUOS-3, launched respectively in 2012, 2013 and January 2015, and four required MUOS ground stations. MUOS-5, an on-orbit spare, also will be launched next year.

Once fully operational, the MUOS network will provide 16 times the capacity of the legacy ultra high frequency communications satellite system, which it will continue to support, and eventually replace. More than 55,000 currently fielded radio terminals can be upgraded to be MUOS-compatible, with many of them requiring just a software upgrade.

LM Conducts Collaborative Unmanned Systems Demo

Lockheed Martin demonstrated its ability to integrate unmanned aircraft system (UAS) operations into the National Airspace System (NAS) using its prototype UAS Traffic Management (UTM) capabilities. During the demonstration on Nov. 18, the Stalker XE UAS provided data and a precise geolocation to the unmanned K-MAX cargo helicopter, which conducted water drops to extinguish a fire, while the UTM tracked the UAS operations and communicated with Air Traffic Control in real time.

"This demonstration represents the path forward for flying UAS in the NAS using Flight Service-based UTM capabilities to extend the technology and systems that air traffic controllers know and understand," said Paul Engola, vice president, Transportation & Financial Solutions. "We were able to successfully modify the existing K-MAX and Stalker XE ground control software to connect to the UTM services and conduct the firefighting mission."

The Stalker XE UAS worked in tandem with K-MAX to identify hot spots and fire intensity with its electro-optical, infrared camera. Its stable, high definition imaging capabilities enable day and night operations. Powered by a ruggedized solid oxide fuel cell, Stalker XE achieves more than eight hours of flight endurance.

Reactel, Incorporated

Reacting First to All Your Filter Needs.

A Sheer Descent into the Noise

High Performance Notch Filters

- High Q
- Bandwidths as low as 0.5%
- Frequency range up to 20 GHz
- Power levels up to 1000 W

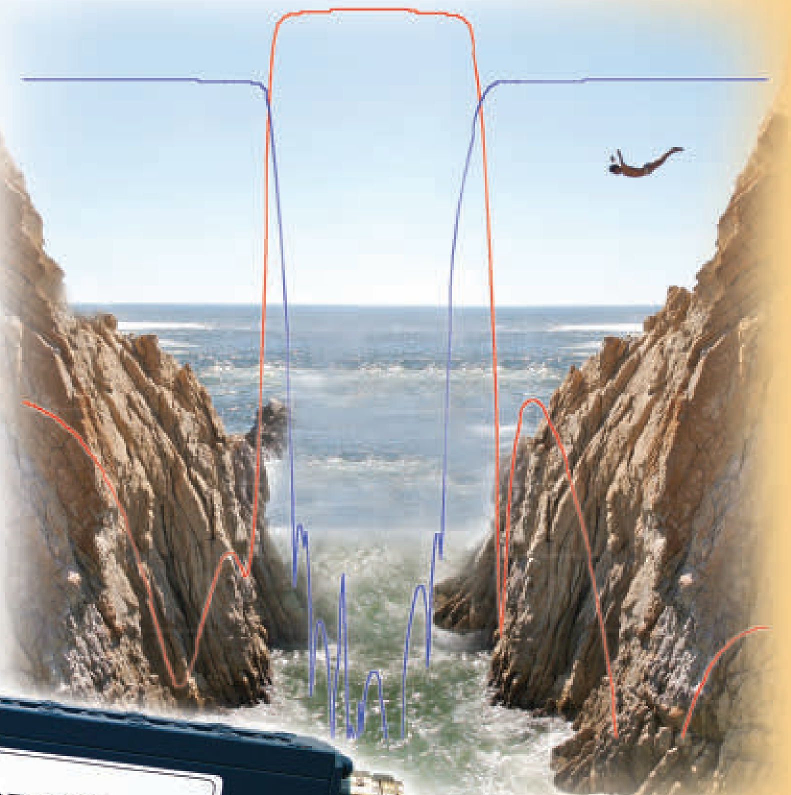

Reactel manufactures a variety of notch filters suitable for most any application.Utilizing Discrete Component, Ceramic, Cavity, Wavegiude or Microstrip technologies, we can create a unit which has extremely low pass band loss, contain up to 16 sections, and can have connectors or surface mount launch options. Contact us with you requirement and let us show you how sharp our notch filters can be.

- Submitting a request for immediate attention will never be easier.
- Full featured App contains expanded RFQ capability, catalog, data sheets and more.
- Available for iPad, iPod and Android devices via the App Store and Google Play.

Available on the App Store

Google play

8031 Cessna Avenue • Gaithersburg, Maryland 20879 • Phone: (301) 519-3660 • Fax: (301) 519-2447
For general inquiries, please email reactel@reactel.com • http://twitter.com/reacteljim • Go online to www.reactel.com to download your Reactel catalog today.

Intertek

RoHS Compliant

@reacteljim

ITU Approves Spectrum for Automotive Radar

At the International Telecommunication Union (ITU) World Radiocommunication Conference (WRC-15) the decision was made that the radio frequency spectrum needed for the operation of short-range high-resolution automotive radar be allocated in the 79 GHz frequency band. The allocation of the 79 GHz frequency band provides a globally harmonized regulatory framework for automotive radar to prevent collisions, which will improve vehicular safety and reduce traffic accidents.

ITU is a partner with the World Health Organization (WHO) on the UN's Road Safety Collaboration and according to UN data, more than 1.25 million fatalities occur each year on the roads around the world. The allocation of the frequency band for automotive radar responds to the call by the United Nations General Assembly and will facilitate the development of one of the most significant technologies in support of this global need.

"...improve road safety worldwide and prevent traffic-related fatalities."

"The decision to harmonize the 79 GHz frequency band for automotive radar will allow the automotive industry to deploy anti-collision radar devices globally," said ITU Secretary-General Houlin Zhao. "This will contribute a great deal towards the UN goal to improve road safety worldwide and prevent traffic-related fatalities."

The decision at WRC-15 culminates extensive studies on the spectrum requirement as well as sharing with incumbent radiocommunication services in the same frequency band. The next "Future Networked Car" is scheduled to take place on 3 March 2016.

IoTUK Announces Boost Partners

IoTUK, a national programme designed to amplify the UK's Internet of Things (IoT) capability and opportunities, has announced the four winning partners for its IoTUK Boost initiative. The IoTUK Boost programme aims to support IoT innovation and adoption across businesses and the public sector, delivering a series of local open innovation challenges and rapid incubation activities across the UK.

The partners selected are Scottish based CENSIS; DataCity – Leeds in Partnership with ODI Leeds & DigicatYorks; Cambridge Wireless Ltd. (CW), which will run the Boost programme in both Bristol and Guildford; and Sunderland Software City, which operates in the North East of England.

"The Internet of Things has the potential to transform businesses and public sector organisations across the UK, as well as drive economic growth and social change. No individual, company or government can do this alone; it can only be achieved through collaboration and bringing together innovators with challenge owners, and it has to especially be achieved at the local level, leveraging the wealth and diversity of talent across the UK. The IoTUK Boost programme will do just this, a coordinated acceleration programme in the IoT across regions to grow new business opportunities in IoT in, and for, the UK," said Maurizio Pilu, executive director for Collaborative R&D, Digital Catapult.

Each Boost partner will bring together up to 20 SMEs with challenge owners such as large companies or local authorities. The support will culminate in a two-day workshop and innovation contest, with winners gaining access to business, technical and mentoring support from the IoTUK team.

"...grow new business opportunities in IoT..."

SEQUOIA Project Reports Advances in PICs

Advances in silicon photonics have been reported by the SEQUOIA project, which runs until September 2016. The project targets the heterogeneous integration of novel III-V materials – quantum dot (Qdot) and quantum dash-based (Qdash) materials – on silicon wafers through wafer bonding, with the ultimate goal of developing and demonstrating transmitters having a total capacity of 400 Gbps (16 × 25 Gbps).

To enable such advance, the consortium is betting on two elements: first, thanks to the properties of their III-V materials, SEQUOIA's hybrid III-V lasers are expected to result in better thermal stability, higher modulation bandwidth and the possibility of generating a flat wavelength-division-multiplexing comb. Then, by integrating these materials with silicon, the team expects to combine their respective advantages: optical filters can be directly integrated with hybrid quantum dot/quantum dash/silicon lasers to create chirp-managed lasers, boasting an enhanced modulation bandwidth and extinction ratio compared to directly modulated lasers.

...better performance at reduced cost...

Project coordinator III V Lab in France recently announced that the two final Photonics Integrated Circuits (PICs) demonstrators have successfully been designed: chirp-managed lasers (CML) directly modulated at 25 Gbps and comb laser integrated with cascaded ring resonator modulators. These PICs, which provide the desired capacity of 400 Gbps through the use of 16 WDM channels, promise better performance at reduced cost as well as enhanced functionality through the use of SEQUOIA's III-V materials and novel integration processes.

For More Information Visit mwjournal.com for more international news

III V Lab also reports that the quality of Qdot/Qdash materials has been significantly improved during the first period of SEQUOIA, whilst the University of Kassel has recently demonstrated Qdot lasers with a record 34Gbps bit rate in direct modulation. In parallel, Qdot wafers have been successfully bonded onto silicon wafers.

European Commission Invests €16B in Research and Innovation

The European Commission will invest almost €16 billion in research and innovation in the next two years under Horizon 2020, the EU's research and innovation funding scheme, following a new Work Programme for 2016-17. The new funding opportunities offered by the Work Programme are directly aligned with the policy priorities of the Commission of President Jean-Claude Juncker, including building stronger industry and making Europe a stronger global player.

Carlos Moedas, commissioner for Research, Science and Innovation said, "Research and innovation are the engines of Europe's progress and vital to addressing today's new pressing challenges like immigration, climate change, clean energy and healthy societies. Over the next two years, €16 billion from Horizon 2020 will support Europe's top scientific efforts, making the difference to citizens' lives."

Horizon 2020 will be open to innovation, open to science, and open to the world. The new Work Programme 2016-17 offers funding opportunities through a range of calls for proposals, public procurements and other actions like the Horizon Prizes, together covering nearly 600 topics. The programme's structure is a reflection of the overall flexibility of Horizon 2020 which focuses on the EU's long-term priorities and the most pressing societal challenges while allowing it to swiftly address emerging problems such as outbreaks of diseases.

The programme will support a range of cross-cutting initiatives: the modernisation of Europe's manufacturing industry (€1 billion); technologies and standards for automatic driving (over €100 million); the Internet of Things (€139 million) to address digitalisation of EU industries; Industry 2020 in the Circular Economy (€670 million) to develop strong and sustainable economies; and Smart and Sustainable Cities (€232 million) to better integrate environmental, transport, energy and digital networks in EU's urban environments.

The new Work Programme is also set on improving the impact of Horizon 2020 funding. First, it will ensure more money is available for innovative companies thanks to new leveraging opportunities supported by the European Fund for Strategic Investments (EFSI), in addition to over €740 million dedicated to support research and innovation activities in nearly 2000 small and medium enterprises (SME).

Echodyne Brings First Metamaterials Based Radar Antenna to Market

Echodyne Corp. recently announced limited availability of its first metamaterials electronically scanning array (MESA) for radar applications. Echodyne's MESA makes high performance radar far easier to deploy by lowering both the cost and weight by up to 10 or more times while decreasing the size of the antenna by up to 5 or more times over traditional electronically scanned arrays. The first product from Echodyne, a metamaterials electronically scanning array for X-Band (MESA X-EVU) is now available for partners and integrators interested in evaluating MESA for radar systems in a variety of commercial markets including maritime, aviation, and surveillance/security among others.

"We are very pleased with the early reception of MESA-X-EVU by key partners and are excited to be able to offer more units to qualified partners and integrators," said Eben Frankenberg, founder and CEO of Echodyne. "Metamaterials based radar has the opportunity to not only change how traditional, heavy, expensive radar systems are deployed but can open up new markets for advanced radar that were never before thought possible because of the cost, size and weight of traditional electronically scanned arrays."

Echodyne's MESA X-EVU combines ultra-low C-SWAP (cost, size, weight and power) with ultra-fast beam steering (sub-microsecond) in an electronically scanning array that can be integrated into new or existing radar systems.

Unlike conventional mechanical apertures which steer a radar beam using motorized gimbals, Echodyne's MESA requires no moving parts to steer its beam. And unlike Phased Array radars or Active Electronically Scanning Array (AESA) radars that use complicated, expensive, and inefficient transmit/receive modules which include phase shifters, amplifiers, circulators, and low noise amplifiers behind every single antenna element, MESA uses a vastly simpler metamaterials architecture. The net effect of this simplified architecture is dramatically lower cost, size, weight and power.

Echodyne's MESA-X-EVU operates at X-Band and has a broad field of view (±50° in azimuth and ±45° in elevation) which it can scan very rapidly given its sub-microsecond beam switching speed. The MESA-X-EVU subsystem includes the metamaterial array, the array control driver circuitry, and the beam steering computer. Fully assembled without packaging, the subsystem is a mere 50 × 18 × 2.5 cm with a total weight of only 1.4 kg. While this size and weight already demonstrates a vast improvement over traditional electronically scanning arrays, Echodyne will be decreasing this even further as the company optimizes the technology for various implementations. The aperture is controlled through a simple USB 2.0 interface and requires only a single +12 DC source to operate. Integrators and radar manufacturers interested in evaluating MESA-X-EVU can connect their own Pulsed or FMCW transceivers through a single coax SMA port.

Echodyne has produced a limited number of MESA-X-EVU to share with qualified partners and integrators.

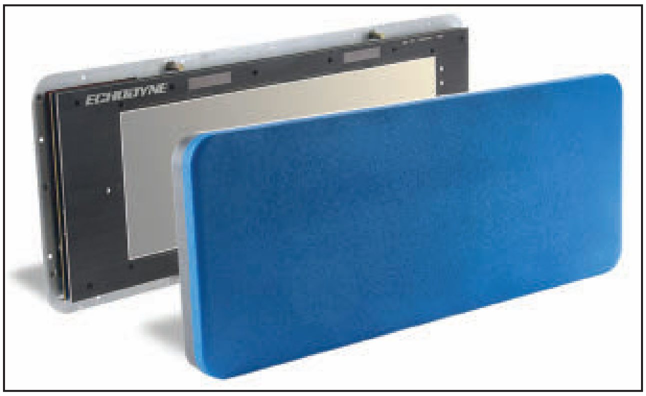

Echodyne X-Band (Source: Echodyne)

Small Cells Surge as Mobile Network Operators Densify Networks

"Many mobile network operators around the world, including Verizon, Sprint, China Mobile and Vodafone, among others, are now investing in network densification," says Nick Marshall, research director at ABI Research. "The results of this can be seen in the ramp of small cells this year. As many networks shift from coverage-centric to capacity-focused, MNOs are finding that small cells are an effective way to boost network capacity in high traffic areas."

In 2015, the challenges of backhaul, power, permitting and siting, which previously stalled small cell rollout, are being overcome with Small Cells as a Service (SCaaS) from vendors and infrastructure owners, including Alcatel-Lucent, American Tower, Crown Castle, Ericsson, Nokia Networks and Towerstream. Several of these companies are reporting in earnings calls that small cell-related revenue is growing strongly quarter-on-quarter.

> "...small cells are an effective way to boost network capacity in high traffic areas."

Additionally, 2015 marks 4G small cells as the fastest growing small cell type in the market driven by venue and dense urban deployments. ABI Research forecasts the number of LTE small cells to double in 2015 and by a similar factor each subsequent year. In 2020, the value of LTE small cells will represent more than 85 percent of the small cell equipment market.

The Asia-Pacific region, given its large size and 4G deployments in South Korea and Japan, as well as the start of commercial TD-LTE operations in China and India, will grow to represent almost 50 percent of the worldwide small cell equipment market by 2017.

For More Information Visit mwjournal.com for more commercial market news

Global Commercial Building Automation Market Revenues Will Reach $45B by 2021

The building automation market will experience steady but incremental growth over the next five years, generating $45 billion in 2021. Europe will be the biggest market in terms of revenues followed by North America and Asia Pacific in 2021. The big four building automation OEMs, namely Honeywell, Schneider Electric, Johnson Controls and Siemens, have more than 60 percent market share and a strong influence in the market. Holding back adoption is the slow return on investment for building owners due to the high costs of installing building automation systems.

Office buildings are projected to be the biggest verticals in the forecast period followed by retail and public assembly buildings. Among the other verticals, hospitality and healthcare are expected to witness rapid growth from 2016 to 2021. In hospitality, the short refurbishment cycles in hotels are becoming a lucrative market for solution providers to upgrade or replace existing systems with more intelligent systems to improve the overall customer experience. In healthcare, increasing regulatory and compliance requirements are driving the use of connected medical devices to improve auditability in the use of high value moveable assets and to control environments to improve patient comfort.

"The Internet of Things and its adoption in consumer markets has a noticeable impact in a traditionally conservative industry with distributed intelligence and cloud-based analytics gaining acceptance," says Adarsh Krishnan, senior analyst at ABI Research.

As the market continues to witness a gradual shift towards more integrated solutions, there is wider acceptance for interoperable systems that foster innovative applications to optimize building environment. This further allows for potential integration of building automation systems with utility deployed smart meters to gain greater insight into energy and water consumption in buildings in order to efficiently manage resources.

Wired field equipment accounts for the majority of commercial building connections in 2015, but wireless is gaining traction for connecting wireless field devices. Wired connectivity solutions adhere to the high Quality of Service (QoS) requirements for applications, such as security, fire and life safety applications that are critical requirements mandated by regulatory compliance. Applications such as lighting and HVAC are increasing their use of wireless technologies accounting for 19 percent and 21 percent of the annual field equipment shipped in 2021.

RF-LAMBDA
THE POWER BEYOND EXPECTATIONS
ITAR & ISO9000
Registered Manufacture
Made in USA
ITAR
LEADER OF RF
BROADBAND SOLUTION
ULTRA BROADBAND
LOW NOISE AMPLIFIER
R50G69GSC
(50-69GHZ LNA)
RLNA00M50GA
(0.01-50GHZ LNA)
ULTRA BROADBAND
POWER AMPLIFIER
RFLUPA01G22GA
(1-22GHZ 8W)
RFLUPA0618GC
(6-18GHZ 25W)
RFLUPA32G38GB
(32-38GHZ 10W)
RFLUPA0706GF
(0.7-6.0GHZ 35W)
BROADBAND RF
SYSTEM AC AMPLIFIER
RAMP27G34GA
(27-34GHZ 10W)
RAMP02G06GB
(2-6GHZ 50W)
www.rflambda.com
sales@rflambda.com
1-888-976-8880
1-972-767-5998
Plano, TX, US
San Diego, CA, US
Ottawa, ONT, Canada

Around the **Circuit**

Barbara Walsh, Multimedia Staff Editor

MERGERS & ACQUISITIONS

Microsemi Corp. has entered a definitive agreement to acquire **PMC-Sierra Inc.** for $2.5 billion – $9.22 in cash and 0.0771 of a share of Microsemi common stock for each share of PMC common stock through an exchange offer. This represents a 77.4 percent premium to the closing price of PMC's stock as of Sept. 30, 2015. This acquisition will provide Microsemi with a leading position in high performance and scalable storage solutions, while also adding a complementary portfolio of high-value communications products. As they integrate the team and drive profitability, the combined company will benefit from increased scale, industry-leading margins, diversified market exposure, consolidated infrastructure and substantial cost savings.

Remtec Inc., a manufacturer of ceramic substrates, packages and submounts using PCTF (plated copper on thick film) metallization, has been acquired by **LTI**, a major player in the field of precision glass-to-metal seals and glass-to-metal hermetic packages. LTI manufactures glass-to-metal seal hermetic packages, high reliability precision quartz crystal holders and specialized solutions for aerospace, defense, telecommunications, medical, automotive and sensor applications. LTI is a RoHS and ISO compliant and ITAR registered company located in Mission, Kan.

NXP Semiconductors N.V. and **Freescale Semiconductor Ltd.** announced the completion of the merger pursuant to the terms of the previously announced merger agreement from March 2015. The merger has created a high performance mixed signal semiconductor industry leader, with combined revenue of over $10 billion. The merged entity will continue operations as NXP Semiconductors N.V. and has become the market leader in automotive semiconductor solutions and in general purpose microcontroller (MCU) products.

Silicon Labs announced the acquisition of **Telegesis**, a ZigBee expert with strong momentum in the smart energy market, providing ZigBee module solutions to many of the world's top smart metering manufacturers. The company was privately held, founded in 1998 and based near London. This strategic acquisition accelerates Silicon Labs roadmap for ZigBee and Thread-ready modules and enhances the company's ability to support customer needs with comprehensive mesh networking solutions ranging from wireless system-on-chip (SoC) devices to plug-and-play modules backed by best-in-class 802.15.4 software stacks and development tools. Telegesis modules integrate the antenna and provide a pre-certified RF design that reduces certification costs, compliance efforts and time to market.

UTC Aerospace Systems has acquired **N2 Imaging Systems LLC** of Irvine, Calif. The acquisition will complement the UTC Aerospace Systems' intelligence, surveillance and reconnaissance business and add new technology to the company's extensive portfolio of capabilities supporting the U.S. Military across the full spectrum of global strategic, operational and tactical operations. UTC Aerospace Systems is a unit of United Technologies Corp. UTC Aerospace Systems' commitment to the U.S. Army's Reconnaissance, Surveillance and Target Acquisition (RSTA) mission is enhanced by the acquisition, ensuring the company's capabilities continue to support the Army's strategic equipping plans.

COLLABORATIONS

NI and **Astronics Test Systems Inc.**, a wholly owned subsidiary of **Astronics Corp.**, announced their collaborative efforts to deliver PXI-based products designed for the aerospace and defense community. The combination of Astronics' strength in test system integration and NI's leadership in PXI-based automated test systems is expected to produce a best-in-class portfolio for automated test equipment (ATE) applications. The first product to be delivered as a result of the collaboration is the Astronics Frequency Time Interval Counter (FTIC) for PXI Express, modeled after the Astronics VXIbus 200 MHz Universal Counter. Designed for full TPS compatibility, the instrument can replace existing VXI-based FTICs and deliver the same capability in a newer PXI-based subsystem.

Ericsson and **Cisco** – two industry leaders in the development and delivery of networking, mobility, and cloud – announced a global business and technology partnership to create the networks of the future. In a world driven by mobility, cloud, and digitization, the networks of the future will require new design principles to ensure they are agile, autonomous, and highly secure. Ericsson and Cisco will meet this challenge together by offering end-to-end leadership across network architectures including 5G, cloud, IP, and the Internet of Things – from devices and sensors to access and core networks to the enterprise IT cloud.

Pasternack Enterprises Inc., a provider of RF, microwave and millimeter wave products, has partnered with **Besser Associates** to offer customers a seamless portal for accessing continuing education courses in the fields of RF, microwave and millimeter wave technologies. As a leading provider of RF and microwave products as well as being a hub for RF technical resources, Pasternack is exposing tens of thousands of new users to the value and capabilities supplied by Besser's continuing education. All training courses are performed either in-person or on demand by Besser Associates.

Anokiwave Inc., an innovative company providing highly integrated core IC solutions for mmW and AESA markets, and **ATE Systems**, a technology innovator and premier developer of mmW test systems, announced the development of a multi-port mmW test station for characterization of Anokiwave's portfolio of Silicon Core IC solutions. Anokiwave selected ATE Systems to develop this unique test capability that features fully automated calibration for

For More Information

For up-to-date news briefs, visit mwjournal.com

scalar power, S-parameter, and noise figure measurements for devices having up to 14 RF ports over temperature, as a solution to the complex test requirements of the highly integrated, multi-function ICs.

Huawei has announced the world's first successful large-scale field trial of 5G new radio access technologies. The field trial was conducted jointly with **NTT DOCOMO Inc.**, Japan's largest mobile service provider. Experts from both companies participated in the field trial in an outdoor test site in Chengdu, China. As an on-going field trial, Huawei was able to stream live video of trial activity to its booth at the CEATEC JAPAN 2015 trade show at Makuhari Messe in Chiba.

CableLabs, a non-profit R&D consortium dedicated to the development of innovative technologies that significantly impact its cable operator members' businesses, is committed to increasing the quality and security of Wi-Fi enabled devices to meet the growing needs of cable operators around the world. For over-the-air (OTA) device testing and compliance, CableLabs has invested in the **Rohde & Schwarz** TS8991 WPTC system that provides its members and device manufacturers with CTIA compliance and validation to ensure that Wi-Fi enabled devices are network ready.

Ducommun Inc. announced an agreement to manufacture private label RF products for **Pasternack Enterprises Inc.** The agreement makes Ducommun's RF products available under the Pasternack brand to customers with 24/7, online purchasing and same-day shipping. Ducommun will provide Pasternack a range of RF products.

Modelithics and **ANSYS** have collaborated under the Modelithics Vendor Partner (MVP) program to make the advanced, substrate scalable, high accuracy parasitic models from Modelithics compatible with the latest version of ANSYS Electronics Desktop and ANSYS® HFSS™ electromagnetic (EM) simulation software. The Modelithics® CLR Library for ANSYS HFSS has just been released and contains over 270 resistor, inductor and capacitor (RLC) component families as Microwave Global Models™. These models represent nearly 9,000 RLC components from the leading vendors. Modelithics models are measurement-based equivalent circuit models that accurately predict substrate and pad parasitic effects on surface mount components over frequency.

NEW STARTS

Ampleon announced the formation of its global business operations following the successful acquisition of the RF Power business line by **Jianguang Asset Management Co. Ltd. (JAC Capital)** from **NXP Semiconductors**. With immediate effect Ampleon takes responsibility for the entire RF Power business activity, including sales and support of the complete line-up of LDMOS and GaN RF power products. With 1,250 employees across 16 engineering, sales and manufacturing facilities worldwide, Ampleon is headquartered in Nijmegen and is founded with 50+ years of product innovation and engineering excellence.

Keysight Technologies Inc. announced a new organizational structure designed to align the company's activities with the development of customer solutions. The organizational changes include the creation of a centralized Corporate Planning and Technology team, and a move to three customer-focused business groups – the Communications Solutions Group, the Industrial Solutions Group and the Services Solutions Group.

ACHIEVEMENTS

Skyworks Solutions Inc. announced that it received the 2015 National Export Award (PNE) from Mexico. The PNE is one of four national awards given by Mexico's federal government recognizing companies, educational institutions and organizations whose efforts have contributed to strengthening Mexico's competitiveness in international markets. Specifically, Skyworks was recognized for being a role model of innovation and efficiency in delivering high value products to global markets. This is the third consecutive award for Skyworks from Mexico's federal government.

Anritsu Co. announced that its ME7834L Mobile Terminal Test Platform has been certified by Softbank as an approved test system for its mobile terminals. With the certification, the ME7834L supports all Softbank-approved communications protocol tests at test houses. The ME7834L is a world-leading test system with 100% verification. The ME7834L supports both the GCF requirements, as well as Softbank's in-house protocol tests, enabling certification tests of LTE/UMTS smartphones, tablets, Wi-Fi routers, and other products delivered to Softbank. Acceptance tests at test houses are required to verify interoperability between mobile terminals and Softbank's network.

The new test package from **Rohde & Schwarz** operates on the R&S CMW500 wideband radio communication tester, which has been selected by SoftBank for conducting interoperability and validation tests. The test package is a comprehensive solution customized for the internal certification labs of wireless device and chipset manufacturers, as well as for test houses. It carries out RF, protocol, and RRM interoperability tests between products developed by different manufacturers and the 3G and 4G networks provided by SoftBank. The departments at SoftBank that develop the company's own unique products also use this test solution.

Copper Mountain Technologies recently received a Frost & Sullivan Global Best Practices Award. On October 22, Copper Mountain Technologies team joined 25 other recipients of Frost & Sullivan 2015 Excellence in Best Practices Awards at a ceremony in Monaco. The Best Practices Awards are presented each year to companies that are predicted to encourage significant growth in their industries, have identified emerging trends before they became the standard in the marketplace, and have created advanced technologies that will catalyze and transform industries in the near future.

Anritsu and **EMITE** announced that the Anritsu MT8821C Radio Communication Tester has been successfully used in combination to the EMITE E500 Reverberation Chamber

and the Anite Propsim channel emulator to test 3CC and 4CC LTE Carrier Aggregation, using 2×2 MIMO for each carrier and more realistic isotropic Urban-Macro (UMA) fading profiles. The tests were performed for a leading U.S. carrier. The MT8821C Radio Communication Analyzer is designed for R&D of mobile devices/user equipment (UE), such as smartphones, tablets and M2M modules. It builds on the technologies of its popular predecessor, the MT8820C, preferred by UE and chipset vendors worldwide.

Semtech Corp., a supplier of analog and mixed-signal semiconductors, announced its LoRa® wireless RF technology has been selected by České Radiokomunikace (ČRa) as the RF platform for the Company's first Internet of Things (IoT)-based pilot program. Working with network partners RWE GasNet and Softlink, ČRa has developed a LoRa-based solution that was tested in the spring of 2015 and has now been launched in select markets. The tests demonstrated the long reach, low power consumption and low operational costs of the LoRa technology. They also exhibited the signal quality and reach to both outside and inside facilities, which is a key parameter for smart metering.

CONTRACTS

Cobham recently received a series of orders from a leading missile manufacturer for electronic components for several missile programs totaling $157.5 million. The work will be performed by Cobham Microelectronic Solutions, a business unit of the Cobham Advanced Electronics Solutions sector. Cobham is a key supplier of RF electronics that enable a missile's guidance and processing. Cobham hardware spans RF converters, synthesizers, and transmitters, otherwise known as Integrated Microwave Assemblies (IMA). The building blocks of these IMAs are based on Cobham's innovative intellectual property for mixers, filters, and custom Monolithic Microwave Integrated Circuits (MMIC).

Harris Corp. has received a four-year, $113 million contract from the **U.S. Naval Sea Systems Command** (NAVSEA) to upgrade the Navy's primary long-range, three-dimensional defense radar. The contract includes an initial $39 million order and three one-year options. The contract was received in the first quarter of Harris' fiscal 2016. Harris was awarded the contract under the Navy's Radar Obsolescence and Availability Recovery (ROAR) program to upgrade AN/SPS-48E radars to the more advanced SPS-48G version, which uses a modern solid-state transmitter. This approach increases fleet readiness to address emerging threats, while lowering the Navy's total cost of radar ownership.

The **U.S. Marine Corps** has awarded **BAE Systems'** team a contract worth $103.7 million for the Engineering, Manufacturing, and Development (EMD) phase of the Amphibious Combat Vehicle (ACV) 1.1 program. The company, along with teammate IVECO Defence Vehicles, will deliver a solution that will be built from the ground up to be an amphibious vehicle and will provide significant ca-

pability improvements to satisfy the Marine Corps' current and future needs. The award is one of two EMD contracts issued. During this phase, BAE Systems will produce 16 prototypes that will be tested by the Marine Corps beginning in the third quarter of 2016.

Mercury Systems Inc. announced that its Mercury Defense Systems (MDS) subsidiary was awarded a firm-fixed-price, indefinite delivery/indefinite quantity (IDIQ) time and material contract worth up to $41.8 million to deliver 200 advanced miniaturized Digital RF Memory modulators (Mini DRFM) to the **U.S. Navy**. The contract was received in the company's fiscal 2016 second quarter. Work will be performed at the company's Cypress, Calif. facility and is expected to be completed in November 2020.

The Econco Division of **Communications & Power Industries LLC (CPI)** has been awarded a $9.7 million sole-source multiyear contract for the production of new power grid devices to support the **U.S. Navy**'s Aegis radar systems. The two-year, firm fixed-price contract was awarded by the U.S. Defense Logistics Agency Land and Maritime in Mechanicsburg, Pa. Work on the contract will be completed in Woodland, Calif. CPI Econco Division has previously provided rebuilt power grid devices for Aegis radar systems and has twice been awarded the U.S. Navy Aegis Excellence Award for Outstanding Performance on the program.

Comtech Telecommunications Corp. announced that its Santa Clara, Calif.-based subsidiary, **Comtech Xicom Technology Inc.**, has received production contract for more than $3.2 million from a U.S. military integrator to supply high-power traveling wave tube amplifiers (TWTA). This is the first installment of a multi-year program for tactical military transportable satellite terminals.

Rice University researchers have won $2.4 million from the **National Science Foundation** (NSF) to conduct the most extensive experimental research yet of wireless technology that uses 100 or more antennas per base station to send tightly focused beams of data to each user, even as they move. The research at Rice's campus in Houston will help the wireless industry determine whether and how to include the many-antenna technology – known in industry parlance as "massive multi-user, multi-input multi-output," or massive MU-MIMO – in upcoming 5G wireless standards.

Antenna Systems Solutions S.L. (Celestia Technologies Group), a provider of antenna measurement solutions for the defence, government and wireless industries, announced that it has won a contract to supply a turnkey antenna measurement system to **Orange Labs** in France. The range will be installed on the premises of the Laboratoire d'Electronique, Antennes et Télécommunications at the University of Nice Sophia Antipolis. Staff from Orange will be able to make measurements from 600 MHz up to 110 GHz with a range of techniques (far field/spherical near field).

We'll help you do the math.
TRM Quality
TRM Resources
+ TRM Experience
YOUR Success
Air
Sea
Land
Space
Dividers
Couplers
TR Switches
Beamformers
Quads & Hybrids
Harmonic Filters
TRM
MICROWAVE
COMPLETING YOUR IDEAS®
Custom Passive RF Components Since 1970.
info@TRMMicrowave.com
A Woman-Owned Small Business
Apps Engineering Support Line 888.677.6877

Around the **Circuit**

PEOPLE

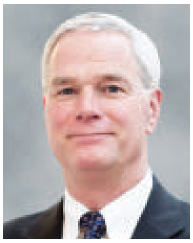
▲ *William W. Boecke*

Anokiwave Inc. announced the latest addition to its leadership team with the appointment of **William W. Boecke** to the position of chief financial officer. Boecke joined Anokiwave in October 2015 and working with the executive management team will insure the company continues to grow on a strong financial foundation. He will promote the creation of value with the development of their technology and will manage their financial and other business risks. This enables Anokiwave to continue to expand, capitalizing on the growing worldwide demand for next generation mmW solutions.

Anritsu Co. announced the appointment of **Paul Innis** as vice president and general manager of the Americas Sales Region. Innis will use his extensive experience to successfully position Anritsu Co.'s wide portfolio of product and services into the telecommunications, general industry and government markets, as well as into emerging industries, such as Connected Car and the rapidly growing Internet of Things (IoT). As vice president and general manager, Innis will be responsible for direct management of all sales, marketing and field support operations and directly responsible for implementation of successful market and supporting product strategies in North and South America.


▲ *Ting-Yen Shih*

Ting-Yen Shih, a Ph.D. student from the **University of Wisconsin-Madison**, was announced the 2015 winner of the FEKO Student Competition. The competition is an ideal opportunity for the students to showcase their work with FEKO, the electromagnetic solver of Altair HyperWorks®. With Shih's winning entry entitled, "Design of Platform-Mounted HF Antennas with Enhanced Bandwidth Using the Characteristic Mode Configuration in FEKO," he successfully developed a method using the characteristic mode configuration in FEKO to systematically and efficiently approach the bandwidth limitation of a platform mode. This resulted in Shih achieving the bandwidths that stand-alone antennas were not able to achieve.

PLACES

Würth Elektronik, a manufacturer of electronic and electromechanical components, has opened a new Design & Application Centre in Barcelona, Spain. The establishment of the new branch in the Catalonian capital will also make it possible to devote more effort to the development of customer-specific solutions and applications. Competence and resources for personal support in the areas of product management and application development are also being reinforced. With its excellently equipped laboratory, the centre will not only enhance the current cooperation programme with the University of Valencia, but also further intensify the collaboration projects with cooperation partners and research institutes throughout Catalonia.

Directional / Bi-Directional

COUPLERS

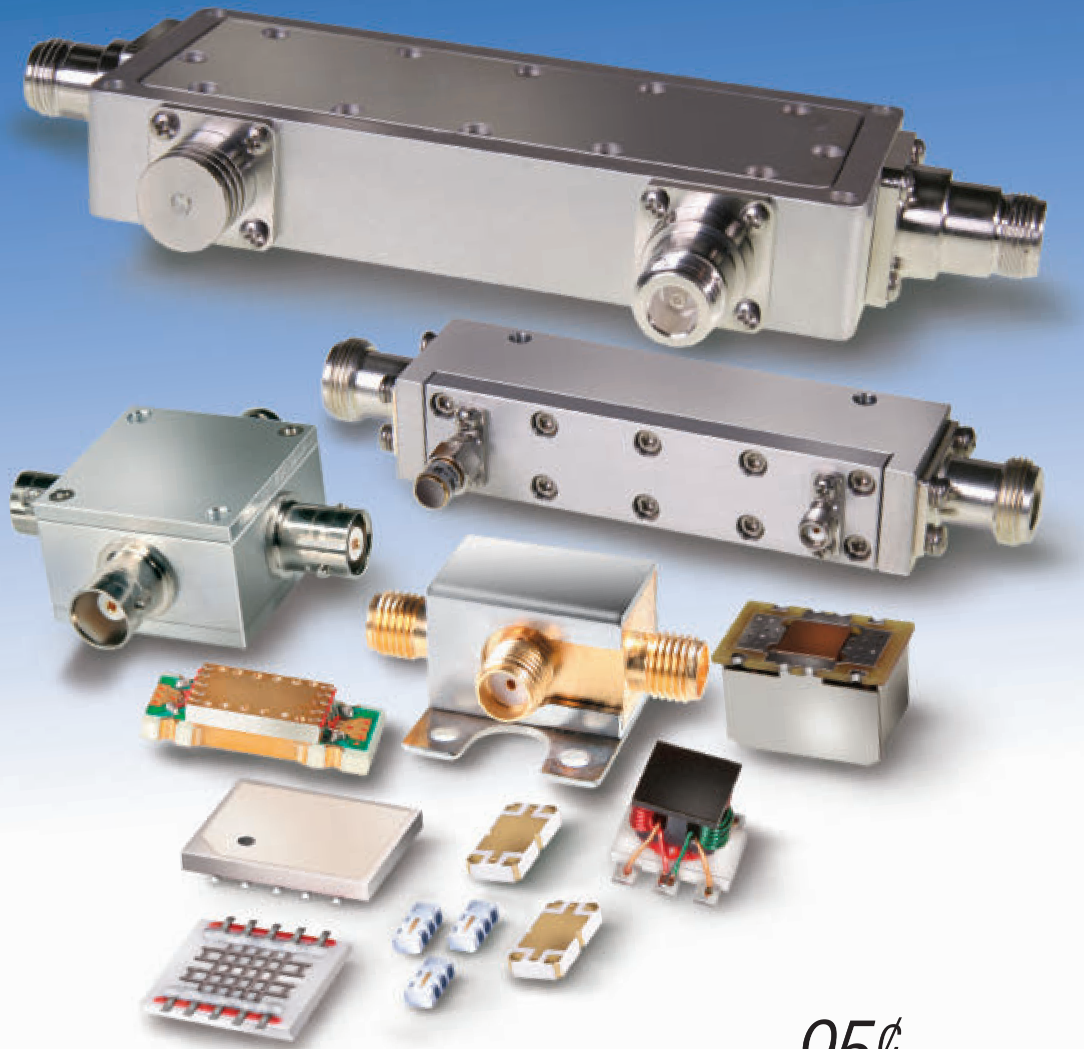

5 kHz to 18 GHz up to 250 W from 95¢ ea. (qty. 1000)

Now! 475 ~~326~~ models in stock, and we're adding even more! Looking for couplers or power taps? Mini-Circuits has 475 models in stock, and we're adding even more! Our versatile, low-cost solutions include surface-mount models down to 1 MHz, and highly evolved LTCC designs as small as 0.12 x 0.06", with minimal insertion loss and high directivity. Other SMT models are designed for up to 100W RF power, and selected core-and-wire models feature our exclusive Top Hat™ for faster, more accurate pick-and-place.

At the other end of the scale, our new connectorized air-line couplers can handle up to 250W RF input power, with low insertion loss and exceptional coupling flatness! All of our couplers are RoHS compliant. So if you need a 50 or 75Ω, directional or bi-directional, DC pass or DC block coupler, for military, industrial, or commercial applications, you can probably find it at minicircuits.com, and have it shipped today!

Mini-Circuits®

www.minicircuits.com P.O. Box 350166, Brooklyn, NY 11235-0003 (718) 934-4500 sales@minicircuits.com

495 rev E

INVITED PAPER

Optimizing Radar Matched Filters

David Brown
Phonon Corp., Simsbury, Conn.

Pulse compression radar achieves processing gain by matched filtering. First described by D. O. North in 1943 at RCA Princeton Laboratories, systems can implement matched filtering for wideband radar receivers by using dispersive surface acoustic wave (SAW) devices as pulse compressors when designers are seeking large time-bandwidth products, low latency and high dynamic range. Usually the transmitter side waveform generator is also a dispersive SAW device, making an expanded pulse "the chirp."

Modern systems can improve on this matched filter system by "matching the matched filter." The concept is to precisely measure a particular dispersive SAW compressor using a high resolution VNA and generate an expanded pulse that is matched to that particular SAW compressor, rather than manufacturing custom compensation networks for each SAW compressor. The advantage of this strategy is improved sidelobe performance and the opportunity to compensate for system-wide errors in the transmitter.

An example system is characterized as bandwidth B = 460 MHz and an expanded pulse width T = 12.5 µs, centered at Flo = 331.8 MHz. The quadratic phase law for this linear FM (LFM) example can be expressed in normalized time t_n as:

TABLE 1

THREE TIME INSTANTS THAT FULLY DEFINE A QUADRATIC LFM WAVEFORM

Time Instant t_n (Normalized)	*Phase Angle φ/2π (Rotations)*	*Instantaneous Frequency f (MHz)*
–0.5	–1355	101.8
0.0	0	331.8
+0.5	2792.5	561.8

$$\varphi(\text{radians}) = 2\pi(2875t_n^2 + 4147.5t_n) \quad (1)$$

where

$$-0.5 \le t_n \le +0.5 \quad (2)$$

Normalized time is related to time by the scale factor:

$$t_n = t/12.5\text{e-}6 \quad (3)$$

with derivative

$$\frac{d(tn)}{dt} = \left(\frac{1}{12.5\text{e}-6}\right) \quad (4)$$

The instantaneous frequencies can be evaluated by taking the derivative and scaling:

$$F = (1/2\pi)\frac{d(\varphi)}{dtn}\frac{d(tn)}{dt} \quad (5)$$

The last factor arises from the derivative chain rule.

Table 1 indicates values at the start, middle and end points. This is an up-chirp, as the frequency is rising in time, and the difference in frequency from start to end is 561.8 - 101.8 = 460 MHz, the dispersive bandwidth of the expander. A digital waveform generator can be built based on a quadratic phase accumulator cascaded with a cosine angle-to-amplitude process and a digital-to-analog converter (DAC). A suitable sampling system can be based on F_{sam} = 4 × 331.8 = 1327.2 MHz, yielding a Nyquist bandwidth sufficient for this example.

In practice, the phase match must be accurate to better than 0.1 degree to achieve high quality sidelobe suppression. Phase errors in wideband dispersive SAW compressors are observed to have a significant cubic error term on

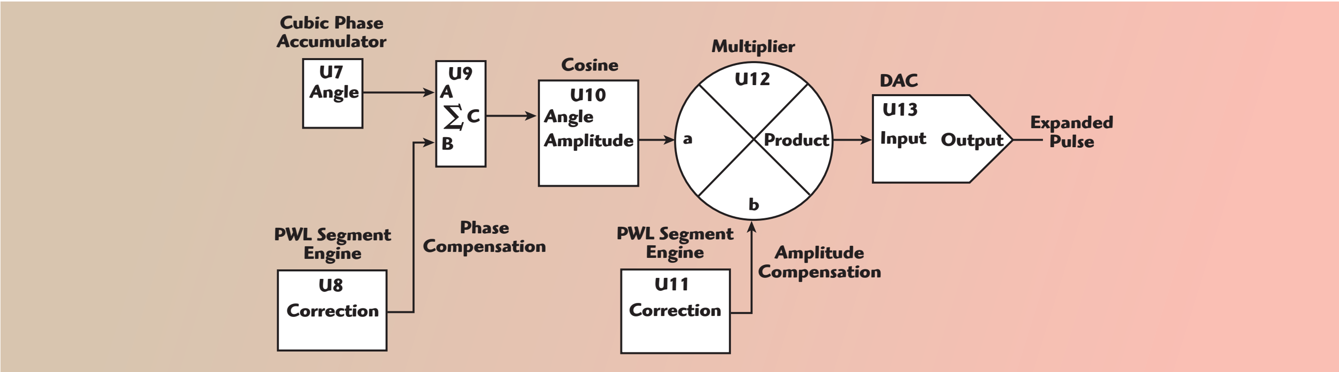

▲ *Fig. 1 Digital waveform generator.*

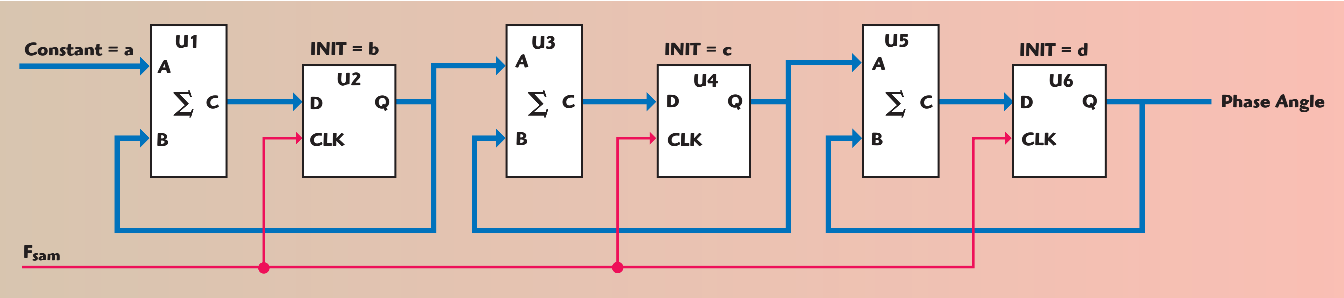

▲ *Fig. 2 Cubic phase accumulator.*

TABLE 2

PHASE LAW POLYNOMIAL AND REAL NUMBER EQUIVALENT DIFFERENCE EQUATION VALUE RELATIONSHIP

Register Initialization	*Value as a Real Number (Continuous Number Line)*
a_{real}	$6 \times a_3/(F_{sam} \times T)^3$
b_{real}	$(2 \times a_2 - 3 \times a_3)/(F_{sam} \times T)^2 + 6 \times a_3/(F_{sam} \times T)^3$
c_{real}	$(a_1 - a_2 + 0.75 \times a_3)/(F_{sam} \times T) + (a_2 - 1.5 \times a_3)/(F_{sam} \times T)^2 + a_3/(F_{sam} \times T)^3$
d_{real}	$a_0 - (a_1/2) + (a_2/4) - (a_3/8)$

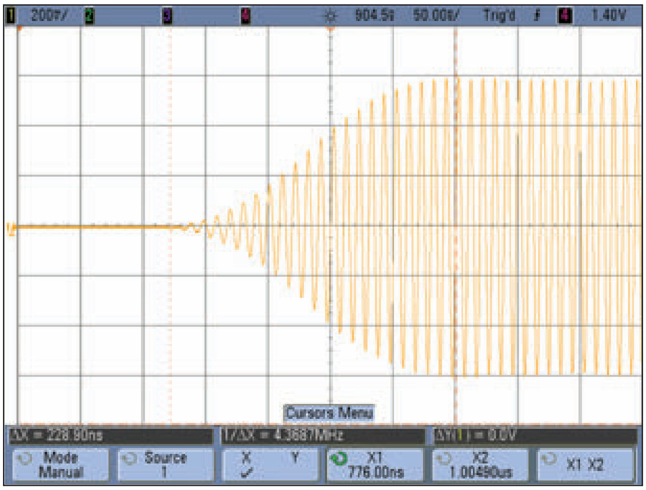

▲ *Fig. 3 Chirp waveform.*

the order of 30 degrees peak-to-peak, in addition to small higher-order terms.

PRECISION DIGITAL

Accordingly, the design has been elaborated beyond the basic approach by using a third-order polynomial for the phase law, adding a secondary phase modulator based on piece-wise linear segmentation and adding an amplitude modulator, also based on piece-wise linear segmentation. The overall organization of the digital waveform generator is shown in ***Figure 1***. A phase domain modulator is an adder, while a multiplier is used in the amplitude domain. This generator uses a cubic phase law accumulator (U7) and modulators (U9 and U12) to modify the instantaneous phase and amplitude. The modulators are driven by piece-wise linear segment engines that correct high order imperfections. All digital processing is clocked at the rate F_{sam}.

The structure of the cubic phase accumulator is simply an extension of the quadratic form (see ***Figure 2***). This block diagram lays out the structure of the phase accumulator (U7 in Figure 1): U1 is a two-port adder; U2 is a pipeline register, clocked at F_{sam}. The third-order system is a cascade of the U1, U2 structure with two additional sections (U3, U4 and U5, U6) to achieve cubic phase. The constants a, b, c and d are described below.

The polynomial form of the cubic phase law is:

$$\varphi / 2\pi = a_3 \times t_n^3 + a_2 \times t_n^2 + a_1 \times t_n + a_0 \qquad (6)$$

As this is a sample data system, normalized discrete time is integer multiples (m) of the clock period:

$$t_n = -0.5 + m / (F_{sam} \times T) \text{ for } 0 \le m \le F_{sam} \times T \qquad (7)$$

The cubic phase accumulator requires initial values loaded into the registers before the start of waveform gen-

eration. The values are partially developed in ***Table 2***.

It might appear unnecessary to include a constant a_0 in the phase law, but it proves useful in controlling the phase to exactly 270 degrees at the instant of the start of chirp. This corresponds to a rising zero-crossing of the cosine function and is readily observable on an oscilloscope. Furthermore, in the example there are 1,355 rotations from the start to the middle, so that point should also be 270 degrees modulo 360. The end point of the chirp is another 2,792.5 rotations, so that will correspond to a falling edge zero-crossing. ***Figure 3*** illustrates the precise location of the start of the chirp waveform, which was created for this example by a definition for a_0 such that the phase is 270 degrees at t_n = -0.5. Note the waveform starts before t_n = -0.5 to allow for edge shaping. The marker at two divisions past center indicates the rising zero crossing, where the instantaneous frequency is 101.8 MHz.

A phase accumulator could be implemented in hardware handling floating point numbers, but that would consume significant resources. Conversion by scaling and casting to integers allows for a simple accumulator, and scale factors that are powers of 2 provide for simple manipulation. For example, a 32-bit accumulator would apply a factor of 2^{32} to each of the register initialization values. Hence the constants for Figure 2 are

$$a = a_{real} \times 2^{32}, b = b_{real} \times 2^{32},$$
$$c = c_{real} \times 2^{32},$$
$$d = (d_{real} \text{ modulo } 1.0) \times 2^{32} \quad (8)$$

The reals are cast to integer values and loaded into the accumulator at the starting instant. By meeting the Nyquist criteria, we are assured that a_{real}, b_{real} and c_{real} are all less than 1. The phase angle result at U6 is produced once every period of F_{sam}. Removal of the 2^{32} factor is trivial: move the (conceptual) binary point from after the LSB to before the MSB of the digital word. ***Figure 4*** shows the error that arises when the values from Equation 1 are applied to a third-order phase accumulator with a_3 set to zero. The errors are fairly small for chirp applications, considering that the chirp has 4,147.5 rotations. In fact, it seems possible to correct for that error with a subsequent phase modulator, as it is known to be exactly repeatable — but wait, it gets complicated.

A more complete error model requires understanding the contribution of a cubic term. Chebyshev polynomi-

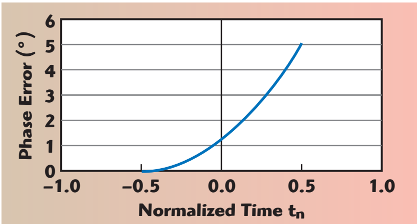

▲ *Fig. 4 Phase error in a 32-bit phase accumulator with only quadratic terms.*

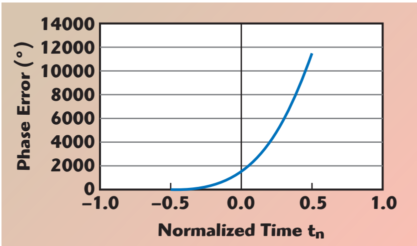

▲ *Fig. 5 The 32-bit accumulator fares poorly when a cubic term is introduced.*

als are a convenient way to add a small ripple to the pure quadratic form. For example, a scaled $T_3()$ is $32 \times t_n^3 - 6 \times t_n$, which adds two full rotations from start to finish (720 degrees). This tiny $T_3()$ is directly added to the corresponding powers in equation 6. The same 32-bit phase accumulator produces dramatically different and poorer results (see ***Figure 5***). Now the end point error is 11,500 degrees, which is a tall order for the subsequent phase modulator to correct. The heart of the problem is that the introduction of the cubic term has increased the rate at which error accumulates. Moving to a 48-bit accumulator looks much better (see ***Figure 6***).

In application, there is one more consideration: the coefficients in equation 6 are convenient for dynamic control of the phase accumulator. If small changes are needed, due to temperature variations for example, it is simple to adjust those parameters. However, by perturbing the coefficients by small amounts, additional errors become visible. A Monte Carlo analysis with the coefficients varied over a range of ±450 ppm indicates that a 52-bit phase accumulator meets the requirements. ***Figure 7*** shows the phase error at the last sample, which is always the largest error. The worst case error does not exceed ±0.03 degrees. Operationally, this means when a small change is made to the cubic polynomial, the phase accumulator might have a change in error of twice this amount, or 0.06 degrees. The end point errors are random; they arise due to small rounding errors when the real numbers in Table 2 are cast to integers.

A worst-case bound can be calculated by assuming that the coefficient errors (eps) are all the same magnitude and the same sign at each stage of the phase accumulator. Normally the eps will be of different signs and magnitudes, and some might even be exact machine numbers. Also, some eps will cancel out the contributions of other stages. The mathematics to use for error accumulation is almost the same expression as for phase accumulation; it really is an error accumulator. Using this assumption, for n accumulations of a coefficient quantizing error eps, the total phase error is:

$$\text{error} = n(n-1)(n-2)\frac{\text{eps}}{6} + n(n-1)\frac{\text{eps}}{2} + n \times \text{eps} + \text{eps} \tag{9}$$

The first product term isn't present for quadratic phase accumulators. It can be seen that the cubic phase ac-

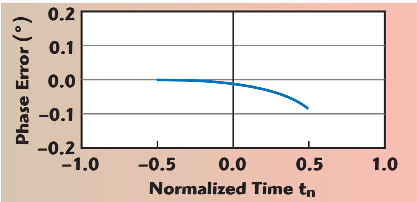

▲ *Fig. 6 Reduced phase error in a 48-bit phase accumulator with a cubic term.*

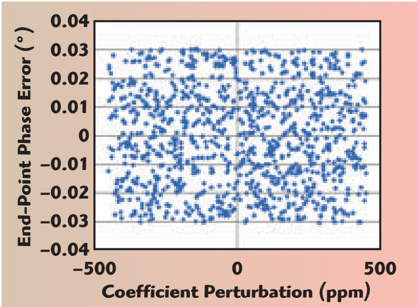

▲ *Fig. 7 52-bit cubic phase accumulator error vs. coefficient variation, where B = 460 MHz, T = 12.5 μs and F_{sam} = 1327.2 MHz.*

HUBER+SUHNER
Excellence in Connectivity Solutions

Minibend CTR
Phase Invariant Cable Assemblies

HUBER+SUHNER introduces the Minibend CTR phase invariant cable, developed for phase critical applications requiring both matched and stable electrical length connectivity.

- Excellent phase and insertion loss stability over temperature
  <300 ppm absolute phase change over -50 to 125 °C temperature range
- Frequency up to 40 GHz
  Phase vs Flexure of 1.2° @ 18 GHz
- Revolutionary minibendTM bend-to-the-end flexibility
  0.20 inches (static) minimum bend radius

aerospacedefense.hubersuhner.com

HUBER+SUHNER AG 9100 Herisau/Switzerland
HUBER+SUHNER INC. Charlotte NC 28273/USA

cumulator has a large first term. Using equation 9, ***Figure 8*** shows that for a phase accumulator of M bits, a worst-case rounding error eps = ½ (2^{-M}) occurs at each increment and the relative position in the accumulator cascade magnifies the contribution. This provides design guidance on keeping the error less than 0.03 degrees. This example system was actually implemented at greater than 52-bit accumulator word size to allow for much larger expanded pulse durations (T). A duration of 47 µs is easily accommodated.

COMPENSATING THE EXPANDED PULSE

A demonstration of the programmable compensation capability of the digital waveform generator is provided by observing its behavior when self-correcting. The goal of self-correcting is to generate constant amplitude and pure quadratic phase. This performance (see ***Figure 9***) is the result of a cubic phase accumulator, piece-wise linear phase compensation of 122 segments and piece-wise linear amplitude compensation, also 122 segments. The demodulated amplitude and phase responses (with respect to a perfect quadratic) show a peak-to-peak amplitude error of 0.0875 dB and a peak-to-peak phase error of 0.375 degrees over a 460 MHz bandwidth. The expanded pulse was auto correlated, and two time spurii were seen positioned at 51 dB at 7 ns, and 57 dB at 10.56 ns. They were not paired-echo responses. The cause of these spurii was not investigated but most likely arose from return loss errors around a bandpass filter, and return loss error on the 41 inch long coaxial cable leading to a high performance oscilloscope.

The phase ripples in Figure 9 are a 90-degree shifted version of the logarithmic amplitude ripples, curiously like a Hilbert transform, and suggesting a minimum phase system. Strangely, the ratio of the amplitude ripple in dB to the phase ripple in degrees is 0.375/0.0875 = 4.28, which is better than the expected ratio for a minimum phase system of 6.6. Note that the phase accumulator and piece-wise linear phase and amplitude modulators require initial data as waveform parameters. In this example, there

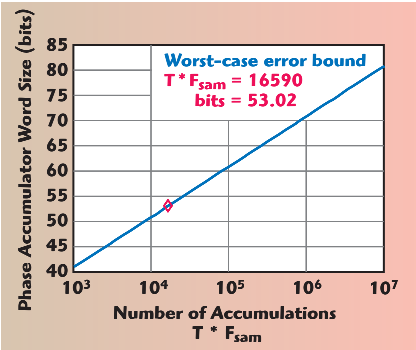

▲ *Fig. 8 Accumulator field width vs. number of accumulations needed to keep the phase error less than 0.03 degrees.*

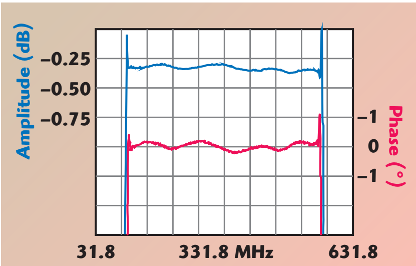

▲ *Fig. 9 Demodulated amplitude and phase responses (with respect to a perfect quadratic) of the expanded pulse from the digital waveform generator.*

are 4 × 52 bits in the phase accumulator and 122 × 2 × 32 = 7,808 bits in the piece-wise linear descriptions. In comparison, an arbitrary waveform generator (AWG) based on a lookup table of waveform samples would require 1,327.2 × 12.5 × 14 = 232,260 bits of storage. The phase accumulator is only using 3.4 percent as much memory storage. This compact waveform format has opened avenues to new capabilities. In particular, 28 sets of piece-wise linear segments are available to encode the temperature behavior of a non-ovenized SAW compressor without any additional storage.

Figure 10 demonstrates the performance achieved when the goals of the programmable digital waveform generator are a flat expanded pulse amplitude and a phase function that is the matched-filter for the compressor, including the phase errors of the dispersive SAW compressor. The matched filter affords 36 dB process gain, the compressed pulse width is 3 ns at -3 dB and 8.4 ns at -30 dB and the undesired sidelobes are more than 35 dB below the compressed pulse.

Pulse compression results in the output signal-to-noise increasing by the bandwidth-time (BT) product. Assuming a lossless compressor, a signal of amplitude 1 and time length T will result in an output signal having amplitude $(BT)^{1/2}$ and a time length of B^{-1}. The resulting peak power gain is BT. Since noise does not correlate, its amplitude remains unchanged.

HARDWARE PERFORMANCE

Figure 11 shows the SAW dispersive delay line.[1] The linear frequency modulated SAW compressor is fabricated on a yz-LINBO3 wafer and assembled in a 3" × 1.25" × 0.5" connectorized package. The compressor is centered at 331.8 MHz with a dispersive bandwidth (B) of 460 MHz and a time dispersion of 12.5 µs (T). For a 460 × 12.5 BT product without amplitude weighting, the resulting signal-to-noise gain is 37.6 dB. With a 50 dB Taylor weighted amplitude response, the output signal-to-noise ratio degrades 1.6 dB. The net signal-to-noise gain through the SAW compressor is then 36 dB; if the input chirp power level is at the noise level, for example, the compressed pulse peak is 36 dB above the noise.

Referring to Figure 11, the compressor is comprised of two slanted aperiodic interdigital transducers. The transducer buss bars are resistor terminated, balanced, microstrip transmission lines. With 140 percent bandwidth, harmonic suppression is important. Transducer interdigital electrode periods determine the frequency response harmonics. Unwanted input-output combined responses below the tenth harmonic are suppressed by using different transducer periods (electrode sampling) of 4 and 3 electrodes per wavelength. Good harmonic suppression requires tight line width con-

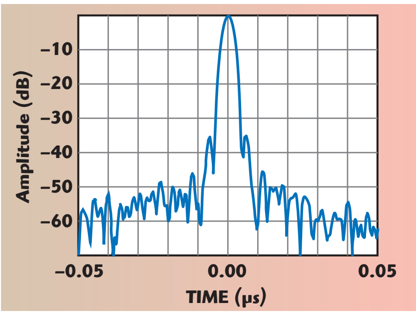

▲ *Fig. 10 Matched filter compressor performance.*

trol of the electrodes, whose periods vary from 0.72 to 5.7 μm.

Figure 12 shows the amplitude and phase vs. frequency responses of the SAW pulse compressor. In this iteration of the pulse compression system, the phase error has been well matched, but an amplitude error is responsible for the -35 dB symmetric sidelobes seen in Figure 10. A simple LC network can compensate for a smooth, low order amplitude error and reduce the time sidelobes to about -42 dB. SAW S-parameter data was obtained over an extended ambient temperature range from -40° to +80°C. Analysis of a discrete data set at ambient temperature increments of 20°C shows the SAW oven can be eliminated by compensating delay, slope and phase variation in the input chirp. Sensing the temperature of a non-ovenized SAW enables this compensation, reducing size, weight and power significantly.

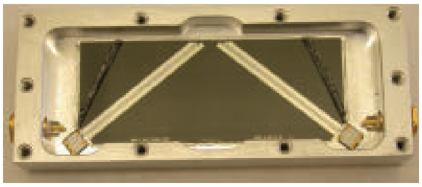

Fig. 11 Phonon dispersive delay line.

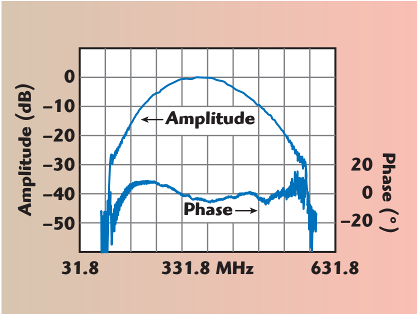

Fig. 12 Measured response of the SAW pulse compressor (B= 460 MHz bandwidth, Taylor weighting), showing the phase response after removing the best-fit quadratic.

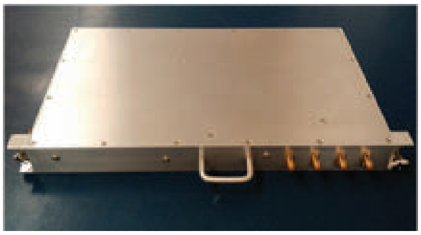

Fig. 13 Highly matched pulse compression system.

Figure 13 shows the programmable waveform generator and the matched SAW compressor fully implemented in system-level hardware incorporating amplifiers and control electronics. The programmable digital waveform generator and the SAW pulse compressor enable a highly matched pulse compression system.

A second dispersive SAWs was also developed and described in the referenced article.[1] The B/F center ratio of the 600 MHz SAW (B = 667 MHz) could be increased to 143 percent (B = 860 MHz). A 23.4 μs dispersion design fabricated on a 4 inch diameter wafer would result in a BT product of 20,000. It is practical to cascade two identical SAWs to achieve T = ~47 μs, a BT of 40,000 and a compression gain of 46 dB. ■

Reference

1. Pierre Dufilie, Clement Valerio and Tom Martin, "Improved SAW Slanted Array Compressor Structure for Achieving > 20,000 Time-Bandwidth Product," *2014 Ultrasonics Symposium Proceedings*, pp. 2019–2022.

INVITED PAPER

Editor's Note: This article is a two part series about the design of anechoic chambers giving a thorough treatment of the subject that could be used as a reference piece. Part one covers RF absorber approximations for rectangular far field ranges. Part two will cover compact and near field ranges and will be published in the February 2016 issue.

Basic Rules for Anechoic Chamber Design, Part One: RF Absorber Approximations

Vince Rodriguez
MI Technologies, Suwanee, Ga.

The task of adequately specifying performance for an indoor anechoic chamber without driving unnecessary costs or specifying contradictory requirements calls for insight that is not always available to the author of the specification. While there are some articles and books[1-3] that address anechoic chamber design, a concise compendium of reference information and rules of thumb on the subject would be useful. This article intends to be a helpful tool in that regard. It starts by recommending the proper type of range for different antenna types and frequencies of operation. Rules of thumb are provided to select the best approach for the required test or antenna type. The article concentrates on rectangular chambers. Simple approximations are used for absorber performance to generate a series of charts that can be used as a guide to specify performance and appropriate facility size.

The ability to measure an antenna is an important design requirement in determining if energy is radiating properly and in the desired direction, as well as how much energy is traveling in undesired directions. To measure antennas (like many other devices that are being measured), there is the desire to have the antenna unaffected by its surrounding environment. This is where the anechoic chamber becomes a viable solution. The anechoic chamber provides an environment free of echo or other radiated signals to reduce the effects of these undesirable signals.

This article covers applications where an antenna is radiating or receiving a given signal, and its performance as a function of direction is being measured.

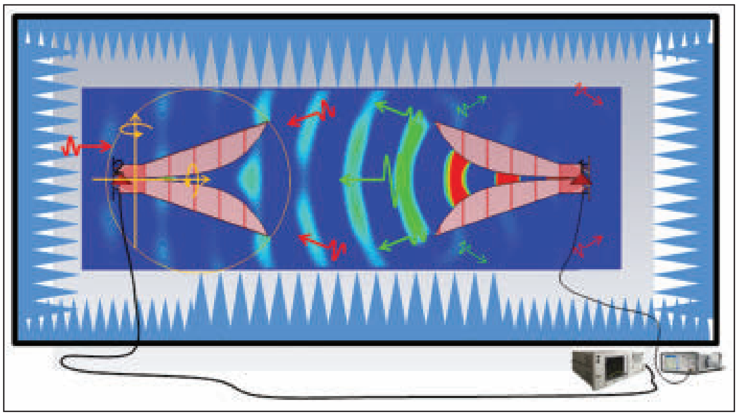

▲ *Fig. 1 General geometry of an indoor range - two antennas are located in the range (one for transmitting and one for receiving).*

RANGE TYPE SELECTION

The general range geometry is shown in ***Figure 1***. There are several methods of measuring the radiation patterns of antennas in-

doors: far field illumination, near field measurements and compact range. While they all present pros and cons, there is not a single solution that is ideal for all types of antennas and situations. The type of range most suitable for a given type of antenna is driven by two parameters: frequency and electrical size of the antenna under test (AUT). The far field condition given by the following equation drives the selection:

$$r \geq \frac{2D^2}{\lambda} \quad (1)$$

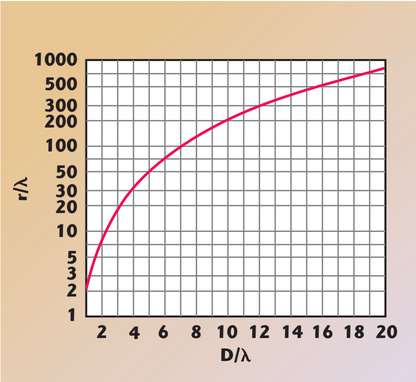

Fig. 2 The far field distance plotted related to the wavelength.

TABLE I

FREQUENCY RANGES AND ANTENNA SIZES FOR THE DIFFERENT INDOOR ANTENNA MEASUREMENT APPROACHES

Indoor Ranges	*Antenna Size in Wavelengths*		
Frequency	*Far Field Illumination*	*Near Field*	*Compact Range*
100 MHz	<2λ	>2λ	Not ideal
500 MHz	<2λ	>2λ	Not ideal
1 GHz	<5λ	>5λ	>5λ
2 GHz	<10λ	>10λ	>10λ
≥ 4 GHz	<10λ	>10λ	>10λ

The parameters mentioned above are embedded into the far field equation. D is the largest physical dimension of the antenna. Wavelength is λ, which is related to the frequency of operation on the antenna. For smaller antennas the far field range length, r, can be approximated by:[4]

$$r \approx 10\lambda \quad (2)$$

This equation can be used when the antenna is under one wavelength in electrical size. From Equation 1, the far field distance can be plotted as a function of the electrical size of the antenna, as shown in ***Figure 2***.

As a rule of thumb for indoor ranges, the far field illumination techniques are better suited for antenna sizes under 10λ. This rule is related to the electrical antenna size. Frequency of operation adds another factor that will influence the type of range. An antenna with a size of 10λ will have a far field distance of 200λ, making the test distance 20 times the size of the antenna. At some microwave frequencies this may be a test distance of 200 inches (5 m) so an indoor range may be easy to implement. However, note a 20λ antenna will have a test distance that is 800λ.

For example, consider an 18 inch dish used by a popular satellite TV service. This satellite service operates at 18.55 GHz. The dish antenna is 28.29λ in size. The far field is at approximately 1600λ or 25.86 m (84.84 ft). Clearly, for such an electrically large antenna, a far field illumination approach indoors is not economically feasible. For this antenna, a compact range or a near field approach is more suitable. Conversely, a 10λ antenna at 300 MHz, which is 10 m in size, would be extremely difficult to manipulate at a test distance of 200 m. For this case, the best solution would be an outdoor range.

In general, for frequencies below 100 MHz, an outdoor range is a better approach. Current absorber technology does not support some indoor measurements at those low frequencies. Indoor ranges can be built, but the antenna size should be kept less than 2λ; which limits the far field distance to 8λ (24 m). This distance is close to the 10λ given by Equation 2. ***Table 1*** provides an approximate guide for the different antenna sizes and frequen-

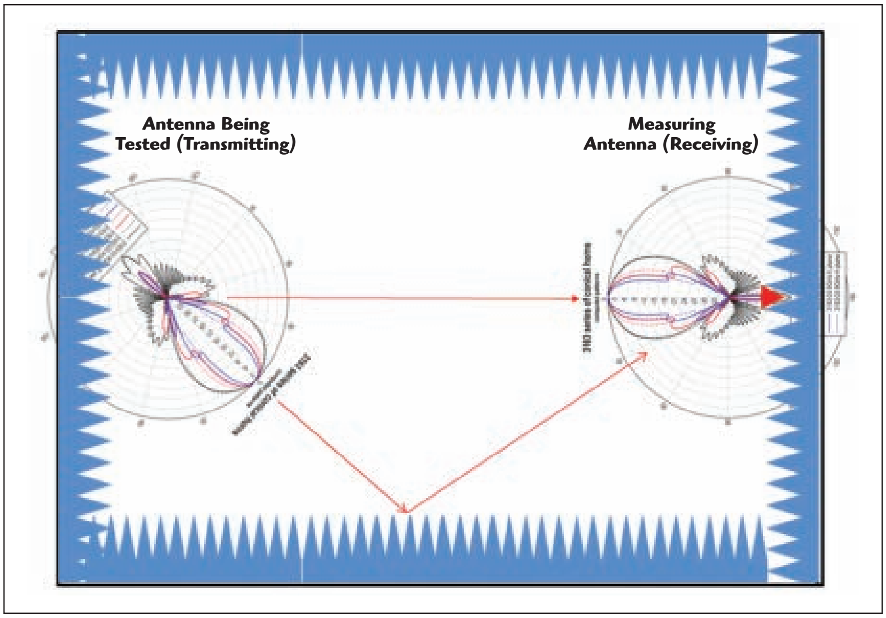

▲ *Fig. 3 An indoor range showing one of the reflected paths and the direct path between the AUT and the source antennas.*

cies of operation.

The values in Table 1 are general guidelines. Spherical near field (SNF) ranges can test antennas as small as λ/2. But for such a small antenna it may be a better approach to use a far field illumination range as it relates to the typical electrical size of the AUT.

When creating an anechoic chamber, the goal is to obtain a volume in the chamber where any reflected energy from the walls of the range (ceiling and floor) will be much lower than any of the features of interest on the radiation pattern. This volume is known as the quiet zone (QZ). Figure 1 shows that as one antenna transmits, it illuminates the receive antenna and all the walls and surfaces of the range. The energy incident onto these surfaces will be reflected towards the QZ.[1,3] The level of reflected energy must be a given number of decibels below the direct path between the transmitting and receiving antennas.

As the antenna being measured is rotated (see ***Figure 3***), its main beam will illuminate different surfaces of the chamber. The range antenna will measure the level of field radiated by the AUT along the direct path between the two antennas. However, the range antenna will also receive the reflected energy from the walls, ceiling and floor. If the reflected energy level is higher than the energy radiated along the direct path between the two antennas, then the radiation pattern in that direction cannot be measured accurately. In Figure 3, the measuring antenna, (also known as range antenna or source antenna) is pointing at a null, but it is also receiving the reflected signal from the wall that is illuminated by the main beam of the AUT. The range antenna is receiving the reflected signal in a direction of 30°. In that 30° direction, the gain of the range is lower than in the direct path (boresight) to the AUT. The reflected energy is a number of dB lower, for example, 20 dB. Let us assume that the gain in the 30° direction is 10 dB lower than the boresight. The signal received by the antenna on that direction will be -30 dB compared to the energy received when the main beam of the AUT was pointing to the range antenna. If the null is less than -30 dB, the measured pattern will have errors.[5]

RF ABSORBER

A key design item for an anechoic chamber is the RF absorber. The absorber treatment must be such that the reflected energy has a small or negligible effect on the measured data. A typical RF absorber is a lossy material shaped to allow for incoming electromagnetic waves to penetrate with minimal reflections. Once the electromagnetic (EM) energy travels inside the material, the RF energy

STRENGTH IN NUMBERS

Qorvo® GaN technology enables the systems all around you

#1 GaN Supplier In DEFENSE

Industry leader of GaN on Silicon Carbide

9 MRL

Only supplier to achieve MRL 9 using USAF MRA tool

More than 2,608,000 GaN devices shipped since 2008

GaN

Demonstrated MTTF reliability with $\frac{200°C}{10^7 \text{ hrs.}}$

Top supplier of DOCSIS® 3.1 GaN components

125 new products in 18 months

0.013% per million device hour report failures

65,800,000 device hours on 16,920 GaN PAs

qorvo® all around you

For more information text **Qorvo** to **82257** or visit Qorvo.com/GaN transforms into thermal energy and dissipates into the surrounding air.[6] The electrical thickness of the material determines how much energy is absorbed. The reflection level at normal incidence can be approximated by the following equation:

$$R_o(t) = -13.374\ln(t) - 26.515 \quad (3)$$

where t is the thickness in wavelengths. The equation is valid for 0.25 ≤ t ≤ 20. This approximation can be used to get a conservative reflectivity value of an absorber of a given thickness. Most manufacturers provide the information in their datasheets.

Figure 1 shows that some of the absorber in the range is not located in the normal incident wave direction, but rather in an oblique incidence. For oblique incidence, the main reflectivity of the absorber is in the bi-static direction. Backscattering occurs when the distance between the tips of the pyramids is ≥λ.[7] Hemming[1] provides plots that show the estimated bi-static reflectivity of absorber at oblique incidence. A series of polynomial approximations, together with Equation 3, provide a general description of the performance of pyramidal absorbers of different thicknesses and at different angles of incidence. These are conservative approximations. That leaves a margin of error to account for things like lights, doors, positioning equipment and edge diffractions from treatment discontinuities.

The absorber performance in dB is given by the following polynomial:

$$R_\theta(t,\theta) = R_o(t) + A_1(t)\cdot\theta + A_2(t)\cdot\theta^2 + A_3(t)\cdot\theta^3 + A_4(t)\cdot\theta^4 + A_5(t)\cdot\theta^5 \quad (4)$$

The coefficients in this equation are functions of the thickness. When the thickness of the absorber is such that 0.25λ ≤ t ≤ 2λ, the coefficients of Equation 4 are given by the following polynomials:

$$A_1(t) = 1.5252 - 4.8243t + 6.9479t^2 - 3.8332t^3 + 0.7333t^4 \quad (4a)$$

$$A_2(t) = -0.0754 + 0.24782t - 0.3984t^2 + 0.2285 - 0.0442t^4 \quad (4b)$$

$$A_3(t) = 0.0016 - 0.00502t + 0.00938t^2 - 0.00577t^3 + 0.001155t^4 \quad (4c)$$

$$A_4(t) = -1.58\cdot10^{-5} + 4.91\cdot10^{-5}t - 1.015\cdot10^{-4}t^2 + 6.58\cdot10^{-5}t^3 - 1.35\cdot10^{-5}t^4 \quad (4d)$$

$$A_5(t) = 5.84\cdot10^{-8} - 1.78\cdot10^{-7}t + 4.02\cdot10^{-7}t^2 - 2.71\cdot10^{-7}t^3 + 5.7\cdot10^{-8}t^4 \quad (4e)$$

When the thickness of the treatment is such that 2λ ≤ t ≤ 20λ, then the coefficients are given by the set of polynominals:

$$A_1(t) = 0.1751 + 0.149t - 0.0119t^2 + 0.00028t^3 \quad (4f)$$

$$A_2(t) = -0.0105 - 0.00824t + 0.0007t^2 - 1.61\cdot10^{-5}t^3 \quad (4g)$$

$$A_3(t) = 0.00029 + 0.000123t - 1.13\cdot10^{-5}t^2 + 2.57\cdot10^{-7}t^3 \quad (4h)$$

$$A_4(t) = -1.69\cdot10^{-6} - 4.77\cdot10^{-7}t + 5.08\cdot10^{-8}10^{-8}t^2 - 1.14\cdot10^{-9}t^3 \quad (4i)$$

$$A_5(t) = 0 \quad (4j)$$

The domain of Equation 4 is limited by those angles of incidence where 0° ≤ θ ≤ 85°and where θ=0° is normal incidence. Additionally, the domain is limited by the domain of the coefficient polynomials. Hence Equation 4 is valid when 0.25λ ≤ t ≤ 20λ. The range of Equation 4 should also be limited to -55 ≥ R(dB) ≥ 0. For an absorber thickness larger than 20λ, the reflectivity can be approximated using the results for a 20λ thick absorber. ***Figure 4*** shows the bi-static performance as a function of angle for a series of different electrical thickness of the absorber.

Figure 5 shows a comparison of computed results using the method in reference 8, a given manufacturer specifications and the results from Equation 4 for a material of thickness equal to λ and 2λ. If the results of the polynomials presented here are compared to those from numerical computations, the polynomials appear to provide a conservative number for the reflectivity — higher by about 10 dB. The manufacturer specifications were only provided from 45° to 80° and normal incidence. Computed results were obtained only at a few angles.

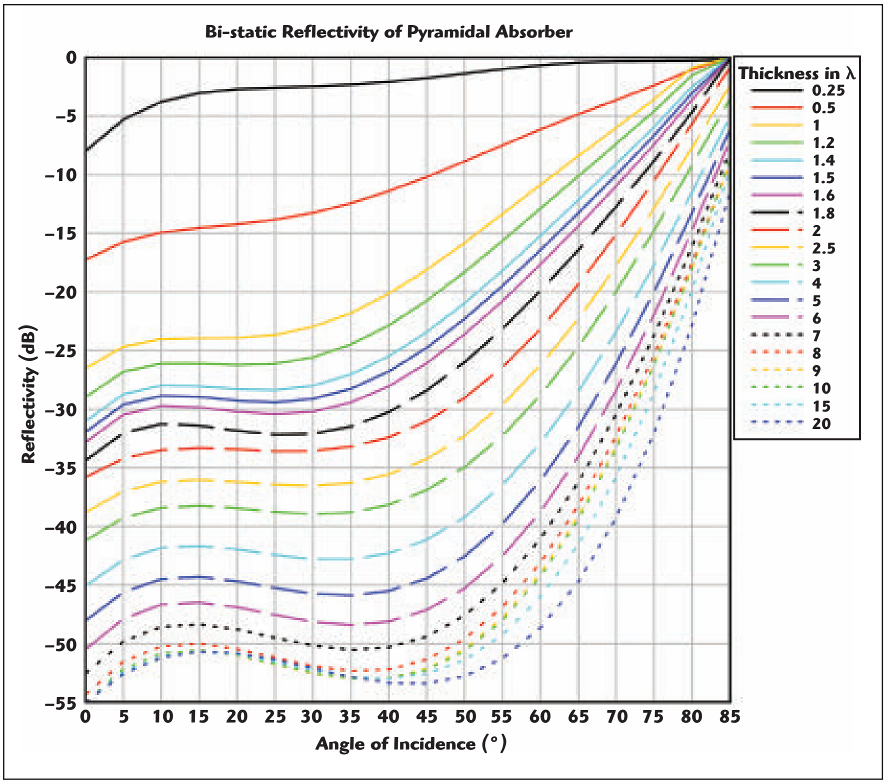

▲ *Fig. 4 Estimated reflectivity of RF absorber as a function of angle of incidence.*

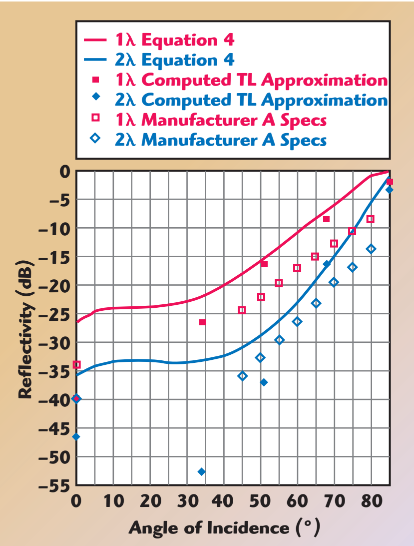

▲ *Fig. 5 Comparison of bi-static reflectivity from a computational approach, manufacturer's specifications and Equation 4.*

For the 1λ thick absorber, the different methods follow similar trends, with the polynomials providing the most conservative number. There is a large difference at 35° between the computed and the polynomial results. However, that null in the reflectivity may shift depending on the material on which the absorber is mounted.[9] In general, the polynomials are a safe approximation for the performance of RF materials at different angles of incidence.

The largest typical absorber size currently available is 72" (1.82 m). This size provides a frequency limit for the use of indoor ranges. At 100 MHz, the thickness of this absorber is 1.64λ with a normal incidence performance at about -33 dB. In an indoor range lined with this material, pattern features -20 dB from the peak will be difficult to measure accurately. There are hybrid absorbers merging ferrite tiles and lossy substrate pyramids of wedges that operate down to 30 MHz or even 20 MHz. These are more suitable for EMC applications as their normal incidence absorption is typically limited between 25 and 35 dB.

RECTANGULAR FAR FIELD CHAMBERS

Sizing the range begins with rectangular far field ranges that have a test distance is determined by Equation 1. It is common to find sources stating the rules of thumb for sizing a rectangular anechoic chamber for far field illumination. Generally, the width and height of an anechoic chamber should be three times the diameter of the minimum sphere that contains the largest antenna being tested. It is

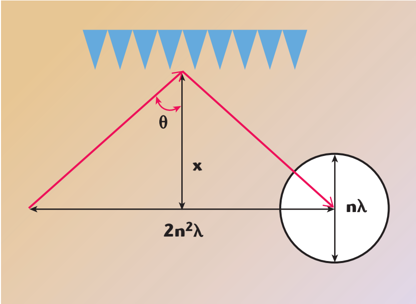

▲ *Fig. 6 Geometry of a far field range.*

important to check that a minimum spacing of 2λ between the AUT and the tips of the absorber is maintained to avoid loading of the AUT. The far field distance is given by:

$$\frac{r}{\lambda} = 2n^2 \tag{5}$$

Where n is the number of wavelengths in size of the AUT. The QZ must be large enough to encompass the AUT. Hence the QZ is nλ. ***Figure 6*** shows a typical rectangular range geometry. From the geometry, an equation for the distance x can be derived. The distance x is the distance from the range centerline to the absorber tips.

$$\frac{x}{\lambda} = n^2 \cdot \cot\theta \tag{6}$$

Equation 6 gives the distance in terms of wavelengths. In Figure 3, the value of θ can be chosen for a desired reflectivity. The curves in Figure 4 will also provide a value for the thickness of the absorber. Hence, if the AUT has features that need to be measured in the -25 dB level, the bi-static reflectivity of the absorber must exceed that level. Absorber 2λ in thickness will exceed -25 dB up to angles of 50°. Hence the width of the chamber is

$$2x = \left(2n^2(0.84) + 4\right)\lambda \tag{7}$$

Where the added 4 accounts for the 2λ thickness of the absorber. If a different thickness of absorber is used, Equation 7 will change. In general, the chamber width can be written as

$$W = \left(2n^2 \cot(\theta) + 2t\right)\lambda \tag{8}$$

Parameters θ and t must be chosen to obtain the required reflectivity. It is important to keep a minimum 2λ spacing from the QZ to the absorber. The length of the rectangular far field chamber is mainly given by the far field distance and the QZ size plus the absorber thickness. Added space should be included for the range antenna and the absorber behind it.

The total chamber or range length (L) is given by:

$$L = \left(2n^2 + n + 2 + t + K\right)\lambda \tag{9}$$

where K is a factor large enough to include the source antenna, the 2λ spacing, and the absorber behind the source. It should be noted, that these equations provide a minimum requirement. Work must be performed inside the chamber — mounting and connecting the antenna, switching

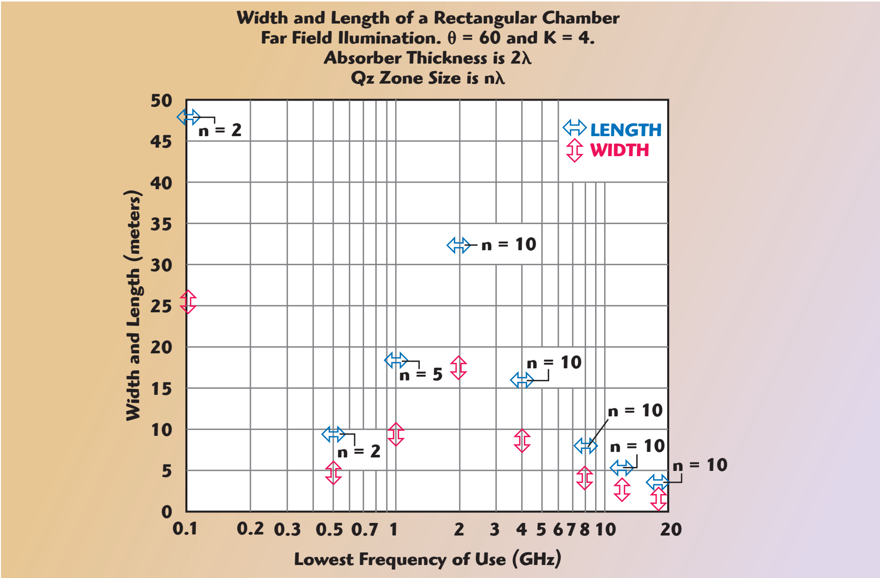

▲ *Fig. 7 Rectangular far field chambers for different lowest frequencies of operation and different largest size antennas at their lowest frequencies.*

Leading Global Communications

PD25-00 0.25μm E / D pHEMT

- 4th generation E/D PHEMT Technology
- High performance 0.25μm E-mode combined with latest generation 0.5μm D-mode switch
- E-mode device: Ultra low noise and high gain
- D-mode device: Compact layout and low Ron-Coff product

Fmin and Gain

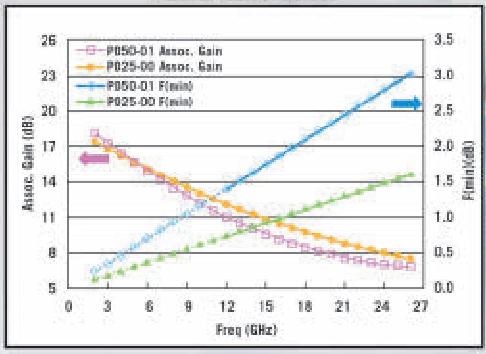

E-mode I-V Characteristics

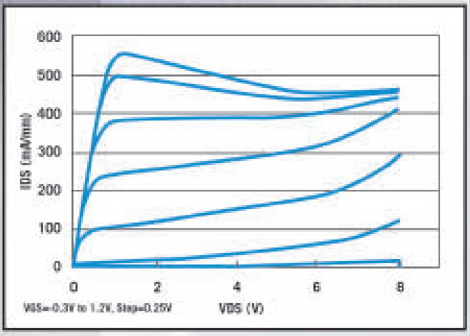

E-mode Transfer Curve

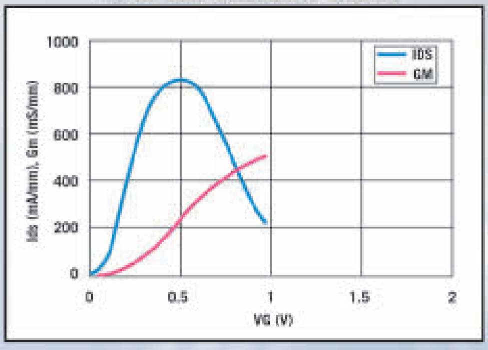

D-mode Switching Speed

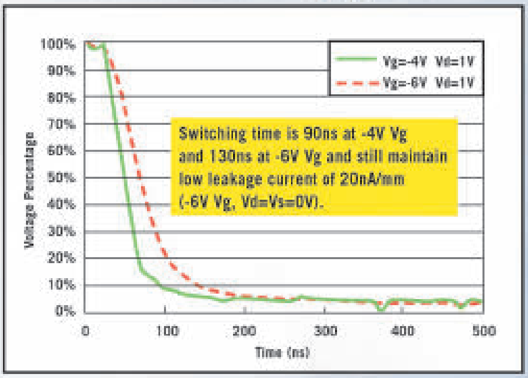

D-mode Device Performance

	PD50-01		PD25-00	
	Single	Triple	Single	Triple
Ron (ohm.mm)	1.9	3.7	1.3	2.2
Coff (fF/mm)	168	83	163	92
RonxCoff(ohm.fF)	316	310	209	198

DUT: NOF x UGW= 5 x 12μm

WIN SEMICONDUCTORS CORP.
Tel:+886-3-397-5999 Fax:+886-3-397-5069 http://www.winfoundry.com

range antennas, etc. The space should be checked to allow for people to perform these tasks inside the anechoic range.

Expected chamber sizes can be examined by entering values into previous equations. It will be assumed that the source antenna is the directive with a sufficient front-to-back ratio. The absorber behind the source antenna will be one wavelength in thickness and the factor K will be set to 4.

In ***Figure 7***, the width and length of a series of rectangular chambers have been plotted versus the lowest frequency of operation. In addition the electrical size of the AUT at the lowest frequency is indicated by the value of n for each chamber size plotted.

If a chamber is designed for an antenna of a given nλ at the lowest frequency, that same chamber is large enough for testing antennas of the same electrical size at higher frequencies. Similarly, as the frequency is lowered, the chamber size must increase. At 500 MHz, a chamber for a 2λ sized antenna is about 10 × 5 m. If the antenna size was increased to 4λ, the chamber would need to be 18 × 10 m. Tapered anechoic chambers should be used at these lower frequencies.[1,10-12] The geometry of the taper chamber uses the specular reflection off the side walls for the AUT illumination rather than reducing its level as it is done in the rectangular chamber. This leads to a physically smaller chamber.

The height of the chamber should be the same as the width. By doing this, the reflections from the ceiling and floor will be similar in level. This is important since the reflected energy from the ceiling and floor will be similar, and the effects of the range on polarization dependant parameters such as cross polarization and axial ratio will be minimized.

Equations 8 and 9 provide a good idea of the space requirements for an indoor range. In most cases, a chamber size can be adjusted. For example, the absorber on the ceiling and floor can be increased in thickness to maintain the reflectivity at more oblique angles of incidence (larger θ). Chebyshev arrangements[13] of the absorber layout can also be used to improve reflectivity.

Figure 3 also reveals another clue to improve reflectivity. The reflected ray arrives at the range antenna at an angle at which the gain of the antenna is lower than in the boresight direction. Using higher directivity antennas as sources reduces the amount of energy received from the side walls, ceiling and floor. Hence, shorter absorbers reduce the chamber size.

CONCLUSION

Part one of this two-part series has dealt mainly with approximations for bi-static reflectivity of RF absorbers and the rectangular design of rectangular RF anechoic chambers. The polynomial equations include a "margin of safety" in their results. This helps in accounting for secondary bounces and edge diffractions as well as light fixtures, vents, doors and other disruptions of the absorber treatment. Part two will provide equations for compact ranges and near field to far field ranges.

ACKNOWLEDGMENT

The author will like to thank Zhong Chen for providing the computed results based on the NIST algorithm.[8] ■

References

1. L. Hemming, "Electromagnetic Anechoic Chambers: A Fundamental Design and Specification Guide," IEEE Press/Wiley Interscience: Piscataway, N.J., 2002.
2. G. Sanchez and P. Connor, "How Much is a dB Worth?" 23rd Annual Symposium of the Antenna Measurement Techniques Association (AMTA), Denver, Colo., October 2001.
3. J. Hansen and V. Rodriguez, "Evaluate Antenna Measurement Methods," *Microwave and RF*, October 2010, pp. 62–67.
4. W. Stutzma and G Thiele, "Antenna Theory and Design," 2nd Ed., Wiley 1997 ANSI/IEEE STD 149-1979 149-1979 - IEEE Standard Test Procedures for Antennas, 1979, reaffirmed 2008.
5. D. Wayne, J. Fordham and J. McKenna, "Effects of a Non-Ideal Plane Wave on Compact Range Measurements," 36th Annual Antenna Measurement Techniques Association Symposium (AMTA), Tucson, Ariz., October 2014.
6. V. Rodriguez, G. d'Abreu and K. Liu, "Measurements of the Power Handling of RF Absorber Materials: Creation of a Medium Power Absorber by Mechanical Means," 31st Annual

Antenna Measurement Techniques Association Symposium (AMTA), Salt Lake City, Utah, October 2009.
7. W. Sun and C. Balanis, "Analysis and Design of Periodic Absorbers by Finite-Difference Frequency-Domain Method," Report No. TRC-EM-WS-9301 Telecommunications Research Center, Arizona State University, Tempe, Ariz., 1993.
8. E. Kuester and C. Holloway, "A Low-Frequency Model for Wedge or Pyramid Absorber Arrays-I: Theory," *IEEE Transactions on Electromagnetic Compatibility*, Vol. 36, No. 4, November 1994.
9. V. Rodriguez, "A Study of the Effect of Placing Microwave Pyramidal Absorber on Top of Ferrite Tile Absorber on the Performance of the Ferrite Absorber," 19th Annual Review of Progress in Computational Electromagnetics (ACES) Symposium, Monterey, Calif., March 2003.
10. W. Emerson and H. Sefton, "An Improved Design for Indoor Ranges," *Proceedings of the IEEE*, Vol. 53, No. 8, pp. 1079–1081, 1965.
11. H. King, F. Shiukuro and J. Wong, "Characteristics of a Tapered Anechoic Chamber," *IEEE Transactions on Antennas Propagation*, Vol. 15, No. 3, pp. 488–490, 1967.
12. V. Rodriguez, "Using Tapered Chambers to Test Antennas," *Evaluation Engineering*, Vol. 43, No. 5, pp. 62–68, 2004.
13. J-R J. Gau, D. Burnside and M. Gilreath, "Chebyshev Multilevel Absorber Design Concept," *IEEE Transactions on Antennas Propagation*, Vol. 45, No. 8, pp. 1286–1293, 1997.

Vince Rodriguez *attended the University of Mississippi, in Oxford, Mississippi, where he obtained his B.S.E.E. in 1994. Following graduation, Rodriguez joined the department of Electrical Engineering at the University of Mississippi as a research assistant. During that time, he earned his M.S. and Ph.D. (both degrees in engineering science with emphasis in electromagnetics) in 1996 and 1999 respectively. Rodriguez joined EMC Test Systems (now ETS-Lindgren) as an RF and Electromagnetics engineer in 2000. He was the principal RF engineer for the anechoic chamber at the Brazilian Institute for Space Research (INPE), the largest chamber in Latin America and the only fully automatic, EMC and satellite testing chamber. In November 2014, Rodriguez joined MI Technologies in Suwanee, Ga. as a senior applications engineer bringing his expertise on numerical modeling, RF absorber and anechoic range design to the development of solutions for antenna, RCS and radome testing facility design.*

Rodriguez is the author of more than 50 publications, including journal and conference papers as well as book chapters. He holds patents for a hybrid RF absorber and a dual ridge horn antenna. Rodriguez is a senior member of the IEEE and several of its technical societies. Among the IEEE technical societies, he is a member of the EMC Society, where he served as distinguished lecturer from 2012 to 2014 and also serves as member of the board of directors. He is an Edmund S. Gillespie Fellow of the Antenna Measurements Techniques Association (AMTA). Rodriguez is a member of the Applied Computational Electromagnetic Society (ACES), where he serves on the board of directors. Rodriguez is a member of several standard committees including IEEE STD 149, IEEE STD 1148 and RTCA DO-213. Rodriguez is also a full member of the Sigma Xi Scientific Research and Eta Kappa Nu Honor Societies.

INVITED PAPER

A Hybrid Hexaband Cellular Antenna

Mark W. Ingalls
Machine2Wireless LLC, Fayetteville, Ark.
Michael D. Glover
University of Arkansas, Fayetteville, Ark.
Ed Liang
MCV Microwave Inc., San Diego, Calif.

Typically, an internal antenna may be custom designed and integrated into a radio's printed wiring board (PWB) or case and implemented as a separate component. Matching elements are then attached to the PWB or remotely connected to the radio with a cable and connectors. These alternatives suffer from inflexibility and poor economy. A new hexaband cellular antenna that is partly integrated into the PWB and compatible with mass production has been designed and tested. The new design offers the benefits of customization and high volume production without requiring a separate matching network.

There is a trend toward connecting machines to the Internet and to each other wirelessly, using radios that have been integrated into the machine's packaging. Equipment manufacturers, wanting to provide a product that is generally serviceable at a reasonable cost, desire that their products, in general, and particularly the installed antenna, operates as flexibly and economically as possible. In addition to being capable of receiving and transmitting wireless information the antenna must be designed to be compatible with the radio equipment to which it is connected. It is said that the antenna and radio equipment must be "matched."

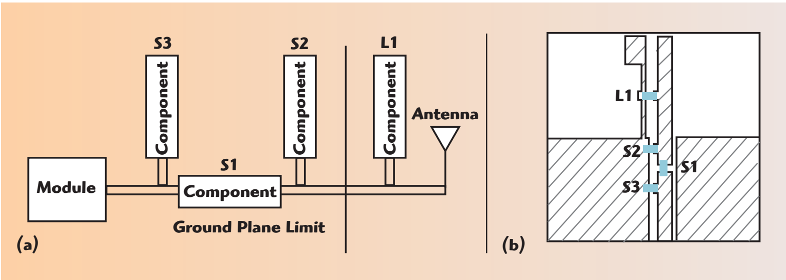

▲ *Fig. 1 Typical matching network block diagram (a) and layout (b) recommended by an antenna manufacturer.*[1]

The essential characteristic of being matched is that information will be passed from antenna to radio and from radio to antenna without reflection of the electromagnetic waves upon which the information is superposed. One must ensure that all elements are matched to one another, by selecting and inserting extra circuit elements (see ***Figure 1***) or by modifying the design of the elements. This process is not too difficult for the non-radiating elements of the signal path, because these elements are relatively immune to influence by other system changes, such as the package that contains the radio equipment. Once the circuit connections to and from the non-radiating elements in the signal path are quantified and have been matched, no further tuning is usually necessary. For example, a system designer usually specifies that an am-

▲ *Fig. 2 Antenna integrated into the package.*[2]

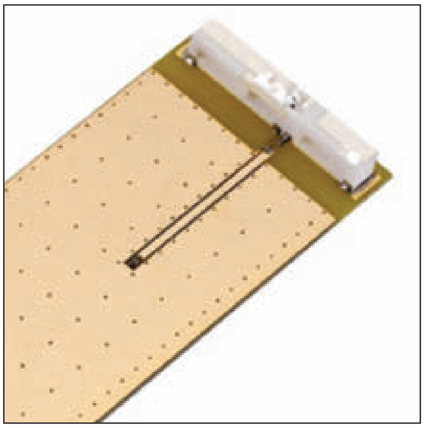

▲ *Fig. 3 Discrete antenna mounted to a PWB.*[3]

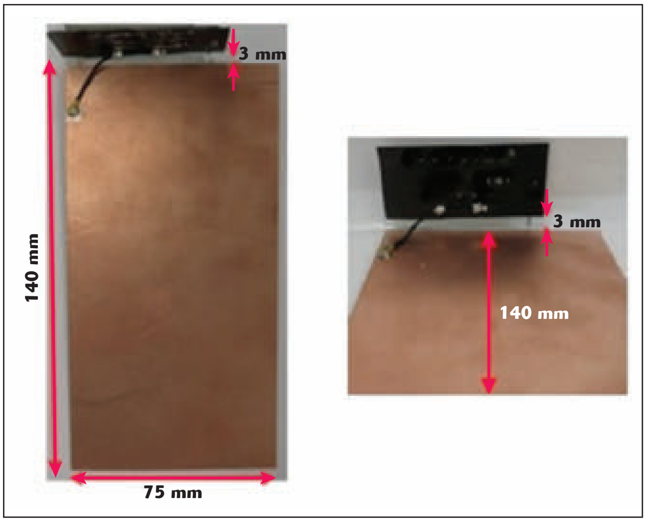

▲ *Fig. 4 Discrete antenna connected to the PWB with a pigtail.*[4]

plifier, filter, switch, mixer, connectors, cables and other elements all match when incorporated into a system. The vendors of these elements are able to provide these components to many system designers for integration into different systems, as long as the system matching requirements are similarly defined.

However this is not necessarily the case with the antenna. The antenna, by virtue of its unique role in the transmission and reception of information-bearing waves, is susceptible to the influence of local but non-connected elements, such as the package that contains the antenna or the PWB that supports other system components. One way to deal with this problem is to place the antenna far away from anything that might influence its characteristics and connect it to the radio with a cable. Another approach is for the antenna manufacturer to precisely define the characteristics of the package that houses the antenna. Unfortunately, forcing these definitions on the equipment manufactures is not "flexible." A third way to deal with the influence of non-connected elements on the antenna is to custom tune the antenna for each situation — every possible style of packaging, for example. This requires designing different antennas for different packages, which is not economical unless the radio equipment will be manufactured in large quantities.

There is a need for an antenna that is customizable to a particular installation at minimum cost and without the need for additional matching elements to be purchased and installed into the radio. An antenna may be incorporated into a packaged radio by integrating it into either the PWB or the radio package (see ***Figure 2***). In this instance, the antenna cost is low because the PWB and package have to be manufactured anyway. But the antenna's performance may be compromised because the materials used to manufacture the PWB or package are not suited to the requirements of the antenna design. The main drawback is that the cost of custom designing an integrated antenna is high. Another approach is to design the antenna as a discrete element that is attached or connected to the PWB (see ***Figure 3***). This usually results in better performance at higher cost. The antenna

Planar Monolithics Industries, Inc.

100 dB ISOLATION

UNPARALLELED PERFORMANCE
100 MHz TO 40 GHz SWITCHES

- Amplifiers
- Attenuators - Variable
- DLVA & ERDLVA & SDLVA's
- DTO's & Frequency Synthesizers
- Filters
- Form, Fit & Function Products
- IFM's & Frequency Discriminators
- Integrated MIC/MMIC Modules
- I/Q Vector Modulators
- Limiters & Detectors
- Log Amplifiers
- Pulse & Bi-Phase Modulators
- Phase Shifters
- Rack & Chassis Mount Products
- Receiver Front Ends & Transceivers
- Single Sideband Modulators
- SMT & QFN Products
- Solid-State Switches
- Switch Matrices
- Switch Filter Banks
- Threshold Detectors
- USB Products

PMI MODEL No: P2T-100M40G-110-T-512-292FF

- 0.1 TO 40 GHz Frequency Range
- Absorptive/Non-Reflective, +20 dBm CW
- 4.3 dB Insertion Loss (0.1 TO 18 GHz)
  4.3 dB Insertion Loss (18 TO 26.5 GHz)
  5.7 dB Insertion Loss (26.5 TO 40 GHz)
- 86.9 dB Isolation (0.1 TO 0.3, 26.5 TO 40 GHz)
  101.3 dB Isolation (0.3 TO 18 GHz)
  102.7 dB Isolation (18 TO 26.5 GHz)
- 2.4:1 VSWR
- 20 ns Switching Speed
- DC Voltage & Current
  +5 VDC @ 120 mA
  -12 VDC @ 65 mA
- 2.92 mm Female Connectors

PMI MODEL No: P4T-100M40G-110-T-512-292FF-IND

- 0.1 TO 40 GHz Frequency Range
- Absorptive/Non-Reflective, +20 dBm CW
- 3.2 dB Insertion Loss (0.1 TO 18 GHz)
  4.2 dB Insertion Loss (18 TO 26.5 GHz)
  6.6 dB Insertion Loss (26.5 GHz TO 40 GHz)
- 101.1 dB Isolation (0.1 TO 18 GHz)
  99.2 dB Isolation (18 TO 26.5 GHz)
  85.5 dB Isolation (26.5 TO 40 GHz)
- 2.0:1 VSWR
- 20 ns Switching Speed
- DC Voltage & Current
  +5 VDC @ 250 mA
  -12 VDC @ 150 mA
- 2.92 mm Female Connectors

PMI MODEL No: P8T-100M40G-95-T-512-292FF-IND

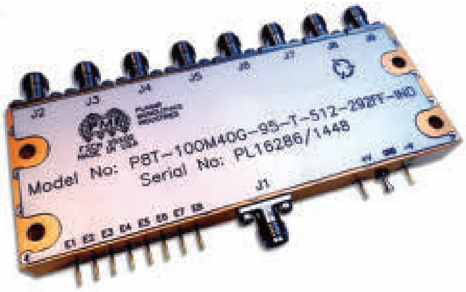

- 0.1 TO 40 GHz Frequency Range
- Absorptive/Non-Reflective, +20 dBm CW
- 5.8 dB Insertion Loss (0.1 TO 18 GHz)
  6.6 dB Insertion Loss (18 TO 26.5 GHz)
  9.5 dB Insertion Loss (26.5 TO 40 GHz)
- 105.3 dB Isolation (0.1 TO 18 GHz)
  97.8 dB Isolation (18 TO 40 GHz)
- 2.8:1 VSWR
- 60 ns Switching Speed
- DC Voltage & Current
  +5 VDC @ 500 mA
  -12 VDC @ 200 mA
- 2.92 mm Female Connectors

All Data Taken From Existing Units

West Coast Operation:
4921 Robert J. Mathews Pkwy, Suite 1
El Dorado Hills, CA 95762 USA
Tel: 916-542-1401 Fax: 916-265-2597
ISO9001:2008 REGISTERED
Email: sales@pmi-rf.com

East Coast Operation:
7311-F Grove Road
Frederick, MD 21704 USA
Tel: 301-662-5019 Fax: 301-662-1731
ISO9001:2008 REGISTERED
Website: www.pmi-rf.com

Hermetic Sealing, High Reliability To MIL-STD-883, Small Quantity Requirements Accepted & We Welcome Custom Designs Too.

cost is slightly higher, and it typically requires a custom matching network which contributes to the total manufacturing cost of the antenna. The design cost is lower but now includes the matching network. A third option to incorporate an antenna into a packaged radio is by providing a short "pigtail" with the antenna (see ***Figure 4***). This method allows the antenna to be placed away from the PWB, allowing more design flexibility; however, the cost of the pigtail, a board connector and the inevitable matching network contribute to the antenna cost.

MULTIBAND HYBRID DESIGN

In the proposed design, some of the antenna's radiating functionality is designed into the PWB, with the remainder designed into a mass-produced element that is attached to the PWB during radio assembly. The radiating functionality is shared between an integrated, customized PWB and the mass-produced portion — a composite of the two.

Prior designs divided the antenna into a PWB portion that operates in one sub-band and an attached portion that operates in another sub-band, i.e., in an uncooperative manner. With this design approach, both the PWB and the attached portion operate cooperatively over the entire frequency range of the design. Tuning is still required for the antenna to be matched to the packaged radio, yet all the needed tuning features are incorporated into the "free" PWB portion (see ***Figure 5***). The PWB may be tuned at one or more separate locations for optimum matching, while the attached portion is designed to be economically mass produced while providing the improved performance associated with the discrete antennas of prior art. The hexaband embodiment is able to work in a variety of packaged cellular radios because it is a composite of a mass-produced portion that radiates efficiently, like the typical antenna mounted on a PWB, and a highly customizable, tunable portion that is essentially free of manufacturing cost, like the typical antenna that is integrated into the PWB.

The applied, mass-produced hardware shown in Figure 5 was realized from a metal stamping, although it may also be fabricated from metallization applied to a supporting structure made from ceramic, plastic, glass or the like. The mass-produced segment may be self-supporting or supported by a non-metallic structure. The key feature of the design is that the antenna's functionality is hybridized, with tunable matching functionality incorporated into the integrated PWB and radiating functionality shared by the PWB and the mass-produced element.

PERFORMANCE

To gauge the performance of the hybrid design, a "real" board layout and components (see ***Figure 6***) were tested. The grounded coplanar waveguide RF trace was interrupted at the radio module's RF pin, and a backside

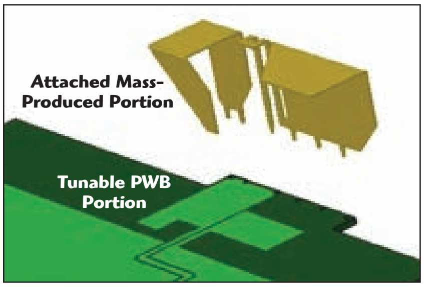

▲ *Fig. 5 Proposed design is a composite of a tunable, low cost, integrated portion and an efficiently radiating mass-produced portion.*

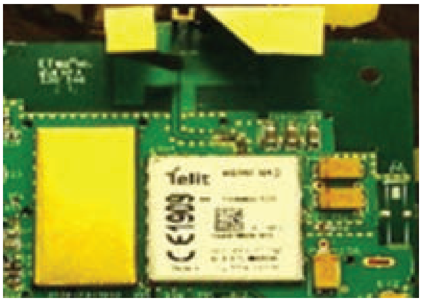

▲ *Fig. 6 Assembled prototype of the hybrid antenna.*

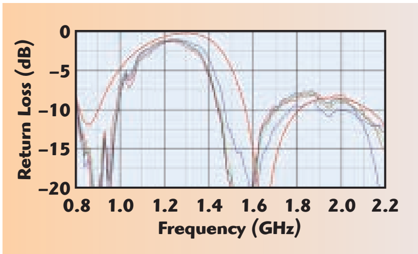

▲ *Fig. 7 Return loss of five samples compared to the simulation.*


IMAGING
BOARD TO BOARD
SMP & SMPM
DELTA
ELECTRONICS MFG. CORP
Connect Here
MODULE TO MODULE
ROBUST & RELIABLE
ARROW
Aerospace & Defense
A.E. Petsche Co.
FOR ALL YOUR
RF INTERCONNECT NEEDS...
A.E. Petsche Co.
Franchised Distributor For
Delta Electronics Mfg. Corp.
www.aepetsche.com
(844) AEP-7600

TABLE 1 MODELED GAIN CHARACTERISTICS OF HYBRID ANTENNA						
Frequency (MHz)	824	880	960	1710	1990	2170
Peak Gain (dBi)	2.56	2.70	2.92	3.98	4.37	4.50

SMA wave launcher was soldered to the modified board. The measured return loss of five prototypes is shown in ***Figure 7***. The modeled peak gains of the new design are presented in ***Table 1***, and the typical simulated antenna radiation patterns are presented in ***Figure 8***.

During simulation, it was noted that adding a shunt inductor to the design improved the return loss of the upper frequency range to –15 dB. This strategy would have improved the input match but at the expense of ohmic loss in the inductor and added manufacturing cost. The measured return loss of the baseline design at the upper frequency was -7.5 dB (0.178 reflection coefficient). If we improve the return loss to -15 dB (0.032 reflection coefficient) with the addition of the shunt inductor, the additional power delivered to the antenna would potentially be $10 \cdot \log_{10}(1 - 0.146) \approx 0.7$ dB. But if we allow for the insertion loss of a lumped inductor, say 0.2 dB, the potential benefit of improving the match amounts to less than a half decibel at the matched frequency. For many applications, this slight improvement in match does not justify the additional cost and complexity of adding the matching element to the bill of materials.

CONCLUSION

A new hexaband cellular antenna partly integrated into the PWB and partly a massed produced component has been designed and tested. The new design demonstrates the benefits of both customization and high volume production, without the need for a separate matching network. Measured and modeled data of the prototypes are in good agreement.

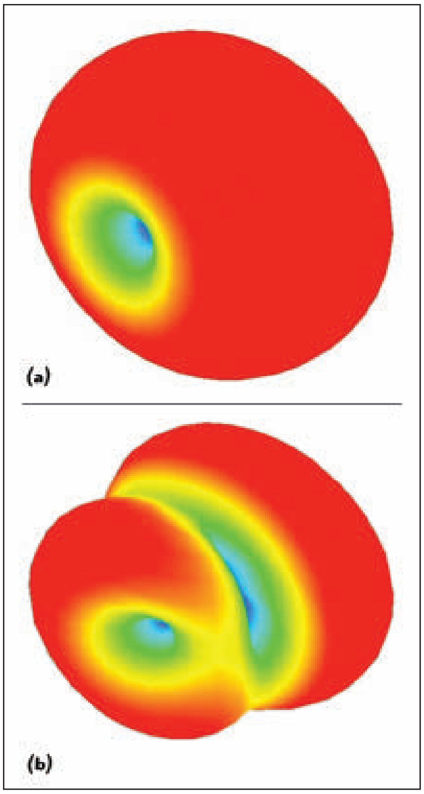

▲ *Fig. 8 Typical radiation pattern of the hybrid antenna in the 824 to 960 MHz (a) and 1710 to 2170 MHz (b) cellular bands.*

ACKNOWLEDGMENT

The assistance of the staff at the University of Arkansas High Density Electronics Center (HiDEC) is greatly appreciated in building and testing the prototypes.■

References

1. “PA.25.A,” Application Note (APN-11-8-002.B).pdf, Accessed May 17, 2015, www.taoglas.com/images/product_images/original_images/PA.25.A%20Application%20Note%20%28APN-11-8-002.B%29.pdf, p. 23.
2. “Baseband and Disassembling the LG Optimus 2X - LG Optimus 2X & NVIDIA Tegra 2 Review: The First Dual-Core Smartphone,” Accessed May 17, 2015, www.anandtech.com/show/4144/lg-optimus-2x-nvidia-tegra-2-review-the-first-dual-core-smartphone/9.
3. “PAD.25 Evaluation Board,” Accessed May 25, 2015, www.digikey.com/catalog/en/partgroup/pad-25-evaluation-board/31496.
4. Embedded_LTE_1002289_20150213.pdf, Accessed May 17, 2015. www.ethertronics.com/files/1414/2386/9980/Embedded_LTE_1002289_20150213.pdf, p. 2.

Full Wave Matching Circuit Optimization Shortens Design Iterations

Jeff Barney and Scott Langdon
Remcom Inc., State College, Pa.

Full wave matching circuit optimization (FW-MCO) is a new technology that combines full wave, 3D electromagnetic (EM) simulation with circuit optimization into a novel approach for solving an age-old RF problem: determining which component values provide the desired match for a given matching network layout. Gone are the days of soldering components in and out of a prototype, trying to achieve the desired performance. This article describes the design process using the design of a matching circuit for a GPS-Bluetooth antenna.

Matching network design is challenging, and RF engineers lack a robust tool for choosing which component values to plug into a matching network layout. Testing a single configuration at a time is expensive, slow and does not result in optimal performance. Existing schematic-based software tools help designers choose a circuit topology to match an antenna according to design goals, such as maximizing efficiency. At low frequencies, the predicted match from a schematic can be comparable to the measured performance of a physical circuit because the connections are very short in terms of wavelengths, the loss is low, and parasitics and coupling with other parts of the geometry are minimal. At higher frequencies, perfect wires become RF components like radiators or lossy transmission lines. Traces couple with each other and with other parts of the geometry. Since the EM interactions are usually more complex than what is represented in the schematic, the resulting physical performance can vary from what the schematic predicts.

Fortunately, full wave electromagnetic simulation captures these complex interactions, so it is possible to perform an optimization which will find the proper circuit component values without trial and error. FW-MCO addresses this missing link in the design process by modeling the RF effects and utilizing that information in the component selection process.

▲ *Fig. 1 Unmatched GPS-Bluetooth antenna.*

MATCHING NETWORK DESIGN WORKFLOW

The workflow for designing any new device is iterative, with multiple false starts, branches and challenges. As engineers gain an understanding of the problem areas and develop more efficient processes, workflow linearity increases and managers shorten their expectations for design cycle lengths. Ignoring the iterative loops, the following are the four main steps to design a matched antenna.

Starting with an unmatched antenna — either a physical prototype or CAD model — an RF engineer's first task is to determine the input impedance and corresponding S_{11} of the radiating structure. The GPS-Bluetooth antenna shown in ***Figure 1*** will be used for this discussion. Two main techniques are used for determining its input impedance. Historically, and in many cases still preferred, a network analyzer measures the impedance in a lab. Recently, the use of full wave, 3D EM simulation has become more popular; Remcom's XFdtd and ANSYS' HFSS have become commonplace for characterizing an antenna. ***Figure 2*** shows the reflection coefficient of the unmatched antenna.

With S-parameter data for the antenna, the second step employs circuit solvers such as

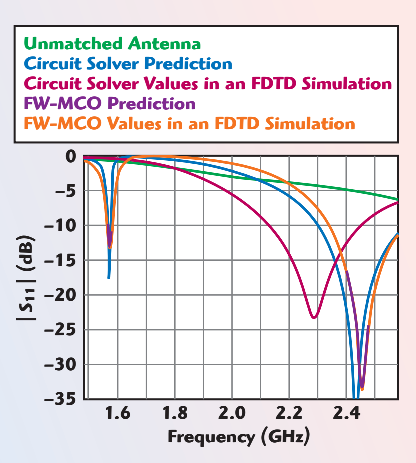

▲ *Fig. 2 Antenna* $|S_{11}|$ *for various cases.*

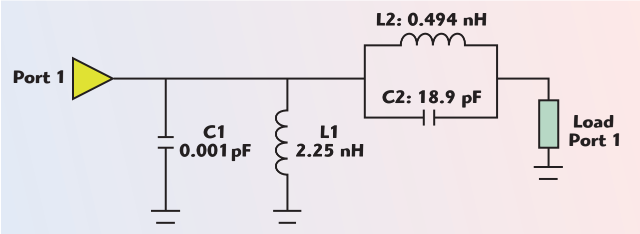

▲ *Fig. 3 Topology for the GPS-Bluetooth antenna's matching network.*

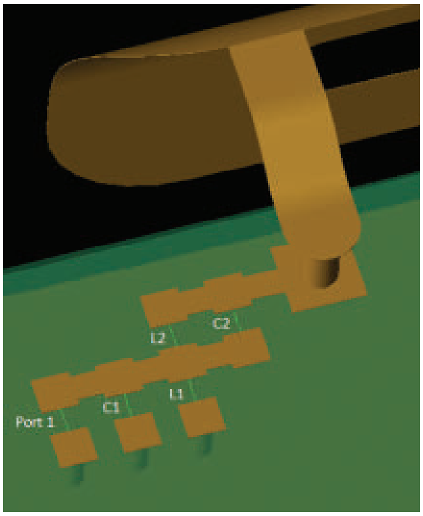

▲ *Fig. 4 Matching network layout.*

Optenni's Optenni Lab and Keysight's ADS. These have schematic-based editors for building matching network topologies, where the schematic comprises the list of components and the nodes that connect them. Circuit solvers analyze the schematic by maintaining voltage and current relationships across the components and at the nodes. ***Figure 3*** shows a four element matching network topology that provides an acceptable match in the GPS and Bluetooth bands. The corresponding S-parameter prediction from the circuit solver is also shown in Figure 2.

Once a matching network topology and initial component values have been generated, the engineer converts the schematic-based topology to a physical layout on a printed circuit board (PCB). Depending on the engineering team's process, mechanical engineers may get involved in the layout process, utilizing software products from Cadence or Mentor Graphics. ***Figure 4*** shows the matching network layout for the GPS-Bluetooth antenna (the lumped components are shown as green lines connecting the copper traces).

At the completion of step three, the RF engineer has an updated physical prototype or CAD model that includes the matching network layout. The layout will reflect the initial lumped component values determined from the circuit solver in step two. If the device is operating at a low enough frequency or the antenna has been isolated from the matching network, a measurement or full wave simulation of the updated prototype will show good agreement with the circuit solver, and the engineer moves forward to product testing. At higher frequencies, a fourth step in the antenna design workflow is generally required, because the updated prototype does not perform as the circuit solver predicted. This difference can be seen by comparing the circuit solver prediction to the finite difference time domain (FDTD) simulation in Figure 2.

In the fourth step, the RF engineers determine the final component values that provide the desired performance with the matching network as it is laid out on the PCB. Until recently, no tools were available to effectively address this problem, so engineers relied on costly techniques that provided sub-optimal performance, such as soldering components in and out of a prototype. FW-MCO technology overcomes this challenge by allowing RF engineers to consider thousands of component combinations and de-

TABLE 1

SELECTED COMPONENT VALUES

	Circuit Solver	FW-MCO
C1	0.001 pF	0.2 pF
C2	18.9 pF	5.6 pF
L1	2.25 nH	1.7 nH
L2	0.494 nH	0.6 nH

termine the optimal antenna performance. ***Table 1*** shows the significant difference between the component values determined by the circuit solver and the optimal ones chosen by FW-MCO. The final two plots in Figure 2 show that the predicted S-parameters from FW-MCO match the validation from an FDTD simulation.

FW-MCO

Specifically created to address the final step in the matching network design workflow, FW-MCO selects the optimal set of lumped component values from the list of allowable components. It uses efficiency and/or S-parameter goals to rate one set against another, accounting for the myriad of electromagnetic phenomena affecting the matching network's performance. There are two main steps to FW-MCO: system characterization and component selection.

FW-MCO's system characterization step utilizes full wave, 3D electromagnetic simulation to analyze the matching network's physical layout and surrounding environment. Unlike a circuit solver, FW-MCO doesn't look at the matching network as a set of lumped components that are connected to nodes by defined transmission lines. Instead, FW-MCO treats each lumped component as though it is plugged into a system made up of a 3D environment containing PCB traces, radiating elements, plastic housing, antenna loading, etc. ***Figure 5*** shows how circuit components are plugged directly into the surrounding physical geometry via the FDTD mesh. The system characterization accounts for field interactions within the matching network, between the matching network and radiating antenna(s) and throughout the entire device. Once characterized, the system is represented by a response matrix that defines the interaction of each component with the system and, consequently, each other. Since FW-MCO abstracts the system into a response matrix, it implicitly accounts for the physical layout of the matching network. For example, it is not necessary to explicitly specify the length of a transmission line because that information is contained in the response matrix.

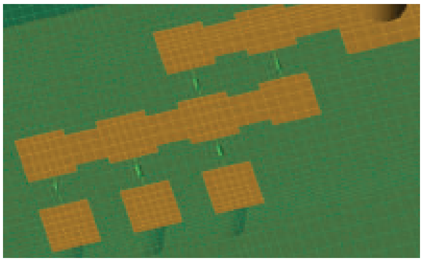

▲ *Fig. 5 Lumped components simulated in a FDTD mesh.*

Once the system has been characterized, it is possible to select any set of components and determine the associated antenna match based on the response matrix without needing to rerun a full wave simulation. FW-MCO's second step, therefore, becomes an optimization problem, where the optimal component values are determined. The RF engineer defines ranges of allowable component values and chooses desired goals for maximum optimization. The list of allowable component values represents the bin of components that can be used in the design. Often, this is equivalent to the list of components available from a component supplier. An individual component can be passive or active; the requirement is that the component be represented in the frequency domain. This provides the flexibility to populate the list with inductors, capacitors and tunable components that are treated as ideal components or realistic ones defined by an *.s2p file. The component values can vary continuously or be restricted to a finite number of fixed values within the desired range, representing actual values available from the manufacturer. Radiation efficiency, system efficiency, S-parameters or a combination can be used to define the goals. In addition, the RF engineer needs to provide the associated threshold over a specified frequency range. For example, one goal could be to find a set of component values that provides greater than 68 percent radiation efficiency over the desired LTE bands.

The optimization treats each component as a variable that can take on one value from the associated list of allowable component values. As such, the optimization algorithm needs to be able to handle multiple variables and be able to identify the global minimum from the multitude of local minima. Particle swarm optimization and genetic algorithms are both able to make this distinction. At the conclusion of the optimization, the optimal set of component values will be available. If some goals fail to be met, then the RF engineer needs to circle back in the workflow and make an adjustment. That may entail changing the physical layout of the matching network, or the change may be as far back in the design process as modifying the antenna structure. If each goal has been met, then these components can be considered the final values and plugged into the prototype for validation and product testing. Since system characterization was completed with full wave, 3D EM simulation, a close match between the FW-MCO prediction and measured results can be expected.

FW-MCO VS. CIRCUIT SOLVERS

While FW-MCO and circuit solvers are both used for matching network design, they are primarily differentiated by the data available to them. For a single port antenna, a circuit solver is provided the source impedance, S_{11}, and radiation efficiency as inputs. When the matching network schematic is analyzed, circuit solvers are limited because they use empirical formulas to maintain voltage and current relationships across the components. They cannot account for field interactions between components, between the components and active antennas and between the components and the rest of the device. FW-MCO, on the other hand, captures all the field interactions that are computed by the full wave EM simulation and selects component values based on that information. As an example, consider the eight element matching network topology in ***Figure 6a***. Physically, it can be laid out as shown in ***Figure 6b*** or ***6c***. While a circuit solver will only return one set of initial component values for this topology, FW-MCO will compute different response matrices for the two different layouts. This leads to the selection of two sets of component values to match the corresponding physical layouts.

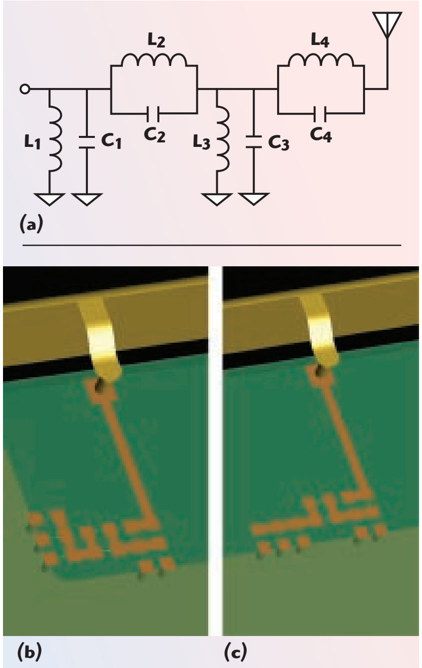

▲ *Fig. 6 Eight element matching circuit topology (a) with two physical layouts (b and c).*

FW-MCO does not replace circuit solvers in matching network design. The two technologies are appropriate for different steps in the workflow. Circuit solvers identify the appropriate topology and provide initial component values in the middle of the workflow. At the end, FW-MCO analyzes the physical layout and returns final component values.

APPLICATIONS

Traditional LC matching network design for a single antenna in free space is used extensively in device design and is readily supported using the FW-MCO approach previously outlined. Consumer demands for reliable connectivity and high data rates, however, are pushing RF engineers beyond traditional design. Fortunately, the flexibility of FW-MCO supports the design of multiple antenna loading configurations and multiple antennas.

Many devices operate under different antenna loading configurations. Consider any hand-held device, where the antenna loading will be different when the device is in free space or being held in a hand. These two configurations lead to different input impedances, so a match-

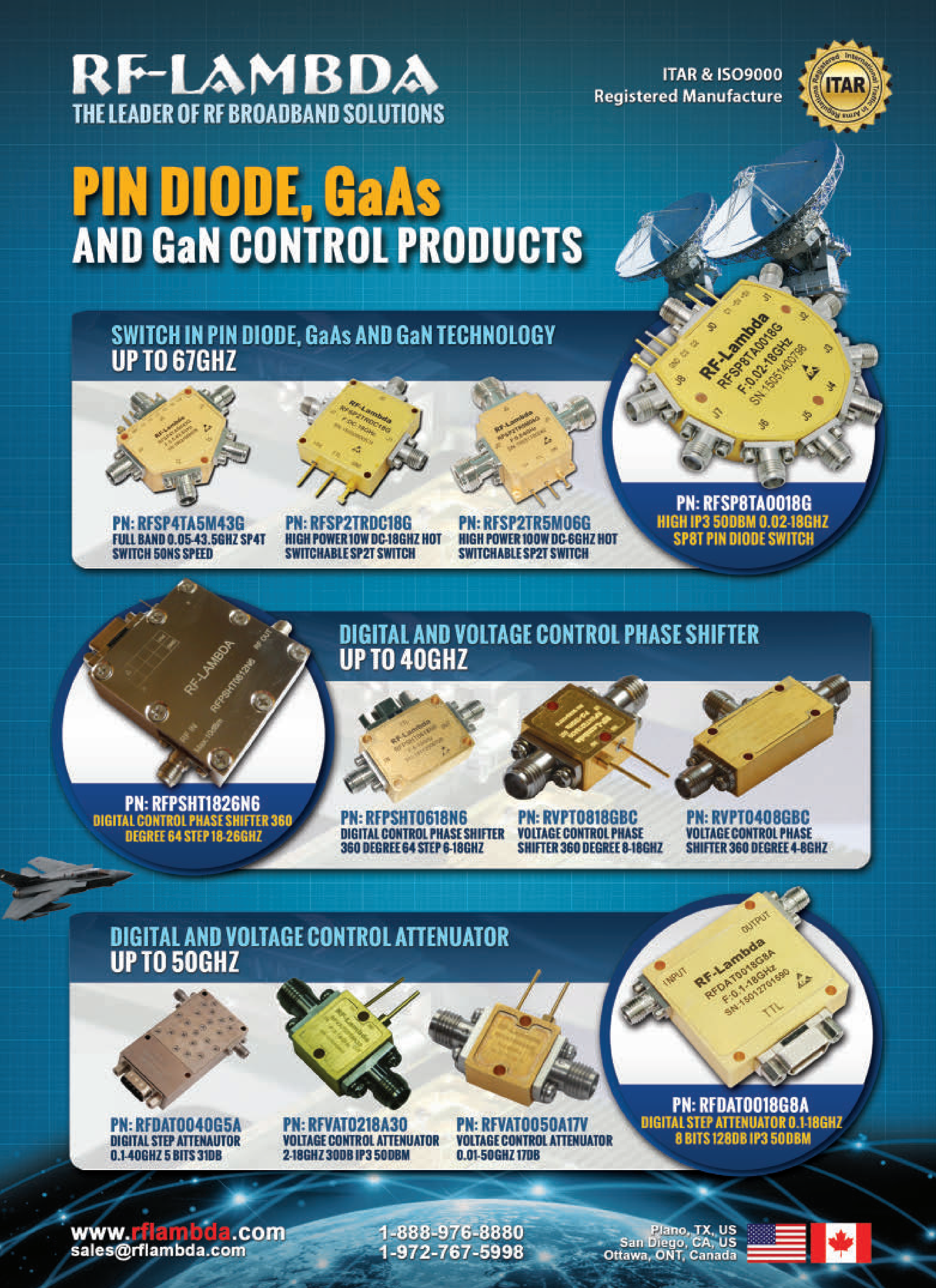
RF-LAMBDA
THE LEADER OF RF BROADBAND SOLUTIONS
ITAR & ISO9000
Registered Manufacture
ITAR
PIN DIODE, GaAs
AND GaN CONTROL PRODUCTS
SWITCH IN PIN DIODE, GaAs AND GaN TECHNOLOGY
UP TO 67GHZ
PN: RFSP4TA5M43G
FULL BAND 0.05-43.5GHZ SP4T
SWITCH 50NS SPEED
PN: RFSP2TRDC18G
HIGH POWER 10W DC-18GHZ HOT
SWITCHABLE SP2T SWITCH
PN: RFSP2TR5M06G
HIGH POWER 100W DC-6GHZ HOT
SWITCHABLE SP2T SWITCH
RF-Lambda
RFSP8TA0018G
F:0.02-18GHz
PN: RFSP8TA0018G
HIGH IP3 50DBM 0.02-18GHZ
SP8T PIN DIODE SWITCH
DIGITAL AND VOLTAGE CONTROL PHASE SHIFTER
UP TO 40GHZ
RF-LAMBDA
PN: RFPSHT1826N6
DIGITAL CONTROL PHASE SHIFTER 360
DEGREE 64 STEP 18-26GHZ
PN: RFPSHT0618N6
DIGITAL CONTROL PHASE SHIFTER
360 DEGREE 64 STEP 6-18GHZ
PN: RVPT0818GBC
VOLTAGE CONTROL PHASE
SHIFTER 360 DEGREE 8-18GHZ
PN: RVPT0408GBC
VOLTAGE CONTROL PHASE
SHIFTER 360 DEGREE 4-8GHZ
DIGITAL AND VOLTAGE CONTROL ATTENUATOR
UP TO 50GHZ
PN: RFDAT0040G5A
DIGITAL STEP ATTENAUTOR
0.1-40GHZ 5 BITS 31DB
PN: RFVAT0218A30
VOLTAGE CONTROL ATTENUATOR
2-18GHZ 30DB IP3 50DBM
PN: RFVAT0050A17V
VOLTAGE CONTROL ATTENUATOR
0.01-50GHZ 17DB
RF-Lambda
RFDAT0018G8A
F:0.1-18GHz
PN: RFDAT0018G8A
DIGITAL STEP ATTENUATOR 0.1-18GHZ
8 BITS 128DB IP3 50DBM
www.rflambda.com
sales@rflambda.com
1-888-976-8880
1-972-767-5998
Plano, TX, US
San Diego, CA, US
Ottawa, ONT, Canada

ing network that passes requirements for free space operation may not be sufficient when the device is held. For simpler, cheaper designs, the RF engineer may use a traditional matching network with LC values that best fit both cases. A more advanced solution would be to incorporate a tunable component into the matching network and a proximity sensor at the device level. In a 3D EM simulator, a phantom hand model would be included in the simulation space for the hand-held configuration. This will lead to different field interactions with the components than the free space configuration. Remember that the response matrix is used to characterize all field interactions affecting the components of the matching network. Therefore, two response matrices are needed to capture the field information for the two loading configurations, which will serve as inputs into a single optimization.

In the advanced case with tunable components, the proximity sensor would be used to detect whether the device was operating in free space or operating while being held. The tunable component's state would then be changed depending on the loading configuration, and this would change the matched impedance. FW-MCO uses similar logic to tie the loading configuration information in the response matrix to the tuner states in setting up the optimization. The goals would be defined to generate better than 93 percent and 75 percent radiation efficiency in the LTE bands for the free space and hand-held response matrices, respectively. As output, the optimization would return two tuner values, one associated with each response matrix. If there were LC components in the matching network, the optimization would also return their fixed values independent of the loading configuration.

The design of multiple antennas also provides a challenge to RF engineers because energy from the active antenna can be lost in the passive antenna, instead of being radiated. This is known as "suck out" and can be identified through S_{21} or reduced radiation efficiency. Using FW-MCO to select optimal component values that reduce suck out is straightforward. The two antennas and corresponding matching networks would be included in the 3D EM simulation space. A single response matrix simulation would characterize the system and determine field interactions affecting all components. Finally, goals would be defined that simultaneously maximized radiation efficiency when antenna 1 was active and minimized S_{21}. Depending on device design decisions, FW-MCO could also be used to identify tunable components that create a poor match at antenna 2 when antenna 1 is transmitting, yet a good match when antenna 2 is transmitting.

CONCLUSION

A new technology, full wave matching circuit optimization, fills the last gap in matching network design. Unlike schematic-based circuit solvers, it accounts for all electromagnetic field interactions with components. Using this information, FW-MCO is able to analyze thousands of component combinations to determine the optimal set that meets design requirements. As the complexity of matching network design increases to support the latest communication requirements, FW-MCO will become a necessity because the number of permutations will be unwieldy without optimization techniques. ■

HIGH
POWER
100 MHz
to 20 GHz

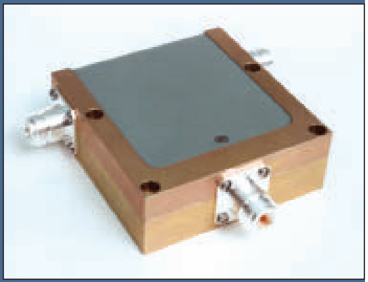

For Military/Radar Applications.

Isolators/Circulators

As one of the leading suppliers of ferrite components in the industry, UTE Microwave has pioneered innovative designs, quality craftsmanship and exceptionally high quality products. Custom designs, standards...many of them off-the-shelf, are the result of over 35 years of experience in the industry. UTE Microwave continues this tradition with new products for ever changing applications. Our broad line of HIGH POWER, low loss circulators and isolators spans the spectrum from below 100 MHz in coax/stripline units to waveguide devices at 18 GHz for both peak and average powers.

325 MHz NEW HIGH POWER Circulator for Radar & UHF Frequencies

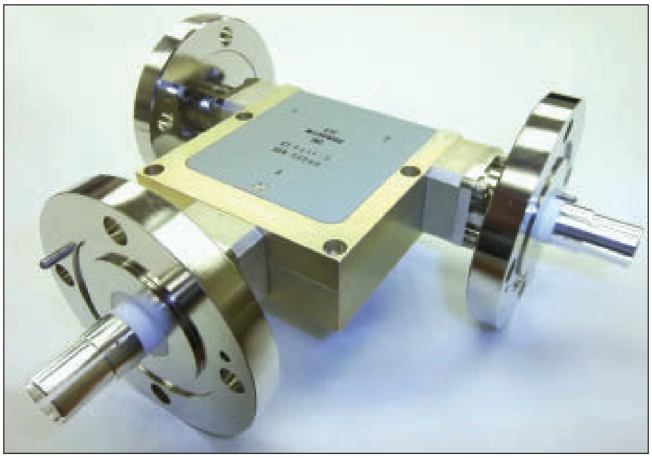

Model CT-1864-S is rated at 60kW peak and 600W average power at 325 MHz. The unit provides 20 dB minimum isolation, 0.2 dB insertion loss and 1.20:1 maximum VSWR. Its extremely compact design has flange to flange insertion length of only 6-3/4" and a height of 5-1/4". For use in radar applications, it has 1-5/8" EIA connectors. It is also available at other UHF frequencies and connector types.

HIGH POWER Drop-in Series

A broad line of low loss HIGH POWER Drop-in circulators are available from VHF to Ku band including Kilowatt average power levels at VHF thru S band. L and S band radar are a specialty. A few of these are shown here.

A) 2.7–3.1 GHZ 1 kW pk, 100 W av

B) 1.2–1.4 GHZ 3 kW pk, 300 W av

C) UHF TV Band 5 kW pk, 500 W av

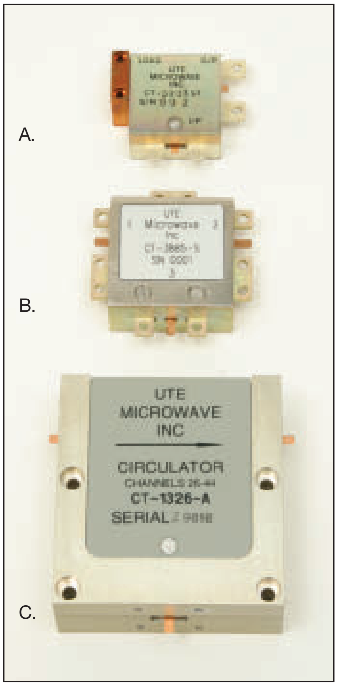

Our "POWER-LINE" serves the COMMUNICATIONS, TELECOM, MEDICAL, SCIENTIFIC, TV, PCS and INDUSTRIAL markets.

The following models are examples of our High Power units

Model No.	Power	Connectors	Freq. Range
CT-1542-D	10 Kw Pk 1 Kw Av	DIN 7/16	420–470 MHz
CT-2608-S	3 Kw Pk 300 W Av	"Drop-in"	1.2–1.4 GHz
CT-3877-S	2.5 Kw Pk 250 W Av	"Drop-in"	2.7–3.1 GHz
CT-3838-N	5 Kw Pk 500 W Av	N Conn.	2.7–3.1 GHz
CT-1645-N	250 W Satcom	N Conn.	240–320 MHz
CT-1739-D	20 Kw Pk 1 Kw Av	DIN 7/16	128 MHz Medical

FEATURES:

- Power levels to 5 KW CW, 75 KW Pk.
- Low Intermod Units
- Low Loss Options
- Extended Octave Bandwidths
- Power Monitors and DC Blocks
- Iso Filter-Monitor Assemblies

Broadband Units • Common Band Devices • High Isolation Units • Multiport Devices • Drop-In Devices • Wireless/PCN Devices • High-Power Industrial/Medical Iso Adaptors Waveguide Junctions • High-Power TV Units • VHF and UHF Devices

sales@utemicrowave.com

UTE MICROWAVE INC.

3500 Sunset Ave., Asbury Park, NJ 07712
Tel: 732-922-1009 Fax: 732-922-1848
E-mail: info@utemicrowave.com

Contact us for more information on our extensive product line and current catalog. We accept Visa, MC, Amex

INVITED PAPER

Scan page using layar app

Pulse Compression Radar System Analysis

Herbert Schmitt
Rohde & Schwarz, Munich, Germany

Today's pulse radar systems frequently use pulse compression. This technique combines excellent range resolution and high energy with low peak power levels. For this purpose, the transmission pulse is initially extended in bandwidth and time by intrapulse modulation. A corresponding matched filter in the radar's receivers compresses the received echo signal in time and increases the peak value by approximately the pulse compression ratio (see ***Figure 1***). This improves the time resolution and thus the range resolution by a factor of the compression. It also reduces the required peak power level, thereby reducing output amplifier and power supply complexity.

The increased pulse length, however, increases the blind range, and an influence of Doppler on range measurement accuracy can be observed. Furthermore, signal processing in a radar system becomes more complex. Depending on the modulation, the compressed pulse will not only have one narrow peak in time (the main lobe) but will also exhibit sidelobes, also known as time sidelobes or range sidelobes. These may cause false alarms or appear as a "blurring" of reflections. Despite these disadvantages, pulse compression is widely used today, as the advantages outweigh the disadvantages.

Typical transmission signal types include linear frequency modulation (LFM) or chirp, nonlinear frequency modulation, binary phase-

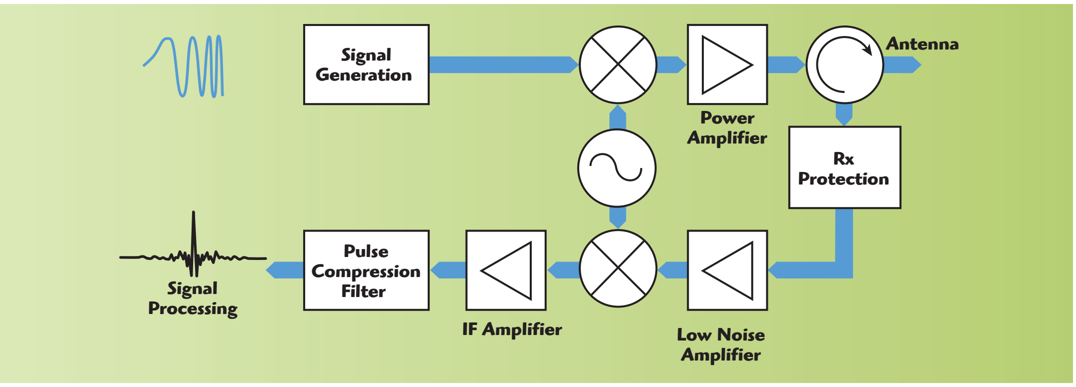

Fig. 1 Radar system using a digital pulse compression filter.

Anokiwave

mmW Solutions. Enabling a new world

Developer Kits for AESA Core Chip Solutions

AWS-0101-DK for the X-Band Low Noise Quad Core IC
AWS-0103-DK for the X-Band High Linearity Quad Core IC
AWS-0102-DK for the K-Band SATCOM Rx Quad Core IC

Enables full evaluation and RF testing of the complex Core ICs reducing system development time and cost

Includes all HW required for device interface

Comprehensive performance data included

Custom GUI to easily control test board

Step by step user's guide for quick setup

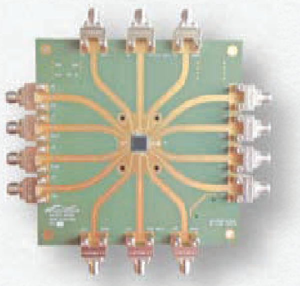

Complete RF test board with RF/DC and SPI connections

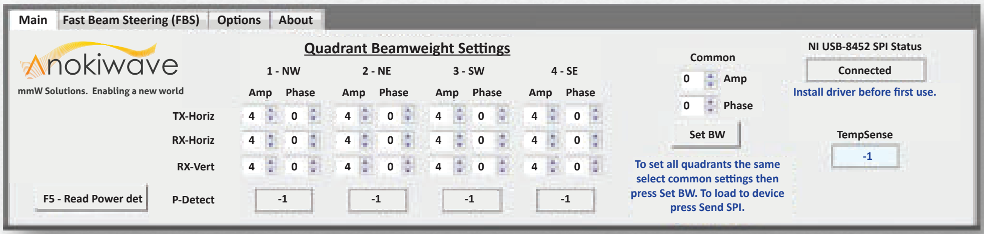

User friendly GUI provides access to all IC controls

mmW Si Core ICs

AESA ASICs

mmW Si Front End ICs

www.anokiwave.com

Fig. 2 *LFM compressed pulse. The correlated magnitude window shows the peak sidelobes are approximately 13 dB down from the peak.*

coded and polyphase-coded signals. An example of a binary phase-coded signal is binary phase shift keying (BPSK) with a Barker code. Although more refined techniques have been developed, LFM and Barker codes are still in wide use. In the case of a pure LFM, the compressed pulse shows a sin(×)/× response, and the level of the highest time sidelobe is theoretically 13.2 dB below the main lobe level. This ratio is also known as the peak to sidelobe level (PSL). The PSL represents the ability of a radar system to distinguish between large targets and small targets in the immediate vicinity. ***Figure 2*** shows an example of an LFM compressed pulse with an approximately 38 MHz linear chirp width, together with intrapulse frequency and phase characteristics.

Amplitude weighting, also known as windowing, can reduce the PSL to the required level, but at the expense of a reduced signal-to-noise ratio. In this case, the matched filter is implemented in the digital signal processing of the receiver as a correlation between the echo signal and the ideal Tx waveform. The basic operation, a convolution in time, is most efficiently done as multiplication in the frequency domain, by first performing a fast Fourier transform (FFT) on the received signal, then multiplying the signal by the reference chirp and finally converting it back to the time domain with an inverse FFT. Windowing is well known in FFT signal processing. Commonly used windowing functions are Hamming, Blackman and Blackman-Harris. ***Table 1*** compares the characteristics of these functions. ***Figure 3*** shows the same 38 MHz LFM signal, now windowed using a Blackman-Harris window; the PSL has dropped to –57 dB.

MEASUREMENT CHALLENGES

As soon as a radar uses pulse compression, measuring the pulse width or the rise and fall times is no longer enough for a measurement-based evaluation of the radar's performance. Any deviation from the desired ideal linear frequency ramp, reflections in the Tx chain, phase and amplitude distortions or modulator inaccuracies will affect the radar's performance, i.e., its range resolution and range accuracy. The effects can lead to a widening of the main lobe of the compressed pulse and may cause additional or increased time sidelobes exceeding the tolerable level or threshold.

Since LFM, BPSK and polyphase codes are adding modulation to the pulse, one might be inclined to treat this as a communications signal and apply error vector magnitude (EVM) metrics used to measure the quality of communications signals. However, EVM is not easily translated into radar performance parameters such as spatial resolution or false alarm rate. Analyzing the sidelobe behavior directly is therefore the method of choice for evaluating the performance of pulse compression radars. In order to track down sources of performance degradation, this needs to be done at different stages in the signal chain. Using a reference target and looking at the radar receiver processing output is not sufficient. Standard pulse analysis using a measuring instrument (typically a signal analyzer) is necessary, yet not enough. The signal analyzer must also analyze the transmission signal using a suitable matched filter and provide a correlation function, similar to how an ideal radar receiver would operate.

As a result of pulse compression, the compressed pulse in the time domain is displayed (see Figures 2 and 3). Any widening of the impulse response (the main lobe) that leads to a poorer range resolution is easy to measure, as well as the sidelobe levels and PSL. Further, frequency error and phase error versus the original pulse length can be shown. In the case of LFM, the frequency error gives a direct measure of the linearity of the frequency ramp.

Many other parameters are used to characterize the compressed signal. With respect to the main lobe, these are the 3 dB width of the main lobe; main lobe power, phase and frequency and the compression ratio. Important measurement parameters for the sidelobes are the PSL, the integrated sidelobe level and the sidelobe delay, i.e., the spacing in time between the main lobe and the closest sidelobe. Main lobe width and sidelobe delay are important system parameters influencing the achievable spatial resolution. Their measurement provides a fast and simple metric to assess the actual spatial resolution achieved in field use. Considering the many parameters that can be used, those most important to the measurement task should be selected. For this reason, any result table should be easy to configure by the user. Figures 2 and 3 show examples of how a signal and spectrum analyzer performs this analysis with its pulse measurement application complemented by a time sidelobe analysis function. The result table has been modified to show only the most important compression parameters. The instrument also provides statistics such as the standard deviation for each parameter, making

TABLE I

PROPERTIES OF SELECTED WINDOWING FUNCTIONS

Windowing Function	PSL (dB)	SNR Reduction (dB)	3 dB Width (FFT Bins)
Rectangular	–13.2	0	0.89
Hamming	–43	1.34	1.3
Blackman	–58	2.37	1.68
Blackman-Harris	–61	2.07	1.56

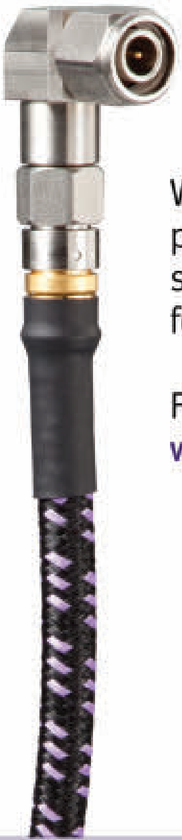

▲ *Fig. 3 Applying windowing in receiver processing reduces the sidelobe level to 57 dB below the peak.*

▲ *Fig. 4 Setting up a reference waveform (matched filter) for a nonlinear FM signal with polynomial coefficients.*

it possible to assess the stability of the radar signal and the repeatability of the measurement.

Another concern, besides the correlation function, is the analysis bandwidth or instantaneous bandwidth of the signal analyzer. The bandwidth of the signal analyzer has to cover the bandwidth occupied by the radar's Tx signal modulation. In the case of a frequency agile radar, the analyzer's bandwidth should also cover the entire frequency band used for agility. Some signal and spectrum analyzers cover internally up to 500 MHz instantaneous bandwidth. Up to 2 GHz of instantaneous bandwidth can be achieved by using a wideband IF output and digitizing this with a high-performance oscilloscope. In such a case, it is essential that the entire measurement chain, including the scope, be fully characterized for amplitude and group delay distortion. The operator should not need to interact with the signal analyzer and oscilloscope separately, instead operating the system from one point, the signal analyzer.

As the time sidelobe analysis is based on a correlation between an ideal Tx waveform, also referred to as the reference signal, and the measured Tx signal, the first step is to select and create the reference signal. For well known techniques such as LFM, nonlinear FM, Barker-coded BPSK or embedded Barker, it should not be necessary to use additional tools to create this reference; the signal analyzer should create this reference internally. ***Figure 4*** shows an example of how such a reference can be defined, in this case a nonlinear FM signal. For standard LFM, different windows such as Hamming, Hanning, Blackman-Harris, Gauss or Chebyshev should be selectable. Waveforms that are more complex than chirp or Barker codes are used today. Many of them are proprietary or confidential for a simple reason: if the codes are disclosed, a jammer can easily modulate its jamming signal to be compressed like the radar's own signal and increase the false alarm rate. To account for confidentiality, an analyzer for time sidelobe measurements has to be able to load user-specific reference waveforms as I/Q data.

For example, the R&S FSW features this function and provides tools to easily convert files created in MATLAB to the internal I/Q data format. Techniques where the analyzer captures the ideal reference signal and uses this signal in the measurement are even easier. Visualizing the properties of the imported I/Q data or the captured signal, including amplitude, frequency or autocorrelation, helps users determine whether the data is correctly imported. This technique also makes it possible to compare the waveforms at different stages in the

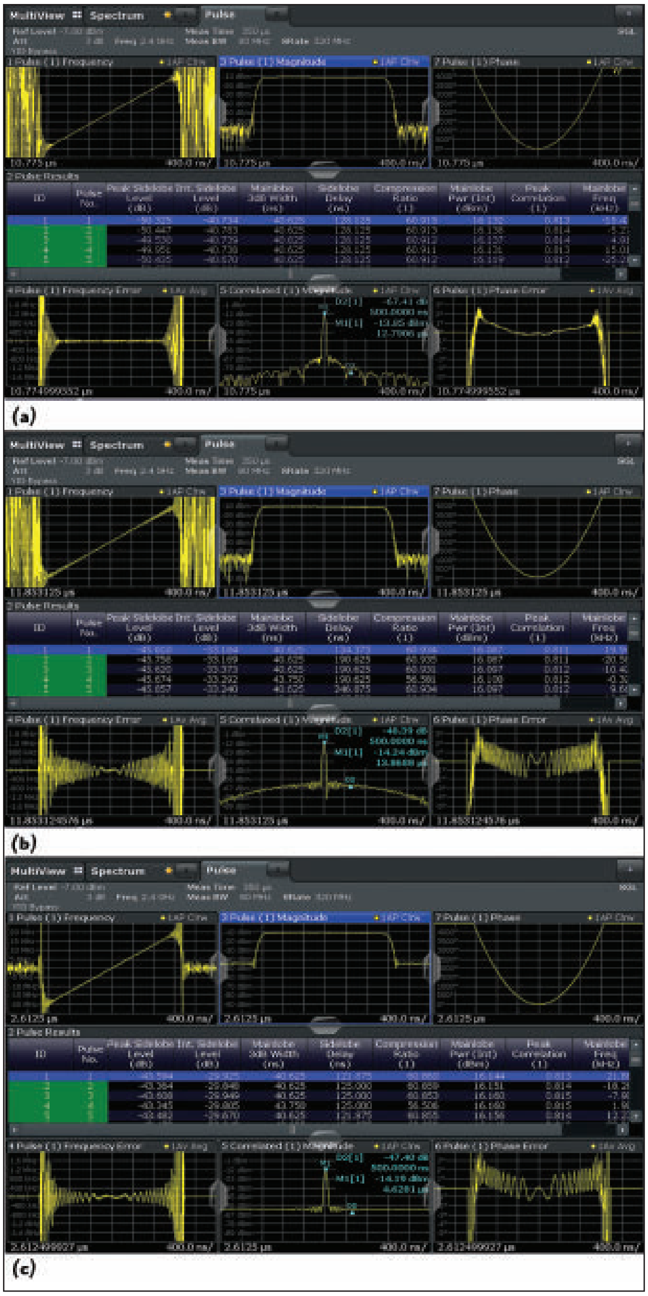

▲ *Fig. 5 Windowed LFM signal with no I/Q impairments (a) with gain imbalance (b) and I/Q offset (c).*

signal chain of the radar and isolate the cause of inaccuracies.

With the time sidelobe measurements well integrated into the analyzer's functions, the user simply displays the correlated pulse and, if necessary, the frequency and phase error and then adjusts tabular results to provide the parameters of interest. Influences from filters, amplifiers or other radar transmitter components are then easy to identify. ***Figures 5a*** and ***5b*** show how an I/Q modulator gain imbalance reduces the PSL from -50 dB to -45 dB. The integrated sidelobe level is reduced even further, from -40 dB in the undisturbed case to -33 dB. An offset on the I/Q modulator will also cause PSL degradation, down from -50 dB to -43 dB (see ***Figure 5c***). The effects can be distinguished by their impulse response as shown in the correlated magnitude display of Figures 5b and 5c.

Notwithstanding the importance of time sidelobe measurements, the more common pulse parameters — pulse width, PRI, rise and fall times, power, droop, overshoot, ringing, or pulse-to-pulse phase — and their statistics provide additional vital information. Therefore, a universal measuring instrument for radar applications should provide both time sidelobe measurements and comprehensive pulse analysis. Since the radar's performance depends on the stability of its oscillators, generally described as phase noise, the instrument should also accurately measure stable oscillators. Advanced signal analyzers provide phase noise measurement functions together with sophisticated pulse analysis, including time sidelobe measurements. They are ideal for many radar systems. To meet highly demanding stability requirements, dedicated phase noise analyzers are commonly used to measure phase noise. The latest measurement capabilities combine ultimate phase noise performance for pulsed signals with signal analysis and pulse analysis capabilities. ■

Scan page
using layar app

Accuracy in Simulation with CST STUDIO SUITE 2016

Computer Simulation Technology (CST)

CST® STUDIO SUITE® is an electromagnetic simulation tool used to design, analyze and optimize devices and systems at all stages of the development process. It is used in industries as diverse as electronics, automotive, aerospace, medical and energy, and covers the electromagnetic spectrum from statics to optics. By replacing physical prototypes with virtual ones, engineers can study how their products work at the earliest stages of design and reduce the number of physical models that need to be constructed.

For virtual prototyping to be a viable option, the simulation tools need to be accurate without sacrificing performance. For this reason, the release of CST STUDIO SUITE 2016 builds on the success of previous versions with a range of new features that make the analysis of systems more powerful while building on CST's reputation for accuracy.

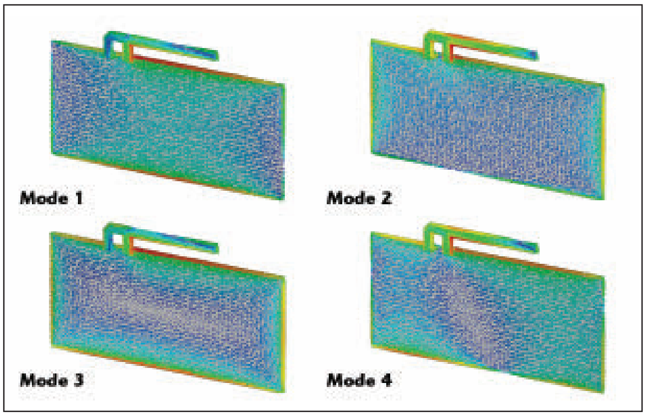

▲ *Fig. 1 The first four modes on a GSM-900 PIFA antenna calculated with CMA.*

CHARACTERISTIC MODE ANALYSIS

Characteristic Mode Analysis (CMA) is a technique developed to provide physical insight into the behavior of a conducting surface by calculating the current-modes that it can support. For example, CMA can be used on a patch antenna to identify the resonant frequencies of the patch. This allows engineers to tune the antenna to the correct frequencies and determine where to place the feed to couple into a particular radiating mode. ***Figure 1*** demonstrates one typical application of CMA to calculate the modes on a GSM-900 PIFA antenna.

The CMA tool is integrated into the method-of-moments (MOM) Integral Equation Solver in CST STUDIO SUITE, and calculates the modal significance (a measure of which modes are dominant at a particular frequency), far field radiation pattern and surface current distribution associated with each mode, with automatic mode-tracking. These features are particularly useful for analyzing and optimizing printed antennas, which often have to be compact and multiband.

REPRESENTING REALITY

To be useful to engineers, a simulation needs to accurately represent the physical system. CST STUDIO SUITE offers an extensive library of material types, such as lossy metals, ferrites and nonlinear materials. The 2016 version adds new advanced types, including arbitrary graded materials and perforated materials. Measured or simulated data can now be used to generate realistic thin panel materials to be included in models. This is particularly useful for modeling composite materials, such as carbon fiber, which have complex electromagnetic properties due to their structure.

Nonlinear circuit elements can be integrated directly into 3D EM simulations through CST's True Transient EM/Circuit Co-Simulation. In CST STUDIO SUITE 2016, the link between circuit and EM simulation is strengthened further by the new Combine Results in Transient Task feature. This allows the results of a 3D simulation to be included in a transient circuit simulation with no post-processing required. This is a feature that will benefit EMC engineers, for example, who need to simulate the behavior of electronic systems affected by pulses or realistic digital signals.

IMPROVED MESHING

The accuracy and performance of a simulation are heavily dependent on the quality of the mesh which describes the structure. Achieving very high mesh quality has previously led to innovations including PERFECT BOUNDARY APPROXIMATION (PBA)® for hexahedral meshes, True Geometry Approximation for curved tetrahedral meshes, and intelligent mesh engines for more efficient discretization. Two important new features have now been added to the repertoire: hybrid curved surface meshing and moving mesh optimization. The surface mesh used by the Integral Equation Solver is very efficient for structures such as reflector antennas and vehicle bodies, which are constructed from large, thin sheets of metal.

With the new version, the surface mesh can now use a hybrid combination of triangular and quadrilateral mesh cells, and these polygons can be curved and conformal to the structure (see ***Figure 2***). This means that a structure can be discretized very accurately with fewer mesh cells compared to traditional meshes, which can accelerate simulation significantly.

Moving mesh optimization is most useful when designing and tuning highly sensitive structures such as filters, which are usually described using a tetrahedral mesh. At each step of an optimization of such a structure, the model geometry changes slightly,

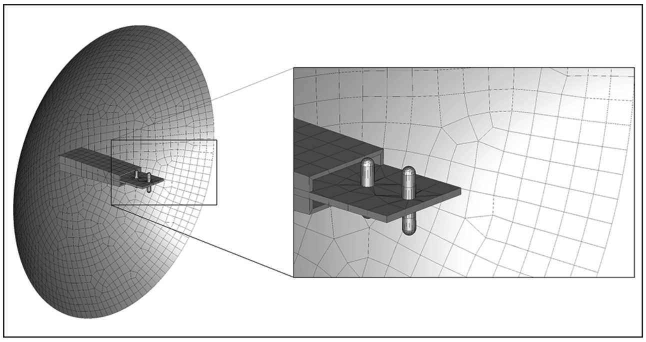

▲ *Fig. 2 Hybrid curved mesh on a parabolic reflector with double dipole splash-plate feed.*

which means that the mesh needs to change as well. Instead of recalculating the mesh from scratch, CST STUDIO SUITE 2016 can instead adjust the previous mesh to fit the new structure. This speeds up the meshing process, and can also improve accuracy by reducing the noise associated with repeated mesh generation.

A range of other improvements to the mesh engines include more intelligent mesh adaptation, sliding meshes for moving part simulation, and the ability to define mesh-independent parameters.

HIGH-PERFORMANCE COMPUTING

For very large or complex simulations that approach the limits of conventional computing hardware, high-performance computing (HPC) can offer significant time advantages. CST STUDIO SUITE supports multi-threading and multi-CPU parallelization in shared memory environments, hardware acceleration (Nvidia® Tesla® GPU and Intel® Xeon Phi®), and cluster computing using distributed computing and MPI.

It was recently certified as Intel® Cluster Ready, and its cluster computing capabilities have been expanded with the ability to perform True-Transient EM/Circuit Co-Simulation on MPI clusters. In addition, the Asymptotic Solver now also supports GPU acceleration, which can significantly speed up bistatic radar simulations and other simulations with large numbers of observation points.

LINUX

CST has supported Linux in HPC compute cluster environments for many years. This allowed simulation jobs to run in batch mode without user interaction. However, Linux-based operating systems are now becoming increasingly common for workstations, and CST STUDIO SUITE 2016 can now be used interactively directly on a Linux machine. This includes the powerful 3D modeling tools and results viewer, greatly increasing the number of tasks that can be performed entirely in a Linux environment.

VENDORVIEW

Computer Simulation Technology (CST), www.cst.com

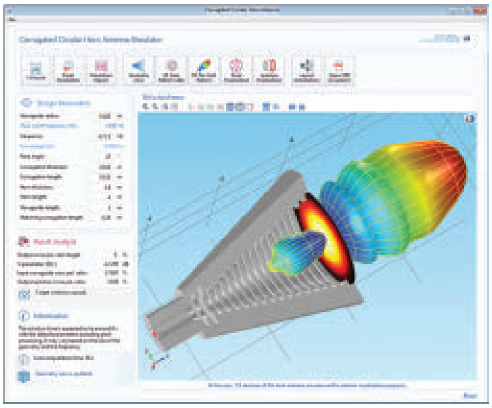

Better Microwave and RF Designs with COMSOL Multiphysics® 5.2

COMSOL, Inc.
Burlington, Mass.

If you have to frequently revise your RF and microwave designs to produce a viable end product, it could be you are not taking the effects of other physics into account. If you use multiphysics simulation software, you can create designs that will be optimized for the real world during the design process. COMSOL Multiphysics® version 5.2 gives all of these benefits plus the ability to wrap your models in an easy-to-use interface that can be shared in the form of apps. Real-world devices and products do not work in isolation. You may want to simulate the electromagnetic properties of a cell phone (see ***Figure 1***). To understand how the device will perform in reality, you need to consider the effects of heat transfer and the chemical properties of the battery. Similarly, if you want to accurately model a microwave oven, you need to simulate the coupled effect of heat transfer on the product design.

COMSOL Multiphysics is an all-encompassing multiphysics simulation tool that offers these capabilities. Going beyond multiphysics simulation, the Application Builder and COMSOL Server™ product enables simulation engineers to build and share applications based on their models. Simulation apps are simplified user interfaces for an underlying simulation. With an app, you can more quickly test parameters and see how different physical elements affect your design.

COMPLETE SUITE OF CAPABILITIES

For a simple, streamlined workflow when simulating your RF device design, use the RF Module, an add-on product to the COMSOL Multiphysics platform. Extensive capabilities make it easy to accurately model electromagnetic wave propagation and resonant behavior; simulate coupled physics effects such as structural deformations and heating; and compute electromagnetic field distributions, reflection, transmission, impedance and S-parameters.

Modeling RF and microwave designs requires just a few simple steps. Set up the geometry of your model as a 1D, 2D or 3D structure and select the required materials from an inclusive materials library. Or you can easily import an existing geometry from a favorite CAD program. Then, you select an analysis type for the simulation, including the governing equations, field formulations, or as an eigenvalue, frequency domain or fully transient problem. Before solving, define the ports and boundaries of your device with a full range of settings. The boundary conditions can represent perfect electrically conducting surfaces, thin lossy boundaries, excitation boundaries for modeling ports and lumped capacitive, inductive, and resistive elements. The RF Module meshes your model automatically. Once the model is solved, you can visualize your results and postprocess them for further analysis directly in the software's user interface.

Version 5.2 of COMSOL Multiphysics, which was released in November 2015, includes improvements to the core functionality, the Application Builder, COMSOL Server and all of the add-on modules. The RF Module includes a new feature specific to microwave and RF modeling: Smith charts are now available for visualizing the impedance of a transmission line and impedance matching (see ***Figure 2***).

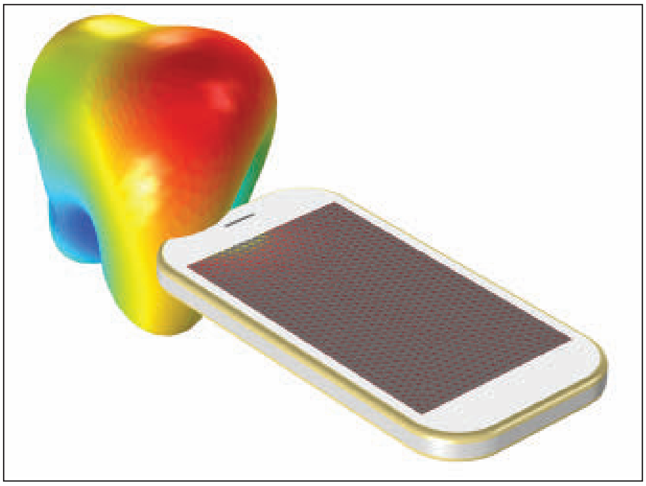

▲ *Fig. 1 The far field radiation pattern of a mobile device antenna, plotted in 3D in the COMSOL Multiphysics simulation software.*

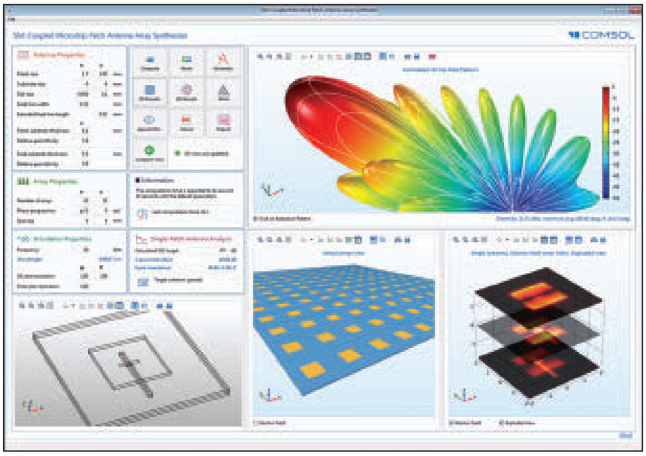

▲ *Fig. 3 The microstrip patch antenna array synthesizer is an RF simulation app optimized for 5G technology.*

In the core software platform, COMSOL Multiphysics now includes more robust meshing capabilities, which provide more accurate and reliable results. You are able to create annotations directly in plots when postprocessing simulation results.

BENEFITS OF SPECIALIZED APPS

Included in the COMSOL Multiphysics software platform, the Application Builder enables models to be saved as applications or apps. For example, you can create a model of an antenna design, save it as an app and add forms for different design parameters such as the length and thickness of the antenna, length of the waveguide, and frequency. In the finished app, these inputs can quickly be changed and the simulation rerun repeatedly to find an optimal combination of parameters. As of version 5.2, the Application Builder allows app users to update simulation plots while the app is solving, to follow the solution's progress. This is especially useful for more complex simulations that may take longer to complete. New editor tools make it easy to create an app to custom specifications.

COMSOL Multiphysics version 5.2 includes many demonstration apps to show how apps are built and used. One of these is the new microstrip patch antenna array synthesizer (see ***Figure 3***), which enables testing different

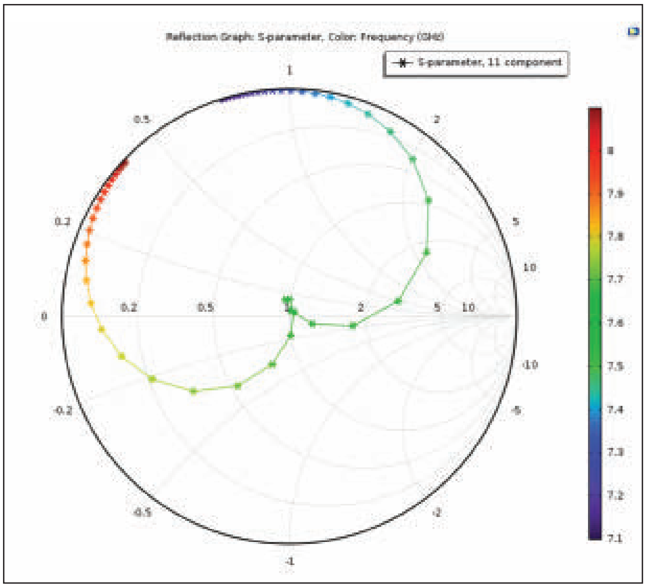

▲ *Fig. 2 Smith chart created with the RF Module.*

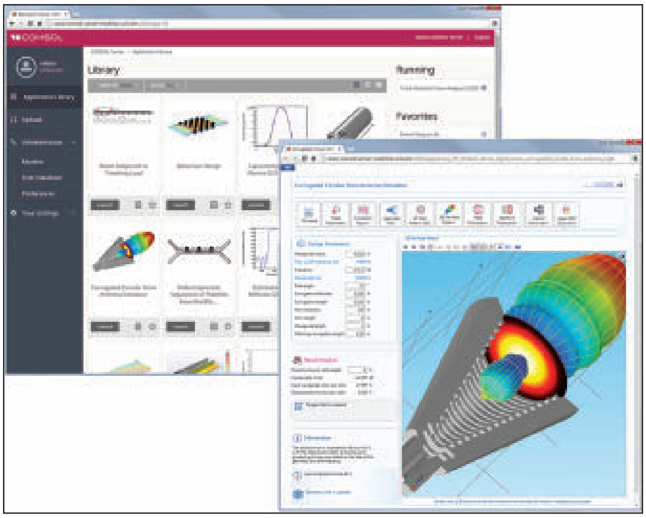

▲ *Fig. 4 A selection of demo apps are available in COMSOL Server™.*

parameters for an antenna array design optimized for 5G technology. Over 50 demo apps are included for a variety of specific uses. You can access the examples in the Application Library in COMSOL Multiphysics or online in the Application Gallery at www.comsol.com/models.

The COMSOL Server product enables sharing apps that you create with those who should use them. Apps can be shared with other design engineers working on the same project, so they can run their own tests without waiting for simulation results. Sales and support teams can use apps to help customers design a specific version of a product or adjust and customize its parameters. Using COMSOL Server, apps run in a web browser or using COMSOL Client (see ***Figure 4***).

During the life cycle of your RF and microwave design process, simulation can help to reduce costs, resources and time — while enabling you to produce more accurate designs.

COMSOL, Inc.
Burlington, Mass.
www.comsol.com

Real-Time Spectrum Analyzers: 10× Lower Size, Weight and Cost

Berkeley Nucleonics
San Rafael, Calif.

Berkeley Nucleonics (BNC) has developed and introduced a next generation, high performance, real-time spectrum analyzer (RTSA) at one-tenth the cost and one-tenth the size and weight of a typical benchtop RTSA. At the same time, it has 10× the performance of a portable handheld spectrum analyzer at half the cost. This leapfrog in technology by BNC is poised to revolutionize the $700 million per year spectrum analyzer test and measurement market. RTSAs allow engineers to see the spectrum as they never have before — in real-time — which means never missing any signals, wanted or unwanted.

An RTSA processes RF fast enough to not miss any signals within its given capture bandwidth, known as its real-time bandwidth (RTBW). It provides views of the spectrum in the frequency and time domains, as well as power spectral density, to enable analysis of signals that may be so fast as to be undetectable to the human eye. An RTSA must also have the capability to trigger on and capture events, recording them for playback and deeper analysis.

The BNC RTSA7500 is a family of PC-controlled RTSAs offered in three upper frequency ranges, from 100 kHz to 8, 18 or 27 GHz. These analyzers are unique in their ability to be operated either remotely over an IP network or by direct connection to a PC. The RTSA7500 features RTBW up to 100 MHz, probability of intercept (POI) as short as 1 µs and a spurious free dynamic range (SFDR) up to 100 dBc. The RTSA7500 consists of software that runs on a PC with Windows 7, 8 or 10 and hardware comprised of a high performance software-defined radio receiver and wideband digitizer.

The RTSA7500 can be utilized anywhere in the wireless ecosystem: R&D, education, manufacturing, deployment and monitoring. Anyone dealing with signals that vary dynamically in amplitude or are agile in frequency can increase their productivity with a real-time spectrum analyzer. Examples include fast intermittent signals, pulsed signals, frequency-hopping signals, signals hidden underneath

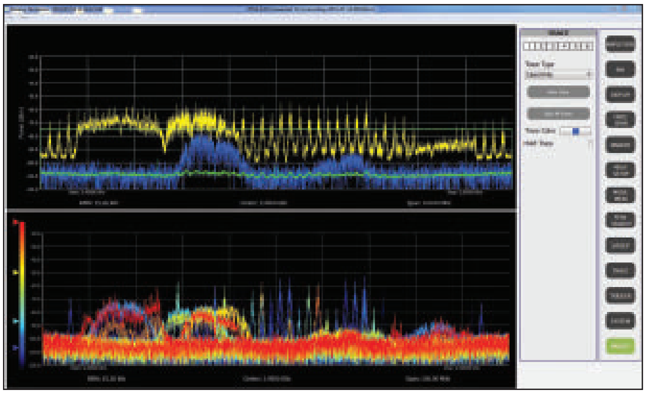

▲ *Fig. 1 BNC RTSA7500 display showing Wi-Fi and Bluetooth signals at 2.4 GHz.*

signals and multi-signal environments sharing the same spectrum in license-free bands (see ***Figure 1***). In addition, the RTSA7500 is versatile enough to be able to analyze conventional CW signals and analog modulation formats.

The BNC RTSA7500 solution consists of the following real-time capabilities: spectrum graph, spectrogram view, power spectral density display (persistence), triggering, I/Q plots, and recording and playback. Users can choose between standard swept-tuned spectrum analysis and real-time spectrum analysis with choices of 10, 40 or 100 MHz real-time bandwidth. Users can also select the high dynamic range mode featuring 100 dBc dynamic range for making critical IP3 measurements.

The RTSA7500 is extensible, which allows OEMs to add additional functionality with a 10 MHz input/output reference for multi-unit synchronization. This allows multiple RTSA7500s to be linked to one another in complete phase-coherence with one another and allowing multiple spectrum to be viewed, in real-time, simultaneously. Analog I/Q outputs can be used with OEM high speed digitizers for 80 or 160 MHz RTBW. The product includes the PC-based Real-Time Spectrum Analysis software, a GPIO port for external triggers and exterior modules such as antenna switches and down-converters and optional support for external local oscillator inputs, to enable phase-coherent radio front-ends.

BNC utilizes industry-leading APIs and open-source code for easy customization and remote control. Programming languages supported are Python™, LabVIEW, MATLAB® and C/C++. Standard protocols and file formats include SCPI, VRT and CSV. For networking and remote applications, the RTSA7500 uses Gigabit Ethernet, making it convenient for the manufacturing environment and remote spectrum management applications. With record and playback files, deeper analysis can be conducted on any PC or multiple PCs running the RTSA software without the instrument being attached.

The cost, size and weight of conventional real-time spectrum analyzers have relegated them to the bench of the mostly R&D intensive military-aerospace industry. BNC's solution now makes RTSAs affordable and portable for all scenarios, whether on the bench for R&D, on the manufacturing floor or in the field for wireless deployment, interference and bug hunting or spectrum monitoring.

Wireless systems are evolving rapidly, with wider bandwidths, higher order modulation and more frequencies — all of which have to coexist. The Internet of Things (IoT) is about to explode, bringing millions of new wireless devices to market that must be engineered, manufactured and deployed. BNC is at the forefront of this technology shift, capitalizing on these new wireless device test requirements with its patented, high performance, low cost, software-defined radio technology, open-source software, standard APIs and a PC-controlled, networked architecture that provides unparalleled performance for the price.

VENDORVIEW

Berkeley Nucleonics
San Rafael, Calif.
(415) 453-9955
rfsales@berkeleynucleonics.com
http://rf.berkeleynucleonics.com/MWRTSA

Wideband Measurement System Characterizes Wireless Networks

The Surveyor 500 is a wideband measurement system for collecting wireless transmissions between 300 MHz and 4.4 GHz. Combining a scanning receiver, computer and software, the system characterizes wireless networks by automatically scanning, collecting and categorizing the signals it receives. The Surveyor 500 is compatible with GSM, CDMA, WCDMA, EVDO, LTE, WiMAX and Wi-Fi and will record the metadata of the detected control channels and associated information. The measurements are passive, meaning the system doesn't require handshaking with the communications network being characterized.

Complementing the wideband receiver, the DCode Pro software interface enables system control and data analysis, with real-time visual notifications. The software includes several recent enhancements: The spectrum viewer provides a spectral display showing cellular modulation types, signals and interferences; The band editor enables the user to identify spectrum that is out of band for the standard band classes; System software is upgradeable, so adding new communications protocols is straightforward.

Designed for fast measurements and low power consumption, the Surveyor 500 is very effective for cellular drive testing. With internal GPS, the system can map the location of base stations. It can also synchronize with external GPS data.

The Surveyor 500 logs data on a removable CFast card, has Ethernet and Wi-Fi interfaces, can be controlled with a USB mouse and keyboard, and includes an HDMI port for showing video. The system is enclosed in an IP66 rated aluminum chassis, measuring 6.4" × 3.5" × 7.9", and weighs 8 lb. It is powered with an external supply between 10 and 32 V DC, typically from an automobile.

QRC Technologies
Fredericksburg, Va.
www.qrctech.com

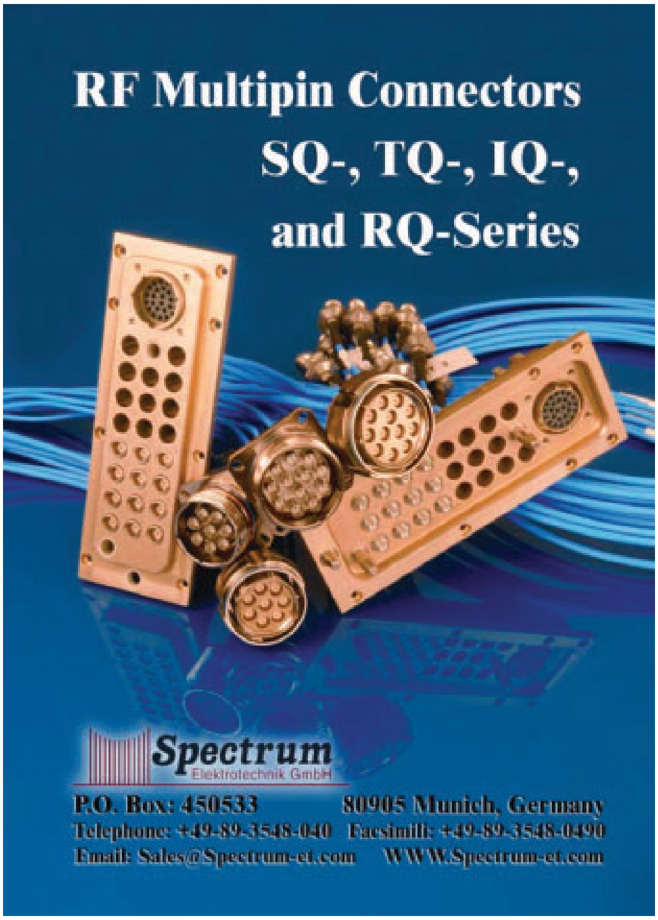

Catalogue RF Multipin Connectors 52 pages showing in detail 4 coaxial Multipin Connector Series, demonstrating how to connect and disconnect up to 23 coaxial lines in seconds and saving space.

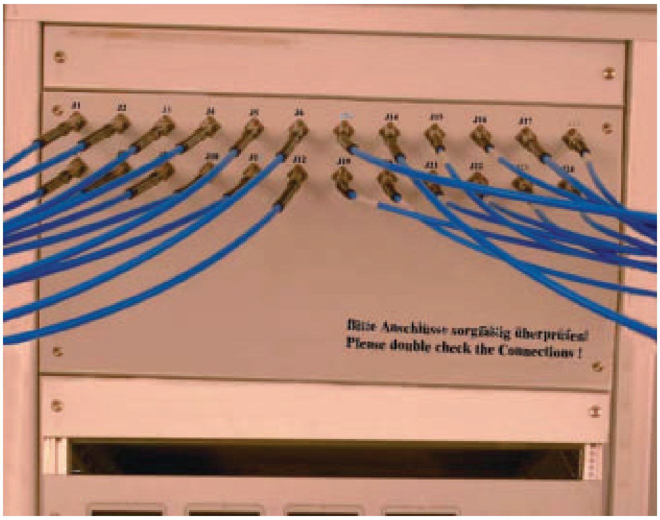

The Problem: In various applications many coaxial microwave links have to be connected and disconnected. This means threadening and unthreadening, torquing and untorquing. Very dense packaging is not possible, as there is still room needed for manual threadening and for the use of a torque wrench. In helicopters and aircrafts all connectors usually have to be safely secured, wiring the coupling nuts of the connectors, using wire holes, a time-consuming process.

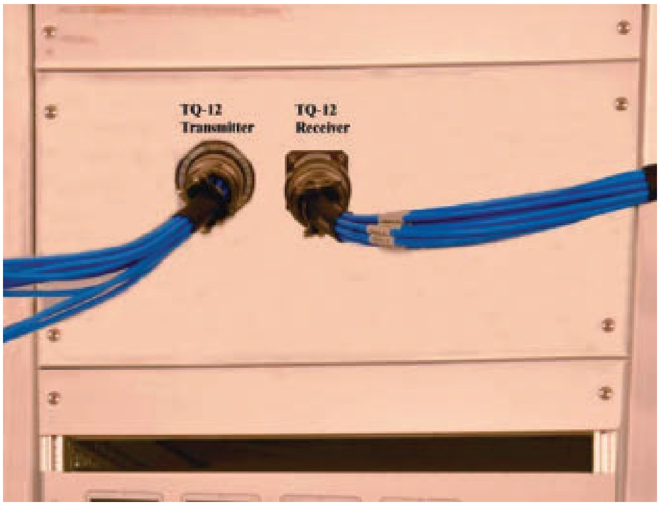

The Solution: Spectrum's Multipin Connectors are available with four (4), seven (7), eight (8), twelve (12) and twenty three (23) coaxial inserts (terminating the coaxial cable assemblies) at the Multipin end, and connecting all the coaxial cable assemblies at once and in seconds with no need of a torque wrench, no need for safety wires and using minimum space.

Spectrum Elektrotechnik GmbH
P.O.Box 450533 80905 Munich Tel. +49-89-3548-040
Email: Sales@Spectrum-et.com www.Spectrum-et.com

RF Signal Generator Delivers Performance and Value

The DSG800 series RF signal generators deliver unprecedented value to engineers needing a full-functioned RF signal generator, yet can't afford the cost of traditional RF test and measurement equipment.

The DSG800 series generates frequencies from 9 kHz to 1.5 or 3 GHz, with 0.01 Hz resolution at any frequency. The instruments achieve output power to +20 dBm, amplitude accuracy of ±0.5 dB and low SSB phase noise of -115 dBc/Hz. An oven-controlled crystal oscillator time-base option provides < 5 ppb temperature stability and < 30 ppb/year aging stability, the most accurate and stable available in this class of signal generator. These signal generators provide conventional sweep functions (step, list, logarithmic and linear) as well as several modulations: amplitude modulation (AM), frequency modulation (FM), phase modulation (ΦM) and an option for pulse modulation. The DSG800 offers an optional pulse train generation capability for those customers needing to translate serial data onto an RF link.

The series includes two models: the DSG815, which covers 9 kHz to 1.5 GHz and is priced at $1,999, and the DSG830, which covers 9 kHz to 3 GHz and is priced at $3,599.

The performance and value of the DSG800 signal generators are attractive to Internet of Things (IoT) designers, engineers integrating Wi-Fi or Bluetooth into higher level products, EMI testers and educators, who are able to have the power of a full-functioned RF signal generator in their labs. These signal generators are the latest in a series of products from the company dedicated to lowering the cost of test. With the DSG800, RIGOL delivers a highly capable, full featured RF source at an extremely affordable price point, providing customers with unprecedented value.

RIGOL Technologies Inc.
Beaverton, Ore.
www.rigolna.com

CatalogUpdate

Quick Reference Guide

VENDORVIEW

API Weinschel's new catalog outlines the latest products offered by Weinschel. Included in this catalog are digital/programmable attenuators to 6 GHz; programmable attenuation, phase shifter and switch units up to 26.5 GHz; COTS subsystems; coaxial fixed attenuators and terminations including new medium and high power models, conduction cooled (Flat-Packs) DC to 40 GHz up to 550 W, high reliability and low passive intermodulation (PIM) designs.

API Technologies Weinschel

www.weinschel.apitech.com

EMC & RF Testing Catalog

VENDORVIEW

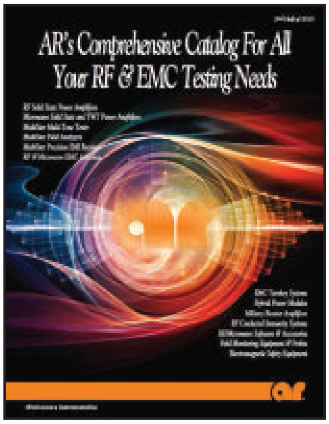

AR's catalog features new RF/microwave amplifier products and new intro sections for its A, W, & S series units. Navigate your way to the hybrid power modules and see photos of the expanded microelectronics lab, read about AR Europe's new partnership with 3ctest. Please contact your local AR sales associate for a hard copy or visit www.arworld.us/html/catalogRequest.asp for a free download, in full or by section.

AR RF/Microwave Instrumentation

www.arworld.us

RF Connector Catalogue

VENDORVIEW

In order to ensure actuality, the HUBER+SUHNER RF connector catalogue has been revised. The main revision of the 550-page catalogue is the addition of the new product series featuring MFBX, Contact-Bridge, XQMA, XQN and 4.3-10. The new connector catalogue also includes all HUBER+SUHNER Astrolab products such as AS12/AS16 contacts, SMPM and SMPM-T. The catalogue is available on the download area of the website or with the PDFolio mobile app.

HUBER+SUHNER

www.hubersuhner.com

RF Catalogue 5.1

INGUN released its new RF Catalogue 5.1. Highlights include — New appearance: cover with products, version number instead of year; New introductory pages to address customers, easy navigation and product search by application; New company pages: INGUN presents itself as an experienced, skilled quality provider with subsidiaries worldwide; Easy reference at work and as a training material with overview of applications, products and technical information; Precise version number on back cover as reference and for reordering. Available today for download at www.ingun.com/download.

INGUN

www.ingun.com

2016 Product Catalog

VENDORVIEW

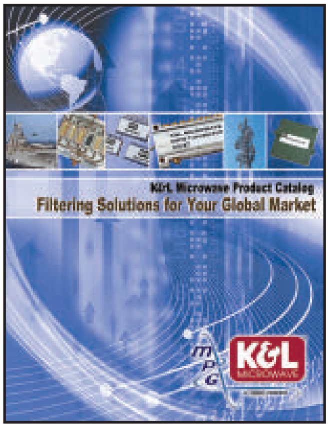

K&L designs and manufactures a full line of RF and microwave filters, duplexers and subassemblies, including ceramic, lumped element, cavity, waveguide and tunable filters. The catalog shows filter responses, loss calculations and standard packages for all products. K&L supplies many of today's most significant military and homeland security electronics programs. Applications include space flight, radar, communications, guidance systems, mobile radio base stations as well as air traffic control and communications. Visit www.klmicrowave.com to download the complete catalog.

K&L Microwave

www.klmicrowave.com

5G Application Note

VENDORVIEW

Keysight Technologies' new application note, "Solutions for Design and Evaluation of 5G Candidate Waveforms," provides deeper insight into using simulation for 5G communication systems and their waveforms. The application note is the latest in the series of Keysight Power of Wireless application notes. They are written to provide a better understanding into the intricacies of the continuously evolving wireless industry and help users accelerate development of their products. Available today at www.keysight.com/find/powerofwireless. Registration required.

Keysight Technologies Inc.

www.keysight.com

CatalogUpdate

DOCSIS 3.1 Product Guide

VENDORVIEW

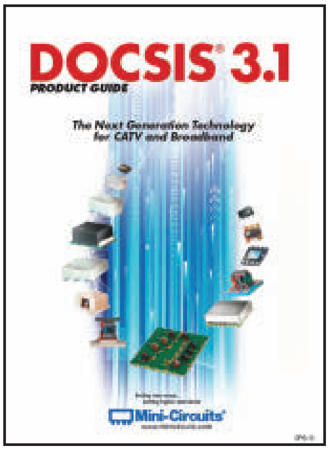

Mini-Circuits' DOCSIS® 3.1 Product Guide, is a 116-page full-color catalog that showcases the company's line of "next generation" products for CATV and broadband markets. The guide provides detailed information on Mini-Circuits' wide range of RF components, all carefully specified to meet DOCSIS 3.1 standards. This includes everything from passive devices such as its transformers, couplers, and splitter/combiners to active elements such as amplifiers, equalizers and more. With over 70 different DOCSIS-compliant models, chances are Mini-Circuits has your application covered.

Mini-Circuits

www.minicircuits.com

2016 RF Product Guide

VENDORVIEW

Pasternack released their new 2016 RF Product Guide. The 264-page catalog contains thousands of in-stock products including an expanded portfolio of RF amplifiers and electromechanical switches, the industry's largest selection of RF cable assemblies, and hundreds of other passive, active and test & measurement components, all available for same-day shipping worldwide. New additions include GaN, GaAs and LDMOS amplifiers, SPDT through SP12T switches, waveguide components, VNA calibration kits, test cables and ultra-high frequency RF adapters. The catalog also features product selection guides as well as other useful charts and resources.

Pasternack

www.pasternack.com

Filters, Multiplexers and Multi-function Assemblies

VENDORVIEW

When being first to react makes all the difference in the world, choose Reactel for your mission-critical filter requirements. You can count on Reactel to satisfy the most demanding requirements for units used in extremely harsh environments. Their full-line catalog features RF and microwave filters, multiplexers and multi-function assemblies for the military, industrial and commercial industries. To request your copy, please e-mail reactel@reactel.com or visit www.reactel.com.

Reactel Inc.

www.reactel.com

Contactless Data & Power Transmission

VENDORVIEW

The new second edition of the Contactless Data & Power Transmission brochure from SPINNER covers all available "contactless slip ring" techniques for use in military and industrial applications. These entirely maintenance-free contactless data transmission modules are available for various BUS protocols up to 1 Gbit/s. They function at up to 4500 RPM, and data transfer cannot be monitored (Wi-Fi is not used). Stand-alone or in combination with data transmission, "rotatable" DC/DC converters are available. Designed for 24/7 usage. Customized solutions are available.

SPINNER GmbH

www.spinner-group.com

Connectors and Cable Assemblies

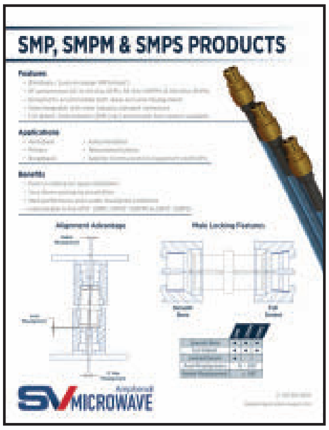

SV Microwave released their new SMP, SMPM & SMPS application note. These high density, high frequency connectors and cable assemblies increase electrical performance while reducing density. The new application note includes features, applications and benefits sections along with technical specifications, product styles available and clarifies radial/axial misalignment data. Visit svmicrowave.com to get your copy today.

SV Microwave

www.svmicrowave.com

Product Selection Guide

VENDORVIEW

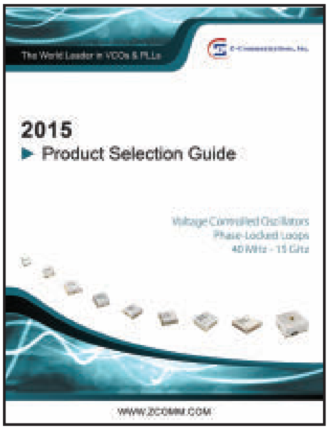

Z-Communications Inc. released its new Product Selection Guide. This short form catalog includes a wide variety of surface-mount VCO (voltage controlled oscillator) and (PLL) phase locked loop synthesizer modules ranging from 40 MHz to 15 GHz. Users can download an electronic version of the product guide in PDF format or contact the company for a hard copy version. A complete listing of all available parts and specifications can be found on the company's website.

Z-Communications Inc.

www.zcomm.com

NEW PRODUCTS

FOR MORE NEW PRODUCTS, VISIT WWW.MWJOURNAL.COM/BUYERSGUIDE
FEATURING VENDORVIEW STOREFRONTS

COMPONENTS

Ku-Band Bandpass Cavity Filter

VENDORVIEW

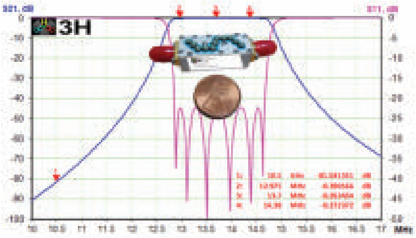

3H Communication Systems offers its new high performance Ku bandpass cavity filter. The filter offers low in-band insertion loss of < 0.40 dB max with > 60 dB attenuation in a connectorized package no larger than 1.23" L × 0.5" W × 0.5" H (excluding connectors) with average power handling of 50 W. Meets Mil-Std-202 conditions. For more information contact: sales@3hcomm.com or call (949) 529-1583.

3H Communication Systems
www.3Hcommunicationsystems.com

50 W Fixed Attenuators

BroadWave Technologies added model series 351-319-XXX (insert desired attenuation value to complete the model number) to its portfolio of 50 ohm fixed attenuators. Standard attenuation values are 3, 6, 10, 20, 30 and 50 dB. The average power rating is 50 W @ 25°C with 1000 W peak power. Maximum VSWR is 1.40:1. Other attenuation values and connector configurations are available upon request.

BroadWave Technologies
www.broadwavetech.com

Power Switch Matrix

Ducommun Inc. released a low power, high reliability, 4 × 3 switch matrix for space applications. The operating frequency range is 7 to 11 GHz with an input power of 200 mW. The operating voltage is 24 to 31 V DC (28 V DC Nominal) at extreme temperature of -20° to +80°C. The 4 × 3 switch matrix is latching type and equipped with suppression diodes and telemetry circuitry. Ducommun's design engineers can create custom versions for your specific applications. Contact them at (310) 513-7256 or (310) 513-7200 for more information.

Ducommun Inc.
www.ducommun.com

24-Bit 2 Msps SAR ADC

VENDORVIEW

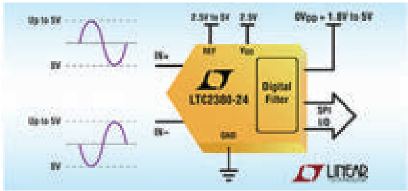

Linear Technology Corp. introduced the LTC2380-24, a breakthrough no latency 24-bit 2 Msps successive approximation register (SAR) analog-to-digital converter (ADC). The LTC2380-24 features an integrated digital filter that averages 1 to 65,536 conversion results real-time, dramatically improving the dynamic range from 101 dB at 1.5 Msps to 145 dB at an output data rate of 30.5 sps. This makes the LTC2380-24 ideal for seismic, medical and many other applications demanding high dynamic range.

Linear Technology Corp.
www.linear.com

50 W Low PIM Attenuators

VENDORVIEW

MECA's line of 50 W low PIM attenuators, within series and between series includes: 4.1/9.5, 4.3/10.0, 7/16 DIN & Type N connectors. With PIM spec of -160 dBc typ, while handling full rated power to +85°C with no power deration over temperature. Covering 0.698 to 2.7 GHz frequency bands and weatherproof IP67 rated. Products are verified for RF performance and PIM tested to the industry standard consisting of 2 × 20 W tones at 25°C in both cell and PCS bands.

MECA Electronics Inc.
www.e-MECA.com

MMSM SP2T PIN Diode Switch

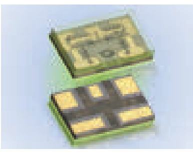

Microsemi announced the MPS2R10-606, a new high power Monolithic Surface Mount (MMSM) series-shunt SP2T PIN diode reflective switch. Optimized for high power UHF and transmit/receive (T/R) switching applications, the switch provides frequency coverage from 0.1 to 1 GHz with 0.2 dB insertion loss and 55 dB of isolation at mid-band. A simple analog control voltage allows this device to achieve 500 nS switching speeds while handling up to 100 W of continuous wave (CW) power.

Microsemi
www.microsemi.com

Cavity GPS Bandpass Filter

VENDORVIEW

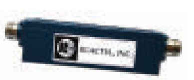

This filter has a passband of 1217 to 1606 MHz passing GPS L1 and L2 frequencies while rejecting extremely close-in iridium and TACAN 123× signals. Utilizing a unique approach to achieve these specs, this filter exhibits low passband loss and a high level of unwanted signal attenuation all while offering a DC thru path via the center conductor of the RF connector pins. Reactel manufactures a wide variety of filters, multiplexers and multifunction assemblies. Contact the company today with your requirements.

Reactel Inc.
www.reactel.com

0.5 to 18 GHz SMA Couplers

VENDORVIEW

RFMW Ltd. announced design and sales support for broadband directional couplers from P1dB. Operating from 0.5 to 18 GHz, these coaxial, SMA connectorized directional couplers offer coupling factors of 10, 20 and 30 dB as follows: P1CP-SAF-R518G30W-10 (10 dB), P1CP-SAF-R518G30W-20 (20 dB), P1CP-SAF-R518G30W-30 (30 dB). All models can handle input power levels as high at 30 W. Directivity for the P1CP-SAF-R518G30W-10 (10 dB), P1CP-SAF-R518G30W-20 (20 dB) is 22 dB while model P1CP-SAF-R518G30W-30 offers 20 dB directivity. All three P1dB directional couplers are standard products and P1dB offers additional coupling factors upon request.

RFMW Ltd.
www.rfmw.com

High Power Handling SPDT Switch

VENDORVIEW

Richardson RFPD Inc. announced the availability and full design support capabilities for a new 700 to 3800 MHz, UltraCMOS SPDT RF switch from Peregrine Semiconductor Corp.

New**Products**

The PE42822 is a HaRP™ technology-enhanced absorptive 50 ohm SPDT RF protection switch designed for use in high-power and high performance wireless infrastructure and small cell applications, supporting frequencies up to 3800 MHz. The new switch features high linearity, which remains invariant across the full supply range, as well as exceptional isolation and fast switching time. In addition, no external blocking capacitors are required if 0 VDC is present on the RF ports.
Richardson RFPD Inc.
www.richardsonrfpd.com

QPL Switches

RLC Electronics introduced seven new QPL switches to its library of over 100 QPL switches that RLC is already manufacturing. Being the only QPL switch provider in the U.S., RLC works directly with the U.S. Government to assign new part numbers frequently. Recent additions include S-8836, iaw M3928/30-01, S-8837, iaw M3928/31-01, S-8838, iaw M3928/31-02, S-8839, iaw M3928/32-01, S-8840, iaw M3928/32-02, S-8841, iaw M3928/33-01 and S-8842, iaw M3928/33-02.
RLC Electronics Inc.
www.rlcelectronics.com

CABLES & CONNECTORS

Ultra-Miniature Cable Assemblies

Fairview Microwave Inc. introduced a brand new family of ultra-miniature UMCX, WMCX and HMCX32 cable assemblies. Commonly used to connect an external antenna to a mini-PCB, these flexible micro-coax jumpers offer operation from DC to 6 GHz and are ideal for use in wireless communications systems. Additional wireless

applications include antennas for GPS and other radio systems, Wi-Fi, wireless LAN, Bluetooth, ZigBee, LTE, mini-PCI and PDA/PCS/cellular handset applications. Fairview Microwave's new UMCX and WMCX cable assemblies are compatible with Hirose® U.FL™ and W.FL™ connectors respectively, and feature miniature snap-on connectors with mated connection heights ranging from only 1.2 to 2.5 mm.
Fairview Microwave Inc.
www.fairviewmicrowave.com

VNA Test Cables

VENDORVIEW

Pasternack released an all new line of ruggedized phase stable VNA test cables operating up to 40 GHz depending on the series. These VNA test cables are specially designed to withstand the rigors of test lab use and production testing for 50 ohm communications systems. The new phase stable cables can be ordered with male or female versions of SMA or Type-N connectors for cables operating to 18 GHz, 2.92 mm connectors for cables operating to 26.5 GHz or 2.4 mm connectors for test cables performing up to 40 GHz.
Pasternack
www.pasternack.com

Field Replaceable Receptacles

SGMC Microwave's 1.85 mm series receptacles are precision grade connectors designed for use with microwave applications requiring excellent performance up to 65 GHz and beyond. Mechanically compatible with 2.4 mm connector series with captivated center contacts. Ruggedized 303 series stainless steel (passivated) construction for repeatability and reliability. Low VSWR and insertion loss. Same-day shipping available from SGMC's stocking distributor C.W. Swift & Associates.
SGMC Microwave
www.sgmcmicrowave.com

COTS SMA and TNC Connectors

SV Microwave drastically increased their COTS SMA and TNC connector selection. Visit SV's new website to view ready to ship factory stock. SV understands that customers need RF connectors fast, but cannot compromise on quality. So come visit SV's website now to check stock and order your favorite connector that can ship the same day. SV's factory inventory includes: SMA, TNC, 2.92 mm, 2.4 mm, SMP, SMPM, SMPS and Mil specs.
SV Microwave
www.svmicrowave.com

AMPLIFIERS

Benchtop Power Amplifier

VENDORVIEW

The 350S1G6 provides wideband high linear output power over a frequency band of 0.7 to 6 GHz. Over 350 W of output power is achieved with only 1 milliwatt of input power. This amplifier is designed using "Hybrid Microelectronics Technology" resulting with an amplifier with greater power density, smaller size and lower production cost than previously possible.
AR RF/Microwave Instrumentation
www.arworld.us/html/18200.asp?id=1271

NewProducts

X-Band SSPA Module

COMTECH PST introduced another new gallium nitride (GaN) amplifier for X-Band applications. This class AB linear design operates over the full 9 to 10 GHz frequency range and is ideal for use in phase array radar applications, as a TWT replacement or for a microwave communication link. The amplifier features phase and amplitude control, internal DC to DC converters and DC filtering, PA self-test and LED fault indications, unique waveguide coupling circuits, an internal isolator and digital control via a magic tee. The small lightweight construction makes it amenable to a variety of platforms and environments.

COMTECH PST
www.comtechpst.com

RF Instrument Amplifier

VENDORVIEW

Mini-Circuits' TVA-4W-422A+ instrument amplifier provides flat gain and high IP3 across the 500 to 4200 MHz frequency range, supporting a wide variety of applications. The amplifier runs on a built-in 110/220 V power supply, making it easy to use in most lab environments. This model features thermal self-protection and withstands open and short loads while delivering signals up to P1dB, preventing damage to the amplifier and providing added reliability. It comes housed in a lightweight aluminum alloy case (15.35" × 8.27" × 3.25") with N-Type connectors, ideal for benchtop use. Two N-male to SMA-female adapters are included.

Mini-Circuits
www.mini-circuits.com

Power Amplifier Module

NuWaves Engineering introduced the NuPower 05E05A, a compact and highly efficient solid-state power amplifier (PA) module for S-Band transmitters and data links. Providing 30 W on average, and 20 W minimum, RF output power, the NuPower 05E05A operates from 2000 to 2600 MHz for continuous wave (CW) and near-constant-envelope waveforms. The connectorized PA module accepts a nominal 0 dBm (1 milliwatt) input signal and provides 44 dB of RF gain while operating at 40 percent DC power efficiency with a +28 VDC supply voltage.

NuWaves Engineering
www.nuwaves.com

Successive Detection Log Video Amplifier

VENDORVIEW

PMI's successive detection log video amplifier (SDLVA) has been designed using cutting edge GaAs technology providing stunning performance and reliability. Its compact package makes it an optimum solution for high speed channelized receiver applications. It has a dynamic range of 65 dB, log slope of 25 mV/dB, a nominal video bandwidth of 32 MHz, and operates between 18 and 40 GHz.

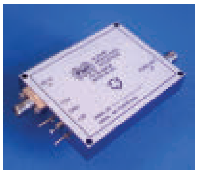

Planar Monolithics Industries Inc.
www.pmi-rf.com

60 W Power Amplifier

RF-Lambda's 60 W power amplifiers feature high output power +48 dBm, aerospace and military application, X-Band radar and high peak to average handle capability. All specifications can be modified upon request.

RF-Lambda
www.rflambda.com

Wideband GaN Amplifiers

Teledyne Microwave Solutions announced a new line of wideband GaN amplifiers that further lowers the form factor threshold in the industry for the 0.1 to 6 GHz frequency range. The new line consists of five GaN wideband amplifier models that raise the bar for SWaP (size, weight and power) in this category of GaN amplifiers, while meeting the stringent airborne requirements of the most demanding commercial and military applications. The dimensions, excluding connectors, are 2.5"L × 2"W × 0.42"H, at only 2.1 cubic inches. The five model numbers are TSA-213241, TSA-213242, TSA-213243, TSA-213244 and TSA-213245.

Teledyne Microwave Solutions
www.teledyne.com

X-Band GaN MMIC Power Amplifier

Wolfspeed's X-Band GaN MMIC power amplifier is rated for 25 W and 8.5 to 11 GHz operation, delivers high performance in a small form factor and features: 37 W typical Pout, 16 dB power gain, 35% typical power added efficiency (PAE), and <0.1 dB power droop. The GaN MMIC is also internally matched to 50 Ω, and is supplied in both a 10-lead metal/ceramic flanged package and a new, smaller form factor pill package for optimal electrical and thermal performance.

Wolfspeed
www.wolfspeed.com

NewProducts

High Gain Power Amplifiers

VENDORVIEW

Z-Communications Inc. introduced a new series of RF amplifier products with the release of the PAC18700T and DRC23000M. Operating in the K-Band, the PAC18700T and DRC23000M provide a unique advantage by allowing quick and simple installation into systems with their integrated supply circuitry allowing to be operated from a single power source and availability in a SMA connectorized module package. These new RF amplifiers are further heightened by their high output power, high gain and superior linearity.

Z-Communications Inc.
www.zcomm.com

SYSTEMS

AutoPoint Alignment System

HXI's AutoPoint System, designed exclusively for HXI Radios, provides mmWave radio path alignment from any remote location. It is the perfect solution to align and maintain high bandwidth directional antennas for many communication applications. AutoPoint is a complete hardware and software solution. It can be used to "fine tune" initial alignment, and more importantly, to re-align your link as required. The web-based user access makes it easy to optimize link performance regardless of the time of day, season or current weather conditions.

Renaissance Electronics & Communications LLC
www.rec-usa.com

W-Band Receiver

VENDORVIEW

Model SSR-9630831560-10-S1 is a W-Band receiver. The receiver has a typical conversion gain of 15 dB with a typical RF input power of -60 dBm in the frequency range of 92 to 100 GHz and IF output frequency range of DC to 4 GHz. The required LO power and frequency range are +5 dBm and 16 GHz. The LO and IF port are both equipped with female SMA connectors and the RF port is a WR-12 waveguide with a UG-387/U flange.

SAGE Millimeter
www.sagemillimeter.com

SOURCES

Ka-Band mmWave Power Module

L-3 Electron Devices introduced its new M1292-02 Ka-Band millimeter wave MPM. The module is available for immediate insertion on advanced Ka-Band communications systems requiring linear output power and high efficiency in an ultra-compact, fully airborne-qualified (up to 50,000 feet) package that enables users to physically mount the MPM extremely close to their transmitting aperture, thus minimizing RF losses. The MPM is also reconfigurable for 100 W of saturated power operation.

L-3 Electron Devices
www.L-3com.com

Pulse Generators

The PicoSource® PG900 Series pulse generators are high speed, low cost instruments for use in single-ended and differential pulsed measurement applications. The series offers two triggered step-generation technologies. The PG911, with integral step-recovery diode outputs, offers a transition time of < 60 ps with a large and adjustable output swing of 2.5 to 6 V on each output. The PG912 uses external tunnel diode pulse heads to deliver a faster transition time of < 40 ps with fixed 200 mV amplitude right at the interface plane. A third model, the PG914 combines both technologies in one space-saving, economical unit.

Pico Technology
www.picotech.com

RF Signal Generator

RIGOL Technologies Inc. introduced the DSG800 series RF signal generator. Delivering unprecedented value to engineers integrating RF technology into their Internet of Things designs, the DSG800 delivers an uncompromised signal generator at very attractive entry level price point. The instruments provide maximum output power up to +20 dBm and low SSB phase noise of -105 dBc/Hz, amplitude accuracy of ± 0.5 dB, and frequency resolution 0.01 Hz at any frequency.

RIGOL Technologies
www.rigol.com

Wideband Selectable Frequency Synthesizer

The FCPH225375-10 is a wideband, low phase noise selectable frequency synthesizer capable of covering 2250 to 3750 MHz in 10 MHz discrete step sizes from a 10 MHz reference. Phase noise at 1 kHz offset is -96 dBc/Hz and at 100 kHz offset is -107 dBc/Hz. Spurious products are suppressed by 70 dBc and output power is +6 dBm, minimum. The package is a surface-mount which is 1.25" × 1.0" × 0.23" (L × W × H) and is powered by a

MICRO-ADS

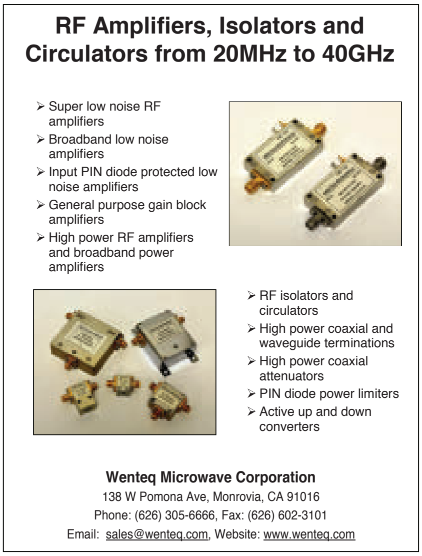

single +5 volt supply drawing less than 200 mA of current.

Synergy Microwave Corp.
www.synergymwave.com

TEST EQUIPMENT

SAR Emissions Measurement System

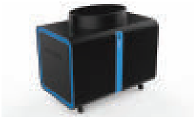

Art-Fi's ART-BODY is the first instant SAR measurement system with a fixed probe-array for large devices. Small cells, divided into microcells, picocells and femtocells, are like lesser basestations that extend mobile coverage into areas where coverage is poor or needs to be improved. Femtocells, the smallest type of small cell, is the size of a normal Wi-Fi router and is used in homes or small offices that have poor coverage. Microcells, the largest type of small cell, are often used in areas of mass congregation where many people need cellular service simultaneously, like sporting events.

Art-Fi
www.art-fi.com

Cross-Correlation Phase Noise Test Systems

VENDORVIEW

Berkeley Nucleonics introduced a new signal source analyzer providing accurate measurements of SSB phase noise as well as full time domain analysis capability and several different modes of noise, spectrum and transient analysis. The 7000 series offers both residual and absolute noise measurements from 5 MHz to 30 GHz, providing operation with either internal or external reference sources and measurements from 0.1 Hz to 50 MHz frequency offset. BNC's analysis time only takes a few minutes, leapfrogging traditional testing hardware and techniques by an order of magnitude.

Berkeley Nucleonics
www.berkeleynucleonics.com

Spectrum Rider

VENDORVIEW

The versatile R&S Spectrum Rider from Rohde & Schwarz assists users during RF transmitter installation and maintenance and also supports measurement tasks in RF development labs and in service. With its high sensitivity of -160 dBm and measurement accuracy of typically 0.5 dB between 10 MHz and 3 GHz, the R&S Spectrum Rider offers class-leading RF performance. The frequency range of the R&S Spectrum Rider can be extended via software upgrades - a feature unrivaled in this instrument class. The base model covers the frequency range from 5 kHz to 2 GHz, which can be expanded to 3 or 4 GHz to support applications that require higher frequencies.

Rohde & Schwarz GmbH & Co. KG
www.rohde-schwarz.com

2016 Microwave Wireless Industry Exhibition in China (MWIE 2016)
2016 International Conference on Microwave and Millimeter Wave Technology

MWIE 2016

Sponsor: Chinese Institute of Electronics (CIE)

Co-Sponsors:
Microwave Society of Chinese Institute of Electronics
Beijing Institute of Technology
Tsinghua University
Southeast University
Kingradio Technology [Shenzhen] Co., Ltd.
Science and Technology on Electronic Test & Measurement Laboratory
Education Development Fund of Lin Weigan
Xi'an HengDa Microwave Technology Development Company

Collaborating Media:
Journal of Microwaves (China), Microwave Journal (USA), MWRF.NET and Rfeda.cn

Date: June 5~8, 2016 Venue: Beijing International Convention Center, P.R. China

The International Conference on Microwave and Millimeter Wave Technology (ICMMT) is one of the series international conferences on microwave and millimeter wave field in China. The bi-yearly Conference is organized by Microwave Society of Chinese Institute of Electronics, etc. and held in every two years (every even year). The ICMMT 2016 (9th ICMMT) will be held in Beijing International Convention Center.

The ICMMT 2016 is supported by Beijing Institute of Radio Metrology and Measurement, Institute of Electronics Chinese Academy of Sciences, 12th Institute of China Electronics Technology Group Corporation, Peking University, Beihang University, Beijing University of Posts and Telecommunications, and Beijing Jiaotong University!

The ICMMT 2016 is supported by IEEE, too! All the presented papers will be included into IEEE Xplore® and indexed by EI.

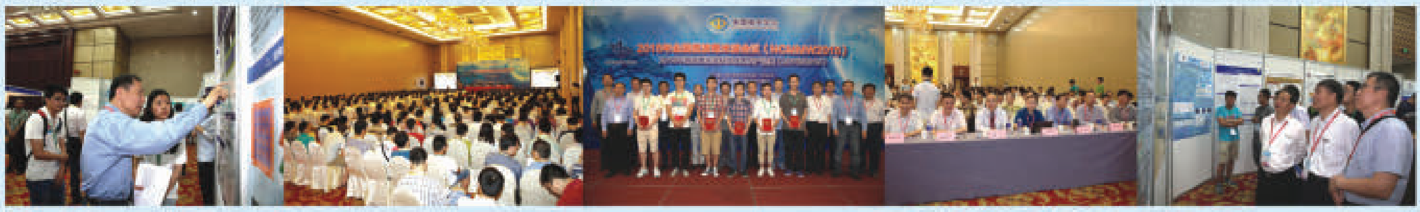

Microwave Wireless Industry Exhibition (MWIE) has been held for over 20 years. It is one of most important event of the International Conference on Microwave and Millimeter Wave Technology held every even year as well as the National Conference on Microwave and Millimeter Wave in China in every odd year.
MWIE 2016 will be another grand exhibition after MIWE 2015 in Hefei, MIWE 2013 in Chongqing, MIWE 2012 in Shenzhen, MIWE 2011 in Qingdao, MWIE 2010 in Chengdu, MWIE 2009 in Xi'an and MWIE 2008 in Nanjing.

2015 Microwave Wireless Industry Exhibition in China (MWIE 2015) & 2015 National Conference on Microwave and Millimeter Wave in China

Exhibitors to be attended:

Manufacturers / distributors for RF / microwave / millimeter wave devices / components: solid state device and circuits (including MMIC): amplifiers, mixers, oscillators, etc. and passive components: filters, duplexers, couplers, attenuators, and antennas etc
Designer / distributor for RF / microwave / millimeter wave software
Manufacturers / distributors for RF / microwave / millimeter wave equipment
Manufacturers / distributors for RF / microwave PCB and connectors
Manufacturers / distributors for microwave absorber
Manufacturers / distributors for microwave / millimeter inductor, capacitor and high power resistor

Contact: Mr. Wei Zilun, Gao Xin, Ms. Liu **E-mail:** mwrf@vip.163.com kingradio@188.com


Information

Transmit Receive Modules for Radar and Communication Systems

Rick Sturdivant and Mike Harris

The concept of the active phased array — more formally the active electronically scanned array (AESA) — has been around for decades. The concept became viable with the development of transmit receive (T/R) modules that met both system performance and cost requirements. Today, AESAs are either in production or are being developed for virtually all military radar systems, and their advantages are being applied to commercial communications links.

"Transmit Receive Modules for Radar and Communication Systems" addresses the T/R module, which routes and amplifies the transmit and receive signals and sets the amplitude and phase for steering the antenna beam. The authors consider all aspects of the module: theory, practical design, fabrication, integration and implementation issues, and they include 44 examples of T/R module analysis, circuits and components.

The book addresses the impact of new semiconductor technologies, principally GaN and SiGe, which are enabling better performance than can be achieved with GaAs MMICs. Since packaging, interconnections and thermal management determine how semiconductor performance is realized at the array level, these topics are treated in detail. Because a large number of T/R modules are used in each array, module manufacturing is a critical process to ensure consistent performance and low cost. The authors address manufacturing and test as well as the other significant contributors to module cost.

"Transmit Receive Modules for Radar and Communication Systems" was drawn from a professional development course on AESAs, making it useful as the text in a workshop for professionals or a one semester course for seniors or graduate students.

The authors bring extensive professional experience to the topic. Rick Sturdivant has been president of Microwave Products and Technology for the last 12 years; his technical interests are in electronic packaging, T/R modules and phased arrays. He earned a master's in electrical engineering from the University of California Los Angeles. Mike Harris has been involved in T/R module programs for over 25 years, including developing semiconductor processes for GaAs PHEMTs and GaN HEMTs. Now retired, he continues to teach professional education courses on T/R modules for phased array radar. Harris earned a master's in electrical engineering from the Georgia Institute of Technology.

To order this book, contact

Artech House
www.artechhouse.com
ISBN: 978-1-60807-979-7
270 pages
$159 for the hardcover edition
Also available in eBook format

Advertising**Index**

Advertisers in blue are enabled with the layar app

Sales Representatives

Microwave Journal
Frequency Matters.

Eastern and Central Time Zones
Chuck Boyd
Northeast Reg. Sales Mgr.
(New England, New York, Eastern Canada)
685 Canton Street
Norwood, MA 02062
Tel: (781) 619-1942
FAX: (781) 769-5037
cboyd@mwjournal.com

Michael Hallman
Eastern Reg. Sales Mgr.
(NJ, Mid-Atlantic, Southeast, Midwest, TX)
4 Valley View Court
Middletown, MD 21769
Tel: (301) 371-8830
FAX: (301) 371-8832
mhallman@mwjournal.com

Pacific and Mountain Time Zones
Brian Landy
Western Reg. Sales Mgr.
(CA, AZ, OR, WA, ID, NV, UT, NM, CO, WY, MT, ND, SD, NE & Western Canada)
144 Segre Place
Santa Cruz, CA 95060
Tel: (831) 426-4143
FAX: (831) 515-5444
blandy@mwjournal.com

International Sales
Richard Vaughan
International Sales Manager
16 Sussex Street
London SW1V 4RW, England
Tel: +44 207 596 8742
FAX: +44 207 596 8749
rvaughan@horizonhouse.co.uk

Germany, Austria, and Switzerland (German-speaking)
WMS.Werbe- und Media Service
Brigitte Beranek
Gerhart-Hauptmann-Street 33,
D-72574 Bad Urach
Germany
Tel: +49 7125 407 31 18
FAX: +49 7125 407 31 08
bberanek@horizonhouse.com

Korea
Young-Seoh Chinn
JES Media International
2nd Floor, ANA Bldg.
257-1, Myungil-Dong
Kangdong-Gu
Seoul, 134-070 Korea
Tel: +82 2 481-3411
FAX: +82 2 481-3414
yschinn@horizonhouse.com

China
Shenzhen
Michael Tsui
ACT International
Tel: 86-755-25988571
FAX: 86-10-58607751
michaelt@actintl.com.hk

Shanghai
Linda Li
ACT International
Tel: 86-21-62511200
lindal@actintl.com.hk

Beijing
Oasis Guo
ACT International
Tel: 86-13011108861
oasisg@actintl.com.hk

Hong Kong, Taiwan, Singapore
Mark Mak
ACT International
Tel: 852-28386298
markm@actintl.com.hk

Japan
Katsuhiro Ishii
Ace Media Service Inc.
12-6, 4-Chome,
Nishiiko, Adachi-Ku
Tokyo 121-0824, Japan
Tel: +81 3 5691 3335
FAX: +81 3 5691 3336
amskatsu@dream.com

Ed Kiessling Traffic Manager/Inside Sales • 685 Canton Street Norwood, MA 02062 • Tel: (781) 619-1963 FAX: (781) 769-6178 • ekiessling@mwjournal.com

FABS and LABS

e2v's Microwave Division Lays New Foundations to Take the Business Forward

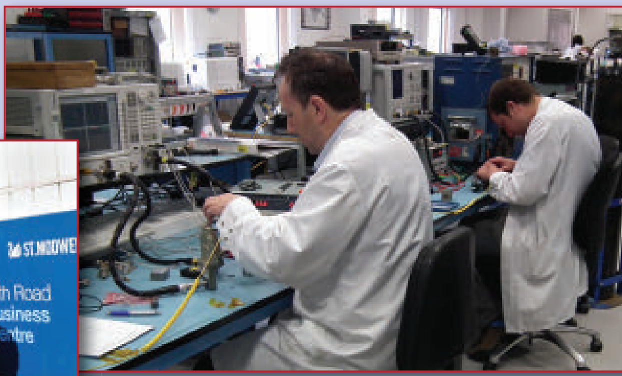

e2v is a leading global provider of innovative technology that employs approximately 1,750 people across 10 countries in Europe, America and Asia and has annual sales of £220 million. A vital cornerstone of the company, with a rich history of innovation and technological advancement is the microwave division, which has now laid down strong foundations for the future with the move to a new facility on Firth Road, Lincoln, UK in December 2015.

The move is part of a general company strategy to simplify and consolidate each core activity into focused businesses that are, by and large, stand-alone. The company still sells thousands of magnetrons a year and will continue to serve its traditional market, but it is also perfectly placed to participate in and benefit from the development of technology at higher frequencies, particularly millimetre wave components and systems.

Prior to taking up residence in the new facility, e2v's microwave business had been disparate with the existing complex on Sadler Road, Lincoln housing the design office, along with development and testing, while manufacturing was at e2v's main site in Chelmsford. The new 1,400 m^2 Firth Road facility will bring design and manufacturing under one roof and will enable e2v to deliver its growth plans, support market demand for new products, provide more efficient delivery to customers and create new employment in the region. The same can be said for the Electronic Safety & Initiation business, which will remain at Sadler Road, and will utilise the new-found space for its own business development.

There is a large office section, substantial manufacturing area plus store and machine shop. Along with the design and development department, which will focus on project management and business development, Firth Road is home to manufacturing and manufacturing engineering, equipment support, purchasing, quality, materials management and logistics. The 45-member staff includes 10 newly created positions, 17 design engineers covering microwaves, electronics, mechanical, ATE and PCB design, plus 15 manufacturing engineers and technicians.

The Firth Road site was also chosen due to its close proximity to the University of Lincoln Campus. The aim is to further strengthen the company's long-standing links with the university's School of Engineering and School of Mathematics and Physics with course specific scholarships and funding for an e2v Technology Research Associate within the School of Engineering.

e2v also has strong links with the University of Nottingham, which materialised when the company's facility on Carholme Road, Lincoln was closed. The large semiconductor Fab processing plant was taken out of the business but e2v needed to keep the core technology. The company made the decision to spin into the University of Nottingham, where it has three employees in the e2v Semiconductor Technology Centre, a state-of-the-art semiconductor 100 m^2 clean room in the University's School of Physics and Astronomy (SPA).

In its five-year collaboration the partnership has made ground-breaking achievements in research and development and device manufacture, including cutting-edge e2v Gunn and Schottky diodes. This joint effort has also spearheaded a wealth of research and development in: Superlattice electron devices (SLED) for millimetre wave components and the manufacture and use of semiconductor PIN diodes for receiver protection. e2v has also been awarded a major, long-term contract to supply semiconductor devices into a key millimetre wave system.

With technology to the fore, consolidated on a dedicated site, the e2v microwave business is set to start 2016 on the right road.

www.e2v.com

WERLATONE®

Celebrating 50 Years of High Power Passive Components

Mismatch Tolerant®

Test & Measurement Couplers

- **Up to 1000:1 Bandwidth**
- Low Insertion Loss
- Power Levels of 20 W CW to 20 kW CW
- Designs for Laboratory use Worldwide
- **Covering Full DC - 6000 MHz!**

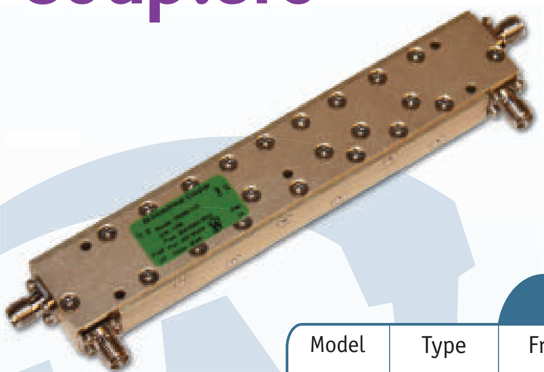

NEW

Directional Couplers

Model	Type	Frequency (MHz)	Power (W CW)	Coupling (dB)	Insertion Loss (dB)	VSWR (ML)	Size (Inches)
C6021	Dual	0.01-1000	500	40	0.45	1.30:1	6.7 x 2.27 x 1.69
C5725	Dual	0.1-1000	500	40	0.5	1.25:1	5.2 x 2.67 x 1.69
C9688	Dual	1-1000	800	40	0.5	1.20:1	6 x 2.2 x 2.2
C7734	Dual	30-2500	100	43	0.35	1.25:1	3.5 x 2.6 x 0.7
C8188	Uni	30-3000	20	20	2.4	1.35:1	6 x 1.5 x 1.1
C3910	Dual	80-1000	200	40	0.2	1.20:1	3 x 3 x 1.09
C8373	Bi	100-2500	200	20	0.8	1.25:1	9.58 x 1.48 x 0.88
C7711	Dual	100-3000	100	40	0.35	1.25:1	3 x 2.2 x 0.7
C7058	Bi	200-2000	200	10	0.3	1.25:1	6.4 x 1.6 x 0.72
C8060	Bi	200-6000	200	20	1.1	1.40:1	4.8 x 0.88 x 0.5
C7248	Bi	300-3000	100	6	0.35	1.25:1	6 x 2 x 0.85
C8000	Bi	600-6000	100	30	0.4	1.25:1	1.8 x 1 x 0.56
C8214	Bi	700-2500	100	6	0.35	1.25:1	6 x 2 x 0.85
C10462	Dual	700-4200	250	40	0.2	1.30:1	2 x 2 x 1.06
C10525	Dual	700-4200	700	50	0.2	1.35:1	2.15 x 2 x 1.36
C10536	Dual	700-4200	1000	50	0.2	1.35:1	2.15 x 2 x 1.36
C10006	Dual	700-4200	2000	50	0.2	1.35:1	3 x 3 x 1.59
C10117	Dual	700-6000	250	40	0.2	1.30:1	2 x 2 x 1.06
C10364	Dual	700-6000	500	50	0.2	1.35:1	2.15 x 2 x 1.36
C8644	Bi	1800-6100	60	20	0.4	1.25:1	1.1 x 0.75 x 0.48

Mismatch Tolerant® Designed to operate, at rated power, into Severe Load Mismatch Conditions

Werlatone, Inc.®
17 Jon Barrett Road
Patterson, NY 12563
T 845 278 2220
F 845 278 3440
sales@werlatone.com
www.werlatone.com

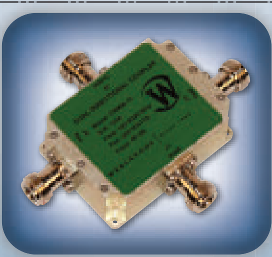

Directional Couplers

0° Combiners/Dividers

90° Hybrid Couplers

180° Hybrid Combiners

Absorptive Filters